Multiscale Interactions in Psychological Systems

by

Aaron D. Likens

A Dissertation Presented in Partial Fulfillment
of the Requirements for the Degree
Doctor of Philosophy

Approved November 2016 by the
Graduate Supervisory Committee

Polemnia G. Amazeen, Chair
Eric L. Amazeen
Nancy L. Cooke
Arthur M. Glenberg

ARIZONA STATE UNIVERSITY

December 2016

ABSTRACT

For many years now, researchers have documented evidence of fractal scaling in psychological time series. Explanations of fractal scaling have come from many sources but those that have gained the most traction in the literature are theories that suggest fractal scaling originates from the interactions among the multiple scales that make up behavior. Those theories, originating in the study of dynamical systems, suffer from the limitation that fractal analysis reveals only indirect evidence of multiscale interactions. Multiscale interactions must be demonstrated directly because there are many means to generate fractal properties. In two experiments, participants performed a pursuit tracking task while I recorded multiple behavioral and physiological time series. A new analytical technique, *multiscale lagged regression,* was introduced to capture how those many psychological time series coordinate across multiple scales and time. The results were surprising in that coordination among psychological time series tends to be oscillatory in nature, even when the series are not oscillatory themselves. Those and other results demonstrate the existence of multiscale interactions in psychological systems.

Dedication

I dedicate my work to my beautiful and loving wife, Nancy. I could have never made this journey without your love and patience. You have kept my spirits up when they were down. You have kept my heart and mind fed. It is an absolute mystery to me how anyone does this without someone like you.

I love you so much!

Thank you!

ACKNOWLEDGMENTS

First, and foremost, I thank my advisor, Nia Amazeen. I thank you for your guidance on this project but also for my career. You took me on as a graduate student one million years ago and have been there for me every step of the way as a mentor and as a friend. I look forward to all of the work for which we never had time and to the new ideas we have yet to invent. Second, I would like to thank Eric Amazeen for my success in this and other projects. I consider you and Nia both mentors and friends, and I am a better scholar and person for having had you in my corner. Third, I would like thank the rest of my committee, Art Glenberg, Nancy Cooke, and Gene Brewer. Your insights were invaluable in the both the development and completion of this project. Fourth, I would like to thank my lab mates, Justin Fine, Cameron Gibbons, and Morgan Waddell. You have all been amazing to work with, and I consider each of you a lifelong friend. I look forward to future collaborations and the many years we have in front of us. Fifth, I thank the research assistants that have helped me over the years. There are too many to list but I want to express a sincere thank you to Angelica Castillo for keeping me sane the last couple of years. Lastly, I thank Mickie Vanhoy for starting me down this path. I wouldn't be here without you.

TABLE OF CONTENTS

Page

LIST OF FIGURES vii

MULTISCALE INTERACTIONS IN PSYCHOLOGICAL SYSTEMS 1

Fractals in Psychological Time Series 2

What it Means to be Fractal 2

The Significance of Fractals in Psychological Time Series 6

Meaning from Ubiquity 6

Fractal Properties and Psychological Constructs 7

Fractal Properties and Multiscale Interactions 9

Overview 11

EXPERIMENT 1 14

Method 15

Participants 15

Apparatus and Procedure 15

Control Condition 17

Movement Perturbation Condition 18

Respiratory Perturbation Condition 18

Analysis Strategy 19

Standard Deviation of Relative Phase (SDRP) 19

Data Preparation 19

Detecting Multiscale Interactions 20

Multiscale Coordination and Performance 24

Page

Results 25
Movement Frequency and Respiratory Rate 26
Movement Frequency and Postural Path Length 31
Movement Frequency and Heart Rate 33
Postural Path Length with Respiratory Rate 36
Postural Path Length with Heart Rate 38
Heart Rate on Respiratory Rate 40
Discussion 42
EXPERIMENT 2 47
Method 48
Participants 48
Apparatus and Procedure 48
Movement Perturbation 49
Go/No-Go Task 49
Analysis Strategy 50
Data Preparation 50
Multiscale Coordination and Performance 51
Results 52
Oz and Cz 56
Performance Results 56
Oz and F3 56
Performance Results 56

Page

F3 and Cz 57

Performance Results 57

Eye Movement Frequency and Heart Rate 58

Eye Movement Frequency and Neural Measurements 61

Discussion 64

GENERAL DISCUSSION 69

Treatment Effects on SDRP 69

Multiscale Interactions 70

Multiscale Interactions in Experiment 1 71

Multiscale Interactions in Experiment 2 75

Multiscale Interactions in Pursuit-Tracking Systems 77

Limitations and Future Directions 79

Multiscale Interactions in Psychological Systems 81

REFERENCES 83

APPENDIX

A MULTISCALE LAGGED REGRESSION 91

B LINEAR MIXED-EFFECTS MODELS FOR EXPERIMENT 1 111

LIST OF FIGURES

Figure Page

1. Time Estimation Series for One Participant from Wagenmakers et al., 2004 4

2. Depiction of the Onscreen Display used in Experiment I. 16

3. MLR Plots Depict (a) Movement Frequency Regressed on Current and Previous Value of Respiratory Rate and (b) Respiratory Rate Regressed on Current and Previous Values of Movement Frequency 27

4. MLR Plot Showing Movement Frequency Regressed on Current and Previous Values of Postural Path Length. (B) MLR Plot Showing Postural Path Length Regressed on Current and Previous Values of Movement Frequency 32

5. MLR Plot Showing Movement Frequency Regressed on Current and Previous Values of Heart Rate. (B) MLR Plot Showing Heart Rate Regressed on Current and Previous Values of Movement Frequency. 34

6. MLR Plot Showing Postural Path Length Regressed on Current and Previous Values of Respiratory Rate. (B) MLR Plot Showing Respiratory Rate Regressed on Current and Previous Values of Movement Frequency. 37

7. MLR Plot Showing Postural Path Length Regressed on Current and Previous Values of Heart Rate. (B) MLR Plot Showing Heart Rate Regressed on Current and Previous Values of Postural Path Length. 39

8. MLR Plot Showing Heart Rate Regressed on Current and Previous Values of Respiratory Rate. (B) MLR Plot Showing Respiratory Rate Regressed on Current and Previous Values of Rate. 41

Figure Page

9. Power Spectrum Average Lag-Wise *B* when Cz is Regressed on Oz with MLR. Note that Peak Power Occurs at a Frequency Very Near the Tracking Stimulus Frequency of 0.80 Hz. The Insert s the Series of Average Regression Coefficients on which the Power Spectrum was Based. 52

10. MLR Plots Depicting Bidirectional Relationships between Neural Measurement Sites in the Go/No-Go Condition. 53

11. MLR Plots Depicting Bidirectional Relationships between Neural Measurement Sites in the Movement Perturbation Condition. 55

12. MLR Plot Showing Heart Rate Regressed on Current and Previous Values of Eye Movement Frequency. (B) MLR Plot Showing Eye Movement Frequency Regressed on Current and Previous Values of Heart Rate. 59

13. (A, C, E) MLR Plot Showing Heart Rate Regressed on Current and Previous Values of Eye Movement Frequency. (B, D, F) MLR Plot Showing Eye Movement Frequency Regressed on Previous Values of Heart Rate. Each Row is a Different Participant. 61

14. MLR Plots Depicting Bidirectional Relationships between Eye Movement Frequency and Neural Measurement Sites in the Go/No-Go Condition. 63

15. MLR Plots Depicting Bidirectional Relationships between Eye Movement Frequency and Neural Measurement Sites during the Movement Perturbation Condition. 64

Multiscale Interactions in Psychological Systems

For over forty years now, researchers have found evidence that humans exhibit *fractal scaling* (e.g., Gilden, Thornton, & Mallon, 1995; Ihlen & Vereijken, 2010; Kello et al., 2010; Likens, Fine, Amazeen, & Amazeen, 2015; Van Orden, Holden, & Turvey, 2003; Voss & Clarke, 1975). Fractal scaling is a curious phenomenon found in the roughness of psychological time series, and was initially intriguing because roughness is a defining feature of many natural phenomena (e.g., coastlines and stock markets; Mandelbrot, 1982). Initial results in cognitive science (e.g., Gilden et al., 1995) were followed by a deluge of related experiments, claiming the presence of fractal scaling in virtually every aspect of human behavior ranging from tapping one's finger (e.g., Chen, Ding, & Kelso, 1997; Lemoine, Torre, & Delignieres, 2006) to recalling members of a category (Rhodes & Turvey, 2007; Szary, Dale, Kello, & Rhodes, 2015). The ubiquity of fractals prompted questions about meaning and significance. Those questions were first answered by physiologists who showed fractal scaling co-varied with health (e.g., Hausdorff et al., 1997; Ivanov, 2001) and later by psychologists who found that fractal scaling predicted performance in many psychological experiments (e.g., Stephen, Broncoddo, Magnusson, & Dixon, 2009; Stephen & Anastas, 2011). Whereas no single model of fractal scaling has reached paradigmatic status, the empirical evidence favors interpretations with two key components: self organization and coordination across numerous scales of analysis. To date, however, empirical evidence of *multiscale interactions* has remained indirect (e.g., Kelty-Stephen, Palatinus, Saltzman, & Dixon, 2013; Ihlen & Vereijken, 2010; Likens, Amazeen, Stevens, Galloway, & Gorman 2014). The primary purpose of this dissertation is to capture multiscale coordination directly.

However, multiscale interactions must be grounded in the other aspects of psychological behavior, and so, the secondary aim is to show that multiscale interaction is an inseparable part of intentional forms of behavior.

Fractals in Psychological Time Series

Fractal scaling is the starting point for theoretical arguments concerning multiscale interactions in psychological performance. In recent literature, researchers have treated fractal time series as the necessary and sufficient evidence to support the hypothesis that psychological performances are best conceived as emerging from nonlinear interactions across the multiple scales that make up even single acts (e.g., Davis, Brooks, & Dixon, 2016; Dixon, Holden, Mirman, & Stephen, 2012; Stephen, et al., 2012; Wijnants, 2014; c.f. Wagenmakers, Farrell, & Ratcliff, 2004; Wagenmakers, van der Maas, & Farrell, 2012). Given the gravity of that claim, it is important to answer the two following questions: (1) what does it mean for a psychological time series to be fractal; and (2) why do fractal time series carry such importance in theoretical discussions of psychological variability? There is no easy path from roughness in stock markets to roughness in reaction times, but the following sections provide a guided tour to the development of theories about fractal scaling in psychology. The tour involves some necessary stops outside the psychological literature, but eventually arrives at the conclusion that fractal scaling in human behavior implies multiscale interactions.

What it Means to be Fractal

The term fractal was coined by Mandelbrot (1967; 1975) to describe natural patterns that cannot be accurately described using Euclidean forms such as circles and squares. Euclidean surfaces and solids fail to describe the rich variability inherent in

nature because, as Mandelbrot (1967; 1975; 1982) noted, nature is rough and irregular. The terms *rough* and *irregular* are also appropriate for observations of psychological performance. Figure 1 (a) is a time series obtained when a participant repeatedly estimated the passing of one second and depicts the roughness typical in psychological time series (Wagenmakers et al., 2004). The time estimation series in Figure 1 (a) also has other important fractal properties – self-similarity and scale-invariance. Those properties can be casually observed by focusing on a reduced number of observations relative to the entire time series observations (i.e., reducing scale size), as shown in subplots of Figure 1 (a). Self-similarity is evident in the fact that the structure of a smaller number of observations resembles the structure of the full series. Scale-invariance follows because, if the variability in a time series is invariant to changes in scale size, then no scale acts as the privileged scale of analysis.

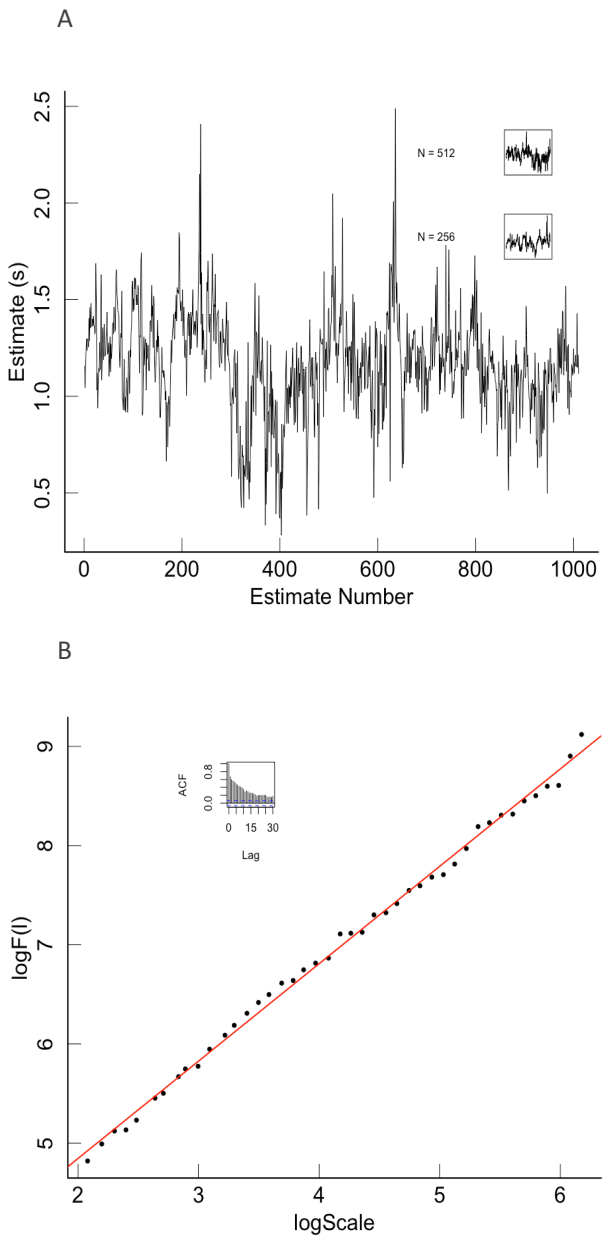

Figure 1. (a) Time estimation series for one participant from Wagenmakers et al., 2004. The subplots show the self-similarity when the time series is halved and quartered. (b) Detrended fluctuation analysis (see Appendix A) of the time series in (a). The subplot in (b) is the autocorrelation function for the time series in (a).

Fortunately, researchers do not have to rely on qualitative judgments like those just given. Like other natural phenomena of interest to Mandelbrot (1982), the roughness in psychological time series is quantifiable (see Eke, Hermann, Kocsis, & Kozak, 2002; Beran, 1994 for general introductions to fractal analysis). Figure 1 (b) demonstrates the quantification of the roughness in psychological time series as a form of self-similar scale invariance. Figure 1 (b) is the output of a procedure called detrended fluctuation analysis (DFA). The procedure is described fully in the Appendix A, but for now, the important point to make is that the ordinate represents a measure of variability and the abscissa is scale size. The linear trend implies that variability in time estimation is invariant over transformation of scale and the slope of that trend ($H_{DFA} = 0.98$, $R^2 = 0.996$) is the *Hurst* exponent, H, a measure of self-similarity. In general, H is defined on the interval (0,1) where $H = 0.50$ indicates a random, white noise process. Values of H on the interval (0.50, 1.0) indicate fractal scaling where the time series exhibits self-similarity in variability but also a slowly decaying, positive autocorrelation function [subplot of Figure 1 (b)]. Values of H on the interval (0, 0.50) imply rapidly decaying, negative autocorrelations. Evaluating H_{DFA} against those criteria reveals the fractal nature implied by the structure in Figure 1 (a). Furthermore, that observation – that time estimation series have fractal properties – provides an answer to question one from above: Psychological time series are fractal when they exhibit an irregular form of roughness characterized by self-similar scale-invariance. The following sections elaborate an answer to question two.

The Significance of Fractals in Psychological Time Series

Meaning from Ubiquity. One reason fractal properties seem important for psychological theorizing is the seeming ubiquity with which they are observed (e.g., Kello, Anderson, Holden, & Van Orden, 2008). In addition to time estimation, fractals arise in psychological time series time series when participants react to both simple and complex stimuli (e.g., Aks, Zelinsky, & Sprott, 2002; Gilden, Thornton, & Mallon, 1995; Van Orden, Holden, & Turvey, 2003); search for hidden objects (e.g., Stephen & Anastas, 2011; Stephen & Mirman, 2010); learn rules and solve problems (Stephen, Boncoddo, Magnuson, & Dixon, 2009; Anastas, Stephen, & Dixon, 2011; Stephen, Anastas, & Dixon, 2012); or even when people perform complicated tasks like making jewelry (e.g., Nonaka & Bril, 2014) or steering a vehicle (Likens, Fine, Amazeen, and Amazeen, 2015). Moreover, self-similar structure appears in a host of physiological outcome variables such as the time difference between successive heart beats (e.g., Peng et al., 1995; Ivanov, 2001), the time between successive breaths (e.g., Peng et al., 2002; West, Griffin, Frederick, & Moon, 2005), and the length of strides while walking (Hausdorff et al., 1996; Hausdorff et al., 2001). Fractal properties are so common in individual performances and processes that some researchers called them pervasive and ubiquitous (e.g., Kello, Anderson, Holden, & Van Orden, 2008; Likens et al., 2015; Van Orden, Holden, & Turvey, 2003). Taken alone, those findings might give the impression that fractal scaling is a purely individual level phenomenon, but fractal properties have also been observed in a number of social contexts where people coordinate their bodies in both rhythmic and non-rhythmic ways (e.g., Coey, Washburn, Hasselbrock, & Richardson, 2016; Davis, Brooks, & Dixon, 2016; Demos, Chaffin, & Kant, 2014; Fine,

Likens, Amazeen, & Amazeen, 2015; Likens, Amazeen, Stevens, Galloway, & Gorman, 2014; Marmelat & Delignieres, 2012). The implication is that fractal properties emerge within the superordinate structure of coordinated action, whether or not the action involves one more people. Fractal properties do appear pervasive (Kello et al., 2008).

The many findings reported in this section are by no means exhaustive but offer a reasonable glimpse into breadth of studies implicating fractal scaling as "The Provenance of Correlations in Psychological Data" (Thornton & Gilden, 2005). The seeming ubiquity of fractal results implies that fractal properties are psychological properties; however, that statement is somewhat unproductive. Clearly, documenting a phenomenon is a vital step in establishing that phenomenon as psychological behavior worthy of study, but continued interest requires making contact with other psychologically meaningful variables (Likens et al., 2015).

Fractal properties and psychological constructs. The fact that fractal properties appear so often in psychological time series leads to deeper questions concerning their meaning and significance. The preceding section gave many examples of fractal scaling involving both individuals and groups, but, as presented, those findings are just facts. What relevance do fractal properties hold for constructs that are of interest to psychologists? The vast literature on fractal scaling has offered several tentative answers.

One case for relevance originates physiological literature, where it is well established that the degree of fractal scaling is associated with health. Earliest observations of that relationship were made concerning the cardiac behavior (Peng et al., 2001; Ivanov et al., 2001). Specifically, the literature has noted two important results: (1)

heat rate time series that exhibit fractal properties are indicative of health, and (2) when the observed physiological process is, on average, fractal, the variability around that average provides further diagnostic advantage. More, but still fractal, variability is associated with a healthier heart (e.g., Ivanov et al., 2001), but cardiac activity is not the only physiological process that exhibits fractal behavior in its healthy state. Healthy breathing rates also tend to be fractal (e.g., Peng et al., 2002), as do postural sway (e.g., Collins & DeLuca, 1995) and neural patterns (Voytek et al., 2015). From these examples, one can infer that the fractal properties are relevant to the physiological domain because they characterize the health of the physiological system in question. The fact that fractal properties distinguish so many instances of physical health leads one to wonder whether fractal analysis of behavioral time series might yield similar benefits.

There is now considerable evidence that fractality is an important psychological property, not only because of its ubiquity, but because self-similarity is an important predictor of other performance data. Fractal variability seems to help people make sense of the vast stimulus array. Fractal movements while wielding an object improves perception of that object's kinematic properties (e.g., Stephen, Arzamarksi, & Michaels, 2010; Stephen & Hajnal, 2011; Turvey & Carello, 2011). Searching arrays in a fractal manner increases the speed with which people find objects (e.g., Stephen & Anastas, 2011). Fractal fluctuations in posture reflect subtle changes in perceptual intent (e.g., Kelty-Stephen & Dixon, 2014; Palatinus, Kelty-Stephen, Kinsella-Shaw, Carello, & Turvey, 2014). Fractality has also been used as an important index of short- and long-term learning: Increases in fractality are associated with development of insight in novel problem solving (e.g., Stephen, Broncoddo, Magnusson, & Dixon, 2009), and fractal

scaling has categorically distinguished more than one form of expertise (e.g., Nonaka & Bril, 2014; Nouritt-Lucas, Tossa, Zelic, & Delignieres, 2015). As hinted earlier, fractal properties also appear to be important for coordinating with other people (e.g., Fine et al., 2014; Marmelat & Delignieres, 2012). Suffice to say, fractal properties are important aspects of human behavior, but despite the many associations among fractal properties, health, perceiving, acting, and learning, a question looms large: why should it be that any of these processes exhibit such a peculiar form of behavior in the first place?

Fractal properties and multiscale interactions. So far, the discussion has given many examples that illustrate the ubiquity of fractal scaling in psychological time series as well as many of the documented relationships between fractal scaling and other meaningful aspects of behavior. Those examples, more or less, represent the state of art concerning the significance of fractal scaling in the study of human behavior. Genuinely understanding the significance of fractals in psychology requires pushing below those surface level descriptions, and below the surface is the development and test of hypotheses that explain the origin of roughness in psychological time series. In the best of worlds, those hypotheses would lead to domain-general knowledge regarding psychological function.

To date, the literature has offered and debated several possible explanations of fractal scaling in psychological time series (e.g., Diniz et al., 2010; Gilden, 2001; Thornton & Gilden, 2005; Ihlen & Vereijken, 2010; Kello et al., 2010; Torre & Wagenmakers, 2009; Van Orden et al., 2003; Wagenmakers et al., 2004). First, the so-called multiscale randomness hypothesis suggests that fractal scaling is nothing more than the superposition of many unrelated sources of noise, captured at the point of

measurement (e.g., Gardner, 1978; Hausdorff & Peng, 1996; Wagenmakers et al., 2004). Second, the shifting strategy (aka regime-switching) model suggests that fractal variation in psychological processes is an artifact of nonstationarity in the data. The nonstationarity stems from changes in the mean that in turn reflect temporal variation in strategy. The example given in Wagenmakers et al. (2004) is of a participant estimating time intervals – changes in the mean occur when the person switches between imagining a clock and simply counting digits.

Third, the two-component hypothesis proposes that noise measured in cognitive experiments has two sources (Gilden, 2001; Thornton & Gilden, 2005). One is a cognitive source of fractal scaling that emerges from dynamical interactions of cognitive processes. Examples processes include time-keepers and memory structure. The other source is a white noise component that reflects the contamination of cognitive emissions of fractal scaling by motor noise involved in generating observable behavior. The latter of the two sources became necessary to account for flat high frequency regions often observed in the power spectra of response time series (see Holden, Choi, Amazeen, & Van Orden, 2011, for an alternative explanation). Fourth, the dynamical systems (aka interaction-dominant) hypothesis suggests that fractal scaling emerges from complex interactions among components that make up a psychological system (Ihlen & Vereijken, 2010; Van Orden et al., 2003: Wijnants, 2014). The hypothesis further implies that control of behavior is distributed among the system's components, a form of control that emerges from coordination across many different time scales, ranging from the rapid time scales of neural oscillations to the relatively slow time scales of the experiment and beyond. Champions of those – and other – approaches have argued their case for two

decades now and articulated the strengths and weaknesses in generous detail. Those arguments will not be recapitulated here (c.f. Van Orden et al., 2003; Van Orden & Stephen, 2012; Wagenmakers et al., 2004; Wagenmakers et al., 2012). Rather, the current work focuses on what has long been a major weakness in the dynamical systems approach – demonstration of the multiscale interactions that is essential to its future theoretical success.

A cornerstone of the dynamical systems hypothesis is the idea that fractal properties self-organize from coordination among the many spatial and temporal scales that compose psychological systems (Davis et al., 2016; Ihlen & Vereijken, 2010; Ihlen & Vereijken, 2013a; Ihlen & Vereijken, 2013b; Kelty-Stephen et al., 2013; Likens et al., 2014; Likens et al., 2016; Stephen, Anastas, & Dixon, 2012; Wijnants, Cox, Hasselman, Bosman, & Van Orden, 2012; Wijnants, 2014). The principal evidence in support of that hypothesis comes from the dozens of studies reported so far concerning fractal scaling in psychological time series. However, fractal findings, while necessary, are not sufficient to substantiate claims concerning multiscale interactions, despite claims to the contrary (Van Orden et al., 2003).

Overview

The primary purpose of this dissertation is to document direct evidence of multiscale interactions among many of the components that make up a psychological act. For over a decade, researchers have claimed multiscale interactions are the source of fractal properties in psychological time series but have yet to demonstrate those interactions directly. Thus, satisfying that purpose fills a large gap in the literature. Furthermore, it has been proposed that fractal properties represent the distributed form of

control inherent in complex, dynamical systems (Van Orden et al., 2003; 2005; Wijants, 2014). If that is true, and if coordination across scales can be quantified, then the degree of coordination across scales should predict psychological performances.

In two experiments, participants performed simple pursuit-tracking tasks while multiple behavioral and physiological measurements were recorded. The general task involved participants coordinating their limbs with oscillatory stimuli (Strayer & Johnson, 2001). Experiment 1 probed how multiscale coordination among motor, respiratory, and cardiac systems predicts one's ability to track and coordinate with oscillatory stimuli. Experiment 2 further explored how multiscale interactions among brain regions, eye-movements, and cardiac activity combine to generate performances in task context similar to Experiment 1.

The tracking task was chosen based on several considerations. First, the task was continuous so that behavior among many interacting systems could be time aligned. Second, the task was simple so that dynamics revealed as multiscale interactions could be cast within the context of an easy-to-understand performance variable. Simplicity in task also permits generalization to more complicated situations. Third, the task was commonly used in the literature to avoid concern that results regarding multiscale interactions might stem from some specialized task.

The task of characterizing the coordination among those different systems at many time scales is no small feat. Although many methods exist for analyzing time series under assumptions of linearity (e.g., Hill, Griffiths, & Lim, 2011) and nonlinearity (e.g., Riley & Van Orden, 2005), very few methods exist that characterize the co-evolution of a system's components. Notable exceptions are those developed in the

economics (e.g., Vector Error Correction Modeling; Hill et al., 2011) and dynamical systems (e.g., joint recurrence quantification analysis, Webber & Marwan, 2015) literature. However, the development of this project made clear the inadequacy of existing methods in capturing multiscale relationships; autoregressive, distributed lag models captured serial dependence but not multiscale relationships. Thus, the current work introduces a new quantitative method capable of unraveling coordination across many temporal scales. The method is introduced in Appendix A along with a number of simulations that showcase the potential of the tool.

Experiment 1

Participants performed a pursuit-tracking experiment in three conditions: one control condition and two experimental conditions that involved a manipulation of movement frequency or respiratory rate as a perturbation within the trial. The aim of the experiment was to demonstrate multiscale interactions, but also to examine how multiscale interactions relate to performance. In pursuit-tracking tasks, the usual variables of interest are limited to the tracking signal and the tracked movement of the participant. That is, researchers derive performance metrics based on the correspondence between the target tracking signal and participant behavior. Several measurements of performance could be used for the purpose of assessment (e.g., root mean square error, Strayer & Johnston, 2001; absolute integrated error, Pew, 1974); however, the oscillatory nature of the task suggests this work may benefit from the work that has been conducted on oscillatory dynamics in motor control. Relative phase measures, standard deviation of relative phase (SDRP), have been and continue to be used extensively to measure stability of coordination (e.g., Amazeen, Amazeen, & Turvey, 1998; Haken, Kelso, & Bunz, 1985; Kelso, 1984; Kelso, 1995; Lamb & Stöckl, 2014). Thus, SDRP measures should be well suited to the task of characterizing performance in a pursuit-tracking. The expectation was that SDRP would be higher during the perturbation than during the non-perturbation periods.

To explore multiscale interactions, several additional measures were recorded while participants performed the pursuit-tracking task. Those measures included several physiological measures (e.g., respiratory rate and heart rate) and postural sway. Multiscale lagged regression (MLR), the new analytic technique introduced in Appendix

A of this manuscript, was applied pairwise to those measurements during three task segments corresponding to the pre-, during-, and the post-perturbation periods. The general expectation is that MLR will uncover meaningful patterns that predict pursuit-tracking performance. Specific patterns that will be revealed are unknown due to the novelty of this technique, but correspondences can be understood from the simulations in Appendix A.

Method

Participants

Twenty participants (Male = 14, M_{Age} = 21.85, SD_{Age} = 3.94) from Arizona State University volunteered to participate in this study. Participants were all non-smokers and reported no injuries to limbs or trunk and no known cardiopulmonary disease. All participants reported normal or corrected to normal vision and 18 were right-handed by self-report. Data from three participants were excluded from further analysis because of equipment failures not detected until after data collection was complete. Data from two participants were excluded because participants failed to comply with task instructions.

Apparatus and Procedure

Experiment 1 involved a pursuit-tracking task similar to that found in Strayer and Johnston (2001). The task required participants to coordinate their movements, depicted as an oscillating circle on a computer screen, with the movements of another circle controlled by a computer program (see Figure 2a, c).

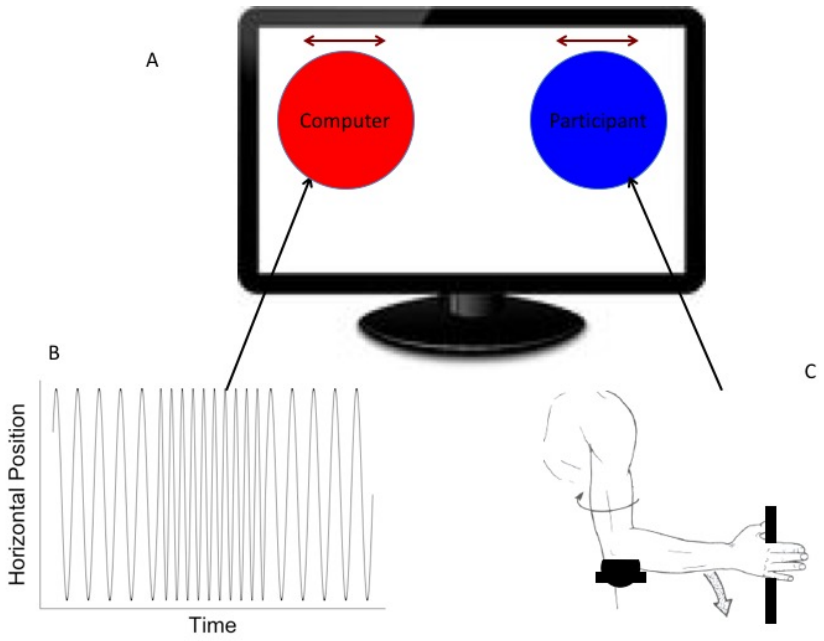

Figure 2. Depiction of the onscreen display used in Experiment 1. (a) Participants coordinated with movements of a circle on a display during Experiment 1. (b) A time series representation of the path involved during the Motion Path Perturbation condition. (c) Participant motion during all conditions of the experiment.

Participants were asked to maintain a 0° phase relationship between the circle they controlled and the computer-controlled circle. Perfect performance meant that red and blue circles in Figure 2a completely overlapped at each moment in time. The path of both the computer- and participant-controlled circles was constrained to the horizontal plane. The path of the participant-controlled circle was mapped to the lateral position of the participant's hand as measured by an Optotrak 3020 camera system. Participants were instructed to control the position of the circle by using external and internal rotation

about the elbow to move a motion-tracked manipulandum (e.g., Figure 2c). Participants were instructed to rest their arm such that the forearm was parallel with the floor. Electromyogram activity corresponding to the external rotation was measured from the infraspinatus fossa located just below the spine of the scapula. Unfortunately, participants failed to keep elbows planted in the fixed position required by the experiment, resulting in unreliable EMG data that was not analyzed further. Postural sway was captured by measuring movement from a marker placed on seventh cervical vertebrae. Respiratory flow was measured using a pneumotachometer (Hans Rudolph, Inc., Kansas City, MO), and electrocardiogram activity was recorded using a Lead III electrocardiogram from a BIOPAC MP150 (Goleta, CA). Those various data sources were synchronized at the hardware level within the Optotrak Data Acquisition Unit. All data were sampled at 500 Hz to accommodate muscular activity up to 250 Hz.

The task was performed under three perturbation conditions, discussed in the next sections. Prior to performing any of the conditions, participants were given a practice trial where they practiced coordinating with the moving circle for seven minutes. During the practice trial, the circle oscillated at 1.0 Hz with the peak to peak lateral distance of about 25 cm (about 14° of visual arc). The duration of the practice trial was chosen for consistency with Strayer and Johnson (2001).

Control condition. In the control condition, participants were instructed to simply match the lateral movement of the oscillating stimulus (i.e., a red circle). The lateral position of the computer-controlled circle was updated once every 33 ms from a 1 Hz sine wave. The trial lasted 15 minutes. Trial length was also chosen for consistency with Strayer & Johnston (2001).

Movement perturbation condition. The path of the computer-controlled circle was generated by a pre-determined sinusoidal function that varied in (1 – 1.5 Hz) over time (Figure 2b). Specifically, the circle moved at 1 Hz for the first five minutes of the experiment; it moved at 1.5 Hz for the second five minutes of the experiment; and it returned to a 1 Hz oscillation for the final five minutes of the experiment. Thus, the trial lasted 15 minutes overall with 5 minute pre-, during-, and post-stimulus periods.

Respiratory perturbation condition. This condition also involved a 15 minute trial with pre-, during-, and post-perturbation intervals. This condition was visually identical to the control condition. Before beginning the trial, participants were told that, at some point during the trial, they would receive a verbal signal to slow their breathing. The specific instruction was that they should notice their current rate of breathing before choosing and performing a slower respiratory rate. Interpretation was left to the participants. Participants were told that they should do their best to return to their original respiratory rate after receiving a second verbal signal. During the trial, the researcher gave the verbal instruction at 5 minutes into the trial, and gave the second verbal instructions 10 minutes into trial. Those intervals were chosen for consistency with the movement perturbation condition. Inspection of respiratory time series showed interpretation of those instructions varied considerably among participants. For example, some participants took deeper breaths without changing the frequency of their breaths. Some participants slowed their breathing for a few cycles but then returned to what was presumably their preferred respiratory frequency. Hence, we were not optimistic about outcomes involving the respiratory perturbation.

Analysis Strategy

Standard deviation of relative phase (SDRP). Standard deviation of relative phase (SDRP) was used as an index of variability around the target frequency. To calculate SDRP, relative phase was calculated as the difference in phase between the target tracking signal and participant movements at each sampled moment (Kelso, 1984). The result was a relative phase time series – SDRP was calculated as the sample standard deviation over the entirety of the time series.

Data preparation. Physiological data streams are rarely, if ever, analyzed in raw data form because those signals tend to very noisy and some form of processing is necessary to extract meaningful information. For example, heart rate and respiratory rate are much more common and more easily understood than raw ECG or flow signals. However, most summary measures discard details that might be informative for our purposes. Therefore, I computed instantaneous frequency for ECG and respiratory flow data using the method outlined in Barros and Ohnishi (2001). Instantaneous frequency of lateral arm movements was computed by Hilbert transform (e.g., Gabor, 1946; Lamb & Stöckl, 2014; Lamoth, Daffertshofer, Huys, & Beek, 2009). Postural path length – the 3D Euclidean distance between successive samples –was calculated as a measure of postural sway (e.g., Gibbons, Amazeen, & Likens, under review; Kerby, Price, & MacLeod, 1987; Rugelj, Tomsic, & Sevsek, 2013). Instantaneous frequency was not computed for postural path length because postural corrections are known to have more than one characteristic time scale (e.g., Collins & DeLuca, 1995).

Detecting multiscale interactions. The current work introduces a new analytical technique called *multiscale lagged regression* (MLR) as a means of capturing multiscale interactions among psychophysiological time series. In this section, I present the MLR algorithm with limited theoretical discussion. That presentation is repeated in the Appendix A with a more detailed theoretical discussion as well as a number of simulations.

Variability in psychological performance is thought to emerge from the multiscale interactions among the many components that make up a psychological system (e.g. Van Orden et al., 2003). The litany of positive results from fractal analysis support that claim, but fractal techniques provide very little information concerning the nature of those interactions. Standard regression, while capturing the monoscale relationship between two series, ignores the multiscale structure inherent in psychological time series. What is needed is an analytical method that can elucidate the time-varying relationships among psychological processes, relationships that may be likewise depend upon the many temporal scales that make up behavior. The following paragraphs propose just such a method.

Recently, Kristoufek (2013; 2015) observed that detrended cross correlation analysis (DCCA; Podobnik & Stanley, 2008) – the bivariate extension of DFA – could be leveraged to develop a multiscale form of regression (see Appendix A for explanation of DFA). The main difference between DFA and DCCA is that DCCA is concerned with the combined fluctuation function, $F_{XY}^2(s)$, between two time series, X_t and Y_t (Podobnik & Stanley, 2008). That is, DCCA performs steps (1) - (3) of the DFA procedure found in Appendix A independently for each time series; however, instead of computing the scale-

wise variance, $F_X^2(s)$, for each variable in step (4), the scale-wise covariance, $F_{XY}^2(s)$, is computed by taking the cross-product of the scale-wise detrended series and averaging at each scale *s*. If the joint fractal properties are of interest to the researcher, then she can examine the linear relationship between the logarithm of $F_{XY}^2(s)$ and the logarithm of *s*.

The resulting slope reflects the average scaling exponent, $\bar{\alpha}_{XY}$, for X_t and Y_t, where $\bar{\alpha}_{XY} = (\alpha_X + \alpha_Y)/2$. However, the current interest is in characterizing how the relationship between X_t and Y_t changes as a function scale and time, not whether the processes have similar scaling properties. Referring to Equation (2) in Appendix A, one can appreciate that the regression coefficient, $\hat{\beta}_1$, is nothing more than the ratio between the covariance of *X* and *Y* and the variance of *X* (Kristoufek, 2015). Thus, the components of the standard regression coefficient are similar to estimates of variance, $F_X^2(s)$, and covariance, $F_{XY}^2(s)$, generated by the DFA and DCCA procedures. Kristoufek (2015) went on to show that scale-wise variance and covariance measures could be used to construct scale-wise regression coefficients,

$$\hat{\beta}_1(s) = F_{XY}^2(s)/F_X^2(s) \quad (1).$$

The current work extends the idea of scale-wise regression coefficient by exploring how the relationships estimated in Equation (1) change as a function of time-lag. Extending the DFA-based regression in this way may help to answer questions concerning how changes in one variable at one time scale might be predicted by changes in another variable at a similar time scale, both contemporaneously and in the past. The outlined steps that follow this paragraph represent the new MLR algorithm. Steps 1 – 6

correspond to earlier work developing fractal analysis and DFA based regression. In step 7, the introduction of time lags, reflects my contribution to the DFA-based regression framework:

1. Normalize each of two time series, X_t and Y_t, to have zero mean and unit variance.
2. Separate each time series into N/s bins of length s.
3. Within each bin, for each time series and several s, estimate the best fitting line and subtract that line from the binned time series. This step requires some justification. In the original DFA algorithm and in many other forms of fractal analysis (Eke et al., 2010), the interest is in analyzing the intrinsic fluctuations of a system, the ebb and the flow. The detrending procedure was introduced in fractal analysis by Peng and colleagues (1994) to address situations where nonstationarities such as a drift and singularities (e.g., sharp peaks or step-like jumps in time series) might bias estimates of scaling behavior by overestimation of long range correlations. However, detrending data before analysis by regressive techniques has long been a recommendation in time series analysis where it has been shown that spurious trends lead to gross overestimation of temporal relationships between variables (Granger & Newbold, 1974).
4. Compute the residuals variances for X and Y as well as residual covariance between the binned series.
5. Compute the average covariance eat each scale, s.
6. For each scale, compute the scale-wise regression coefficient as $\hat{\beta}_1(s,l) = F_{XY}^2(s,l)/F_X^2(s,l)$, where l is lag of X. When l is zero, the procedure in Kristoufek (2015) is recovered.

7. Repeat Steps 1 through 6 for several scales and several lags to obtain an $s \times l$ matrix, B, that contains the regression coefficients for each scale and lag combination. The resulting rows of B give the temporal evolution of relationship between X_t and Y_t.

Those seven steps, encapsulating the MLR procedure, were applied to all possible pairs of the data sources described in the Data Preparation section. MLR was computed over scales ranging from 0.20 s to 32.00 s in increments of 0.20 s and lags ranging from 0.02 s to 32.00 seconds in increments of 0.02 s. For each process pair, MLR was conducted in two directions (e.g., respiratory rate was regressed on past values of heat rate and heart rate was regressed on past values of respiratory rate) to capture possible directional dependencies. The output of the MLR procedure is a matrix, B, of scaled and lagged regression coefficients, $\beta_1(s, l)$. Once B was calculated for each process pair (e.g., movement frequency and postural path; movement frequency and respiratory rate, etc.), a method was needed to summarize results for comparison with SDRP.

There are potentially many ways of summarizing the contents of B, but the results reported here explore only one, involving the Fast Fourier Transform (FFT). The proposed method begins by averaging across rows in B to yield the typical regression coefficients at each time lag. Then, an FFT is applied to the time series of average lags. The underlying mathematics of the FFT suggest that any curve can be approximated by a linear combination (i.e., addition) of sinusoids, or equivalently, complex exponentials (Cochran et al., 1967). That means application of the Fourier Transform to the lag-wise average regression coefficient series should reveal characteristics of the ensemble of scaled and

lagged relationships. In general, the power spectra have strong peaks over a small range of frequencies. For that reason, total power was used as a metric of multiscale coordination, reasoning that if power is clustered within a small frequency band, then total power should generally reflect frequency content observed at multiple temporal scales and thus represent a basic measure of multiscale interaction. Those steps were followed for each process pair, within each condition, and within each task segment (i.e., pre-, during-, and post-perturbation).

Multiscale coordination and performance. The repeated measures nature of the design, along with the mixture of continuous (total power) and categorical (segment and condition) independent variables suggests that ordinary least squares regression and ANOVA will not be sufficient for examining changes in SDRP. Instead, those comparisons were made with linear mixed-effect regression models (Snijders & Bosker, 2011). In each case, model construction followed a similar logic. First, a baseline model was fit with fixed participant effects on the intercept term. Second, power was entered into the model and compared with the baseline model via χ^2 test for improvement in explaining SDRP over and above individual differences in SDRP – the same testing procedure was applied to subsequent models. Total power was chosen as the first predictor variable to enter the model because it is the primary predictor of interest and because this work is exploratory. The latter reason is relevant because there is good reason to suspect that experimental manipulations may strongly predict changes in *SDRP*; however, the effect of total power as derived from *B*s is

entirely unknown. For that reason, I chose to give total power the best chance possible to predict performance. Because it is the theoretical predictor of interest, total power was retained in each modeling step even it was not significant when compared to baseline, as total power could be implicated in higher order interaction terms. Third, time (pre, during, post) was entered and model fit will be assessed to determine if task segment predicts SDRP over and above power. The fourth model added the condition fixed effects on the intercept and the fifth model included fixed effects of condition on time and power slopes. For each process pair, only the final model is discussed. Tables presented in Appendix B identify the output of each model.

Results

The following six sections present pairwise comparisons generated from MLR, along with results from linear mixed-effects models. Each section will consist of two parts: First, graphical depictions of representative *B* matrices will be shown and described. Data from a single, representative participant was used for all graphical depictions. Where those plots deviate from random noise (Figure A4), there is reason to conclude that psychological systems exhibit multiscale interactions. Second, the relationship between a performance measure (SDRP) and total power is assessed along with experimental treatment effects. Those relationships between total power and SDRP were explored across all participants in a linear mixed-effect model. Where total power predicts performance, there is reason to conclude that multiscale interactions play a significant role in the manifestation of psychological behavior.

Movement Frequency and Respiratory Rate

MLR was used to regress current values of movement frequency on current and previous values of respiratory rate at multiple time scales. Presentation of these results is rather involved; however, general tendencies are revealed in this analysis that make reporting on subsequent process pairs less tedious. Figure 3 (a) depicts the scaled and lagged relationship between movement frequency and respiratory rate. Graph colors represent the magnitude of $\beta_1(s,l)$ at each scale and lag, with a color scale range from -1.0 (blue) to 1.0 (red) allowing for comparisons of directionality [e.g., note the obvious difference in color variation between Figure 3 (a) and Figure 3 (b). Values outside the color range are depicted in white. The MLR plots for the remaining process pairs all share these plot characteristics.

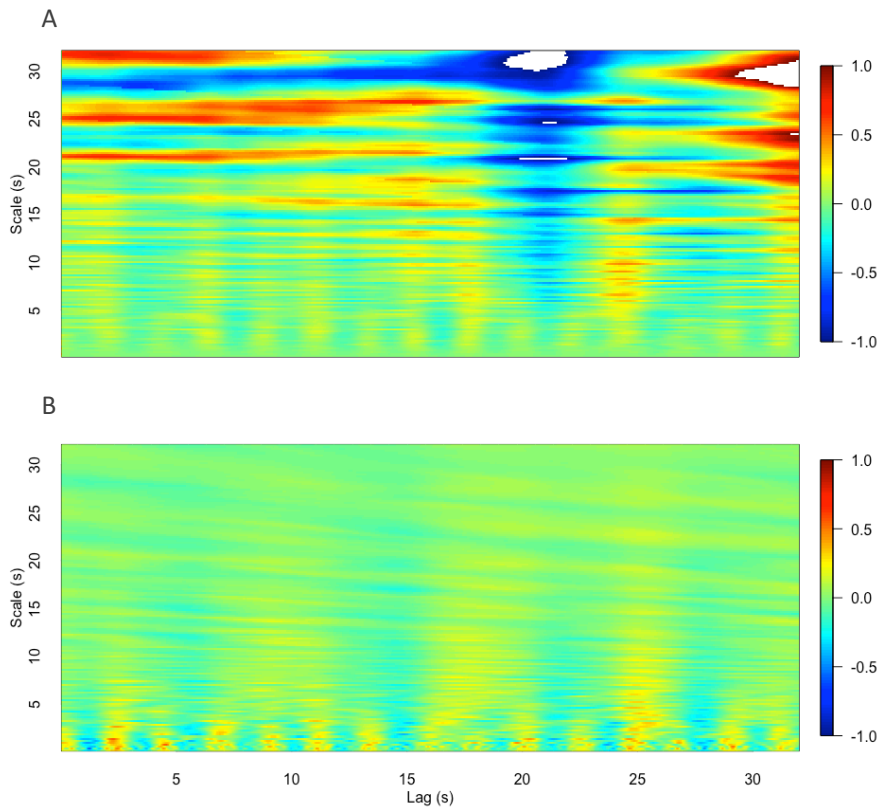

Figure 3 (a). MLR plot depicts movement frequency regressed on current and previous values of respiratory rate and (b) MLR plot showing respiratory rate regressed on current and previous values of movement frequency.

Figure 3 (a) shows that that $\beta_1(s,l)$ seems to increase from small to large scales as can be seen from the large patches of red at scales ranging from ~ 15 to 30 s. In addition, the graph gives the impression of oscillations at both small and large scales, albeit with different frequencies. At the smallest scales (~ 1 - 2 s), there does not appear to be any evidence of oscillation; most $\beta_1(s,l)$ are near zero. However, those weak relationships become a semiregular pattern of oscillation at

scales in the range of 2-5 s. Strong, slower ripples across successive lags appear at the largest scales, implying that the relationship between movement frequency and respiratory rate does indeed depend on scale.

Examination of Figure 3 (b) depicts the MLR relationships obtained by regressing current values of respiratory rate on current and previous values of movement frequency. Comparison with Figure 3 (a) reveals that prediction of changes in respiratory rate from movement frequency are much weaker than predictions of movement frequency from respiratory rate and only appear at smallest time scales (< 5 s). In fact, this plot basically shows the opposite relationship to Figure 3 (a) – the trend is that regression coefficients decrease rapidly over the scale.

To summarize the MLR results, it appears that motor-respiratory coordination takes place across many time scales. Coordination seems to be oscillatory in nature, especially at time scales larger than the time scale of the task. At large time scales, respiratory rate is a much better predictor of movement frequency than vice versa. The motor-respiratory relationship is subtler at small scales but there does appear to be at least some predictive advantage for movement frequency over respiratory rate at finer scales, suggesting an asymmetry in multiscale motor-respiratory coordination.

MLR has revealed the multiscale nature of the motor-respiratory coordination, but the task remains to explore how that relationship might predict performance in the pursuit-tracking task, across all participants in the study. The MLR coefficients in Figure 3 were averaged at each lag before serving as input to

an FFT. Next, the total power in the FFT was computed as a coarse measure of the multiscale coordination present in each instance of MLR (movement on respiration and vice versa).

Two linear mixed-effects models were then estimated, one for each possible direction of dependence with random participant effects on the intercept. The results regarding prediction of respiratory rate from movement frequency are considered first. In the final model, there was a main effect of total power, *Estimate* = -10.53, *CI* = (-20.25, -0.53), $p < 0.05$. There was also a main effect of time, such that *SDRP* was higher post-perturbation than pre-perturbation, *Estimate* = 0.13, *CI* = (0.03,0.23), $p < 0.05$. There was also an interaction effect between time and condition such that SDRP was higher with a movement perturbation than without a perturbation, *Estimate* = 0.35, *CI* = (0.27, 0.48), $p < 0.05$. Lastly, there was condition × total power interaction such that, during the movement perturbation, there was a positive relationship between total power and SDRP but a negative relationship between power and SDRP without a perturbation, $t(109.53) = 2.76$, $p < 0.05$.

Regarding MLR of movement frequency on respiratory rate, there was a main effect of total power, *Estimate* = 2.00, *CI* = (1.25, 2.75), $p < 0.05$. There was also main effect of condition, such that SDRP was higher for the movement perturbation condition than for the control condition, *Estimate* = 0.15, *CI* = (0.02, 0.29), $p < 0.05$. The main effect of condition was modified by an interaction with time such that, when compared to the control condition, the movement condition showed higher SDRP during the movement perturbation, *Estimate* = 0.33, *CI* =

0.19 – 0.46, $p < 0.05$. Lastly, there was a condition × total power interaction, owing to the fact that during the movement perturbation, there was positive relationship between total power and SDRP in the control condition but a negative relationship in the movement perturbation condition, $t(112.23) = 3.17$, $p < 0.05$. These results, and many that follow, are exciting in that they demonstrate a statistical relationship between multiscale interactions, as measured by MLR, and performance in a psychological task.

Many features observed in the Figure 3 recur in coming sections involving other process pairs, and many results involving SDRP and treatment effects will repeat as well. To avoid monotony, repetitive descriptions will be eschewed in favor of pointing out features and effects that seem unique to a process pair or particularly interesting. That goal advances by forecasting the coming results with some general trends:

(1) SDRP tends to increase during the movement perturbation but not during the breathing perturbation; (2) there is some evidence of a time-based trend in SDRP, even after controlling for perturbations; (3) most process pairs exhibit oscillation in their relationships that unfold over time and scale; (4) most process pairs exhibit directional effects such that one process is a much stronger predictor than the other; and (5) most process pairs exhibit scale-dependence where if $\beta_1(s,l)$ is large at large scales, it tends to decrease at smaller scales; large $\beta_1(s,l)$ at small scales tend to decrease at smaller scales.

Movement Frequency and Postural Path Length

Figure 4 (a) shows the result for MLR of movement frequency on postural path length. MLR coefficients increase across scale, similar to Figure 3 (a) but there is also faint evidence of oscillation at small scales. In Figure 4 (b), the MLR of postural path length on movement frequency shows strong oscillations at small temporal scales. In both Figure 4 (a) and Figure 4 (b), oscillations at small scales correspond to the frequency of the tracking stimulus. These results imply that changes in posture are not strong predictors of movement frequency at small time scales but may predict movement frequency at large time scales. That makes sense as a gross change in posture could determine the actual muscles involved in a movement, thereby altering kinematics over large time scales (Andersson et al., 1975). Conversely, it appears the rapid arm movements do predict changes in the postural sway, in a regular way consistent with the requirements of the task.

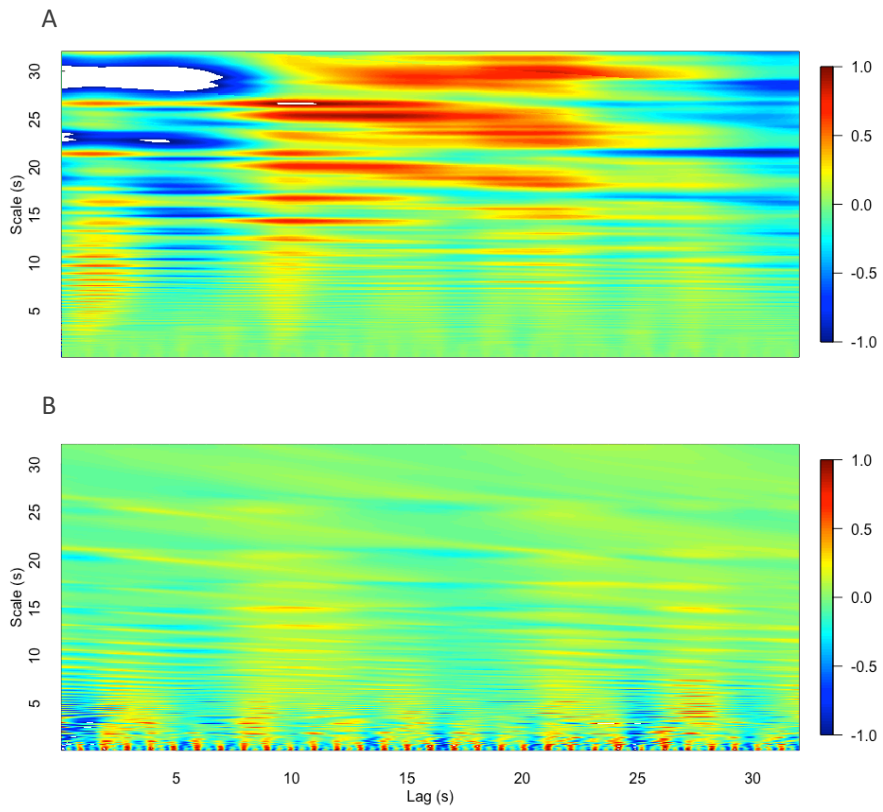

Figure 4 (a). MLR plot showing movement frequency regressed on current and previous values of postural path length. (b) MLR plot showing postural path length regressed on current and previous values of movement frequency.

The relationship between SDRP and power was assessed along with other treatment effects by linear mixed-effect models with random participant effects on the intercept. The results regarding prediction of movement frequency from postural path length are presented first. The model showed that there was a main effect of time, such that SDRP was higher during perturbation than pre-perturbation, *Estimate* = 0.11, *CI* = (0.01, 0.22), $p < 0.05$. There was also an

interaction between time and condition, corresponding to the fact that SDRP was higher during the movement perturbation than during the same task segment without a perturbation, *Estimate* = 0.35, *CI* = (0.20, 0.50), $p < 0.05$. In contrast, results concerning prediction of postural path length from movement frequency showed a main effect of total power, *Estimate* = -1.19, *CI* = (-2.18, -0.21), $p < 0.05$. There was also a condition × time interaction where SDRP was higher with than without a movement perturbation, *Estimate* = 0.38, *CI* = (0.24, 0.53), $p < 0.05$. No other main effects or interactions reached conventional significance.

The results of MLR were consistent across participants, and so these modeling results are not surprising. Essentially, movement frequency strongly predicts changes in postural path length (Figure 4 (b)); prediction of movement frequency from postural path length was much weaker. There are clearly some hot spots at larger scales in Figure 4 (a) but the structure is not nearly as well defined.

Movement Frequency and Heart Rate

Figure 5(a) shows the result when MLR is used to regress movement frequency on heart rate. The plot shows that most prediction in movement frequency comes from moderate to large temporal scales, and seems to oscillate with a period > 10 s. The pattern seems somewhat nonlinear with the troughs (blue regions) being more narrow than the peaks (red regions). Large white patches further indicate that the MLR coefficients at large scales tend to relatively large, compared to those at small scales. Figure 5 (b) shows the result for MLR of heart rate on movement frequency. Surprisingly, prediction of heart rate by movement

frequency is inconsistent. That result is surprising because increases in exertion should clearly lead to increases in cardiac output, yet movement frequency was not as strong a predictor heart rate as one might expect. However, the task was not very vigorous – participants only swung their arms at a maximum of 1.5 Hz, a fact that could be related to that result. Perhaps the "sedentary" task was simply did not have enough physical demand to capture expected relationship.

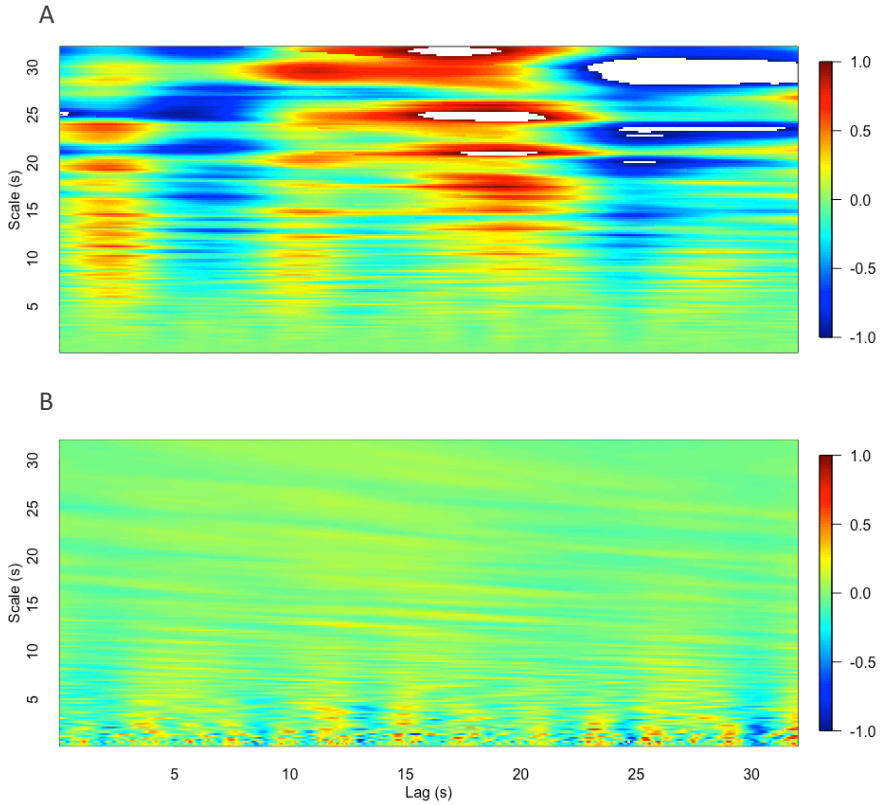

Figure 5 (a). MLR plot showing movement frequency regressed on current and previous values of heart rate. (b) MLR plot showing heart rate regressed on current and previous values of movement frequency.

The relationships implied by the structure in Figure 5 were further explored via linear mixed-effect modeling of SDRP as a function of total power and other treatment effects with random participant effects on the intercept. The model regarding prediction of movement frequency from heart rate are presented first. The results suggest there was a main effect of power, *Estimate* = 0.73, *CI* = (0.49, 0.98), $p < 0.05$. The time × condition interaction was significant, as in previous analyses, *Estimate* = 0.33, *CI* = (0.20, 0.46), $p < 0.05$, because the movement perturbation produced higher SDRP than performing without a perturbation. More interesting was the power × condition interaction, resulting from the fact that there was a negative relationship between SDRP and power during the movement perturbation but a positive slope without a perturbation, $t(113.31) = 3.26$, $p < 0.05$.

MLR results of heart rate on movement frequency are presented next. The model results suggest that there was a main effect of time such that SDRP was higher during the perturbation, *Estimate* = 0.18, *CI* = (0.11, 0.25), $p < 0.05$, and SDRP was also higher during the third task segment than the first, *Estimate* = 0.08, *CI* = (0.01, 0.15), $p < 0.05$. There was also a main effect of condition where SDRP was higher in the movement perturbation condition than in the control condition, *Estimate* = 0.12, *CI* = (0.05, 0.19), $p < 0.05$. Lastly, there was a significant power × condition interaction. The nature of the interaction was such that the slope between SDRP and power was positive during the movement perturbation but negative without a movement perturbation, $t(112.30) = 2.71$, $p < 0.05$.

Postural Path Length with Respiratory Rate

MLR results, for when postural path length is regressed on respiratory rate, appear in Figure 6 (a). Of note is the obvious presence of three scaling ranges with three different oscillation frequencies. The most obvious pattern is the large scale (≥ 18 s) oscillation with a period of around 15 s and MLR coefficients that increase as a function of scale. The period of oscillation at moderate scales (i.e., scales ranging between 3 and 18 s) seems to be around 10 s. At smaller scales (< 5 s), MLR coefficients tend to oscillate every three or four seconds. Do changes in postural sway also predict changes in respiratory rate?

Figure 6 (b) suggests that they do. Within the same scale ranges identified in Figure 6 (a), one sees oscillations across lags with similar frequencies. Both findings are consistent with the literature where it has been shown that respiration is indeed a potent perturbation for posture (e.g., Hodges, Gurfinkel, Brumagne, Smith, & Cordo, 2002), especially when seated (e.g., Bousett & Dechene, 1994). Posture is not expected to be as strong a predictor of respiratory rate because participants remained in an upright seated position (Buchheit, Haddad, Laursen, & Ahmaidi, 2009; Takahashi, Okada, Saitoh, Hayano, & Miyamoto, 2000).

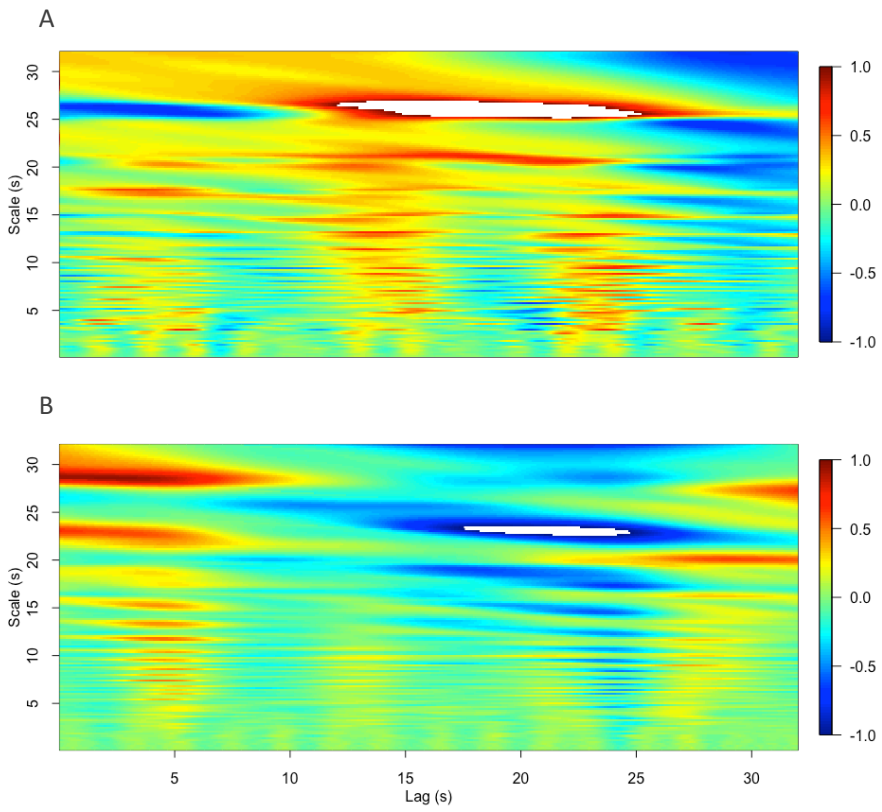

Figure 6 (a). MLR plot showing postural path length regressed on current and previous values of respiratory rate. (b) MLR plot showing respiratory rate regressed on current and previous values of movement frequency.

The relationships implied in Figure 6 were further investigated by regression of SDRP on total power and other treatment effects. The results for MLR of postural path length on respiratory rate are presented first. Despite similarities highlighted in the MLR-generated plots the model only revealed a time × condition interaction, *Estimate* = 0.36, *CI* = (0.21, 0.50).

The results concerning MLR of respiratory rate on postural path length pose a contrasting viewpoint. That model found a main effect of total power, *Estimate* = -4.28, *CI* = (-7.09, -1.47), $p < 0.05$. There was also a main effect of time such that SDRP was higher post-perturbation than pre-perturbation. There was also an interaction between time and condition, *Estimate* = 0.32, *CI* = 0.18, $p < 0.05$. The power × condition interaction was significant because the relationship between SDRP and power was positive during the movement perturbation, $t(113.87) = 2.56$, $p < 0.05$, and during the breathing perturbation, $t(110.18) = 2.23$, $p < 0.05$, but negative in the absence of any perturbation. The modeling results seem to conflict with those depicted in Figure 6. The results of MLR capture expected relationships between posture and breathing, namely, that respiration is expected to perturb, and by extension, predict changes in postural sway (Hodges et al., 2002). The surprising result was that response of respiration to changes in posture predicts performance in the pursuit-tracking task. Perhaps respiratory rate is more sensitive to changes in posture than has been explored in the literature (e.g., Buchheit et al., 2009; Takahasi et al., 2000).

Postural Path Length with Heart Rate. Figure 7 (a) gives the results for MLR of postural path length on heart rate. The patterns are similar to those in Figure 6 (a), as are the patterns in Figure 7 (b), which shows the only scale ranges with coefficients of appreciable magnitude are moderate scales near lags of about five seconds. It is not surprising that there should be a strong relationship between posture and heart rate as those relationships have been studied extensively in the physiological literature where the general finding is that posture

predicts changes in heart rate (e.g., Pomeranz et al., 1985). What is the surprising is that the results of MLR show that the contrary relationship also exists, changes in heart rate predict changes in postural sway, especially at large temporal scales, and the literature has been relatively silent on that particular relationship.

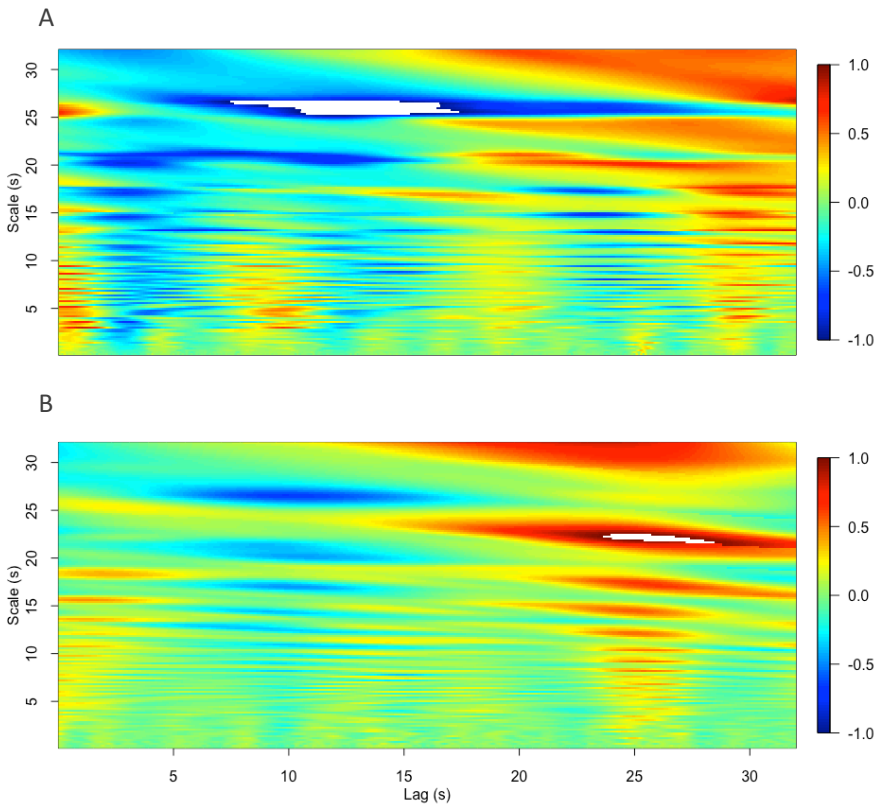

Figure 7 (a). MLR plot showing postural path length regressed on current and previous values of heart rate. (b) MLR plot showing heart rate regressed on current and previous values of postural path length.

As with previous process pairs, linear mixed-effects modeling revealed significant effects of time and condition but did not reveal any effect of power

after controlling for those treatment effects. Null results seem somewhat surprising, given the strong relationship indicated when predicting postural path length from heart rate, not to mention there is considerable evidence that heart rate variability is linked to changes posture (Pomeranz et al., 1985). There are several possible explanations for the lack of an effect. One possibility is that the power measurement is not sensitive enough to capture those relationships as it is a rather coarse measure. Another possibility is that the corrections between posture and heart rate posture are not relevant in the pursuit-tracking task, beyond providing a structural and physiological constraint over which the pursuit-tracking system can develop.

Heart Rate on Respiratory Rate

Figure 8 represents the result of MLR of heart and respiratory rate. The clear delineation of three scaling regions in Figure 8 is similar to what was observed in Figure 7. Other aspects seem puzzling. When respiratory rate predicts heart rate as in Figure 8 (a), there is a negative relationship, but the relationship is reversed when heart rate predicts respiratory rate [Figure 8 (b)]. A full explanation of those results is beyond the scope of the current work, but there are potential physiological reasons for the conflicting patterns.

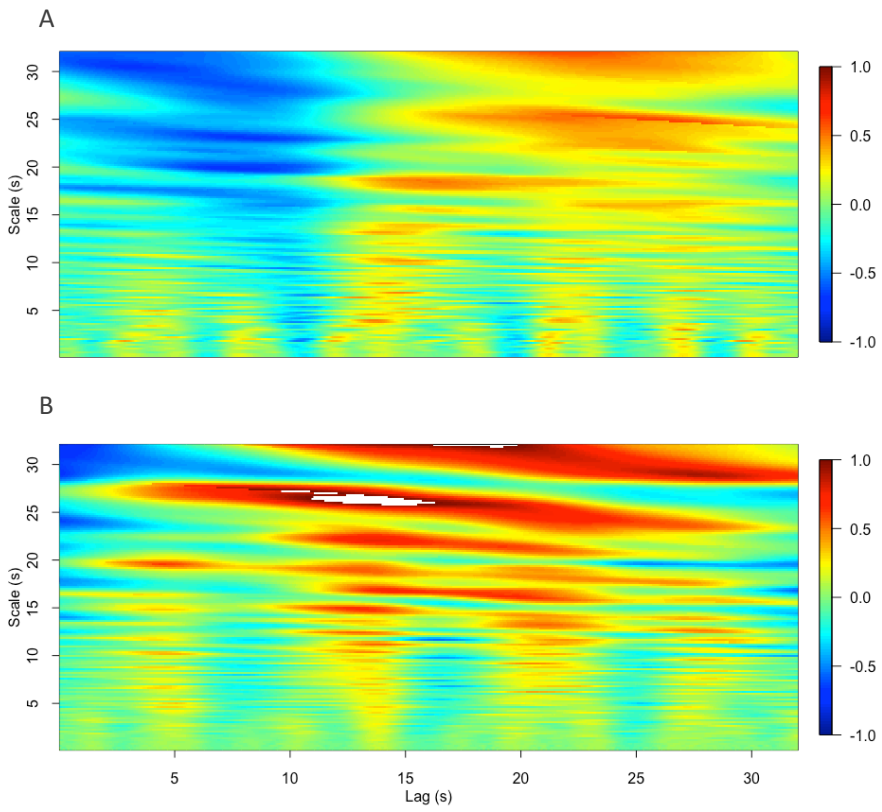

Figure 8 (a). MLR plot showing heart rate regressed on current and previous values of respiratory rate. (b) MLR plot showing respiratory rate regressed on current and previous values of rate.

Respiratory sinus arrhythmia is a known, healthy phenomenon whereby heart rate increases during inspiration but decreases during expiration (Acharya, Joseph, Kannanthal, Lim & Surry, 2006). It is quite possible that participants in this study took longer to inhale than to exhale, on average. If so, then that would lead to lower respiratory rate, on average, because respiratory rate in the current study was calculated instantaneously. A negative relationship follows where decreases in respiratory rate associated with longer inhalations would predict

increases in heart rate. Of course that suggestions would have to be empirically verified, but perhaps MLR reveals two different aspects of the cardiopulmonary relationship. When heart rate predicts respiratory rate, the positive, expected relationship is observed. When respiratory rate predicts heart rate, a surprising, but physiologically plausible negative relationship is revealed.

Discussion

Experiment 1 required participants to perform a pursuit-tracking task under three conditions: a movement perturbation, a breathing perturbation, and a control condition with no perturbation. The general hypothesis concerning performance was that performance, as measured by standard deviation of relative phase, would be worse during the movement and breathing perturbation conditions than the control condition, specifically during the perturbation period. The above results suggest that the movement perturbation consistently increased SDRP but the breathing perturbation had little, if any, effect. The absence of a breathing perturbation effect warrants further discussion. One possibility is that the perturbation was not strong enough to disrupt pursuit-tracking performance. This is somewhat surprising because, informally, several participants mentioned that it was fairly difficult to focus on breathing while performing the pursuit-tracking task. Another, more likely possibility is that the magnitude of perturbation was left to the discretion of each participant, creating sufficient noise in the data as to mask the effect. Both possibilities could be addressed in a future study by providing consistent (across participants) yet graded (across experimental conditions) instances of the breathing perturbation. In addition, a somewhat consistent finding was that SDRP tended to increase across time, perhaps owing to some type of fatigue effect. The fatigue effect

explanation seems reasonable given that trials lasted 15 minutes each and each participant performed 3 trials (one for each condition).

Predictions concerning multiscale coordination were less concrete. Uncertainty comes from two sources – the method is new and both the existence and degree of multiscale coordination in psychological systems is undocumented in the literature. The results presented in the previous section offer many possibilities for discussion, some of which will be addressed in the general discussion. In this brief discussion, however, two key questions will be addressed: (1) do psychological systems exhibit evidence of multiscale coordination; and (2) is multiscale coordination related to task performance, after accounting for treatment effects?

Concerning the first of those two questions, the answer seems to be yes. MLR revealed a complicated set of relationships among the various process pairs examined in the current experiment. Despite that complication, some general trends emerged among the process pairs.

First, it appears that residual relationships between the processes involved is often oscillatory in nature. That fact may seem unsurprising when comparing, say postural path length and movement frequency. After all, the task involved oscillations of the limbs which surely influences the movement of the trunk, possibly generating oscillations in postural sway. In fact, overtly rhythmic postural sway was observed in some participants. However, it is important to recall that postural path length was not regressed on position but movement frequency, the instantaneous rate at which participants swung their arm. One could still argue, of course that participants should move their limbs at different rates during external and internal rotation, based purely on motor kinematics.

Given that the task involved synchronizing rotations with an oscillating stimulus, regularities of the task might correlate with regularities in the speed of rotations about the elbow. As such, it might make sense that the relationship between postural path length and movement frequency might be oscillatory for no other reason than both were involved in an oscillatory task.

That explanation becomes less likely when one considers that postural path length showed evidence of oscillatory relationships with other processes such as heart rate. One could also argue that heart rate, being measured by placing electrodes on the skin, is susceptible to movement artifacts from the jostling of wires during movement. That second argument would be more convincing if raw signals were compared by MLR, but path length was regressed with instantaneous heart rate not the raw signal. The argument regarding heart rate becomes even more untenable when one considers that oscillations between posture and respiratory rate were also observed. Respiratory rate was calculated based on flow which was measured by pneumotachometer and should be far less sensitive to physical perturbations. Thus, the oscillatory patterns revealed by MLR may reflect actual coordinative structure among the systems that made up the pursuit-tracking system.

Second, the relationships observed between process pairs seems to be directional. For example, movement frequency appears to predict changes in heart rate at small scales but heart rate seems to predict movement frequency only large temporal scales. Moreover, the magnitude of predictions made by heart rate on movement frequency are much larger than in the opposite direction. Similar observations were made for each process pair, a possible exception being the relationship between respiratory rate and

heart rate. However, even in the cardio-pulmonary comparison, the plots were not identical, again suggesting directional dependence. Asymmetry in MLR revealed relationships was more the rule than the exception (Figures 4 - 9).

Lastly, the MLR plots further imply that coordination patterns are not constant across scales. In fact, it appears that two general trends can be distilled. Regression coefficients that are large at small scales tend to decrease at larger scales; and regression coefficients that are large at large scales tend to decrease at smaller time scales. The exploratory nature of this study forbids strong conclusions about the meaning of directional dependence; however, the consistency in this pattern permits a few additional words. Directional dependence is a known characteristic in least squares regression, a characteristic that has recently been investigated with respect to determining causal relationships between variables (Sungur, 2005). A complete discussion of that approach is well beyond scope of the current work but provides interesting ideas concerning future extensions of MLR.

Regarding the second question – Do multiscale relationships predict performance? – the answer is a cautious yes. Several of the models presented in the results section implicated total power, a potential metric of multiscale interactions, as an important predictor of pursuit-tracking performance. The most interesting of those findings was the frequent observation of an interaction between condition and power. Leaving limitations for the general discussion, what are the implications of such a finding? The immediate implication is that multiscale relationships are different for steady-state performance (e.g., the control condition) than perturbed performance (e.g., movement and breathing perturbations). If so, then the current results are aligned, at the

least at the surface level, with the large literature on fractal scaling – some of the clearest evidence of fractal scaling is from steady-state performances (e.g., Likens et al., 2015; Wagenmakers et al., 2004), whereas frequent perturbations can lead to decreases in fractal scaling (e.g., Holden, Choi, Amazeen, & Van Orden, 2011; Dingwell & Cusumano, 2010). Furthermore, the condition by power interaction was rarely observed in the breathing perturbation. That finding that is consistent with the idea that changes in fractal scaling accompany changes in the constraints placed on the system. Because performance was unaffected by the breathing perturbation, perhaps the perturbation was not strong enough to elicit a strong compensatory adaptation across psychological scales. An important caveat is that an interaction between power and condition was not always observed within each process pair – perhaps the presence or absence of that effect reflects the degree to which different systems are actively involved in the control of behavior during the pursuit-tracking task. For example, a rigid coupling among heart, lungs, and task could lead to very unwanted outcomes. It is also possible, that in the case of cardio-pulmonary coordination, the task was not vigorous enough to produce an obvious effect.

In summary, the results from Experiment 1 look promising. MLR revealed structure in the multiscale relationships between the components that make up the special purpose pursuit-tracking system. Moreover, that structure may be related to tracking performance. Experiment 2 seeks to extend those findings by examining multiscale coordination with different bodily systems and one additional task.

Experiment 2

Experiment 1 showed that psychophysiological variables exhibit multiscale relationships. Those relationships, as revealed by MLR may have characteristic forms (e.g., oscillation) that vary over both time and scale. Results from Experiment 1 also showed that, at least in some instances, the structure of multiscale coordination predicts performance in a pursuit-tracking task, even after controlling for treatment effects. Experiment 2 continued to explore those relationships by examining multiscale coordination among three different brain regions and other bodily processes while participants engaged in a pursuit-tracking task. In this experiment, neural activity was recorded by electroencephalogram (EEG) while participants performed the same pursuit tracking task in two conditions. The first task was similar to the movement perturbation condition in Experiment 1 – subtle differences are explained in the method section. In addition, participants performed a pursuit-tracking task with a dual-task component, a go/no-go reaction time task. In that task, participants were asked to perform pursuit-tracking while monitoring the color of the tracking stimulus for possible changes. Change to one color signaled go; change to another color signaled no-go. As in Experiment 1, SDRP was expected to increase during the movement perturbation. The result from applying MLR to these new data sources is unknown; however, there is still an expectation that MLR will reveal multiscale interactions, the structure of which should predict pursuit-tracking (i.e. SDRP) and secondary task performance (i.e. RT).

Method

Participants. Eleven participants (*Female* = 6) volunteered to participate in the experiment with an average age of 27.2 years (*SD* = 5.51). Participants were non-smokers with no injuries to limbs or trunk. All participants reported normal or corrected to normal vision.

Apparatus and Procedure. The experimental paradigm was the same pursuit tracking task used in Experiment 1. The goal of this experiment was to extend the analysis to brain activity data. In order to accomplish this, data collection occurred in an EEG lab with different equipment. That change in location made it impossible to collect some of the measures used in Experiment 1, including respiratory rate and 3-D position data from motion tracking, but made it possible to include new measures, including electroencephalogram (EEG) and electrooculogram (EOG). EEG data were recorded with a 32 channel SynAmps (Neuroscan, Sterling, VA) as was electrocardiogram (ECG), electromyogram (EMG) from the medial deltoid muscle of the shoulder, and left and right horizontal electrooculogram (EOG) data. Only left horizontal EOG data were analyzed because the task involved lateral movements and meaningful vertical eye movements were not expected. Medial deltoid activity was recorded in this experiment as an attempt to improve EMG measurement over Experiment 1; however, failure of participants to comply with task instructions resulted in unusable data. MLR was conducted on the pairing of ECG and EOG data but not ECG and EEG data because the precision of instantaneous heart rate at very high frequencies, like those typical of brain activity, is unknown..

The change in experimental venue also required a slight adjustment to the experimental task. Instead of controlling a motion-tracked manipulandum, participants controlled their on-screen circle with a Logitech Extreme 3D Pro joystick (Newark, CA). The following two subsections give additional details regarding specific task conditions but, as in Experiment 1, participants practiced the tracking task without perturbation for seven minutes. The tracking signal during practice oscillated at a frequency of 0.8 Hz.

Movement perturbation. The path of the computer-controlled circle was generated by a pre-determined sinusoidal function that varied in (0.8 – 1.3 Hz) over time (Figure 2b). The speed was slower than Experiment 1 because pilot participants reported the Experiment 1 pace to be too difficult with the joystick. Subsequent pilot testing on the selected range revealed a comparable level of difficulty to Experiment 1. Specifically, the circle moved at 0.8 Hz for the first five minutes of the experiment; the circle oscillated at 1.3 Hz for the second five minutes of the experiment; and the circle returned to a 0.8 Hz oscillation for the final five minutes of the experiment. As in Experiment 1, the trial lasted 15 minutes overall with 5 minute pre-, during-, and post-stimulus periods. SDRP served as the dependent variable and was calculated as the standard deviation in phase difference between the tracking stimulus and lateral joystick movements sampled directly from the device.

Go/No-go task. Experiment 2 also added a go/no-go reaction time task similar to that used in Strayer and Johnston (2001). In this condition, a white target tracking circle presented on a black background oscillated at a constant frequency of 0.8 Hz. Participants controlled a blue circle with a joystick while monitoring the color of the target stimulus. At random intervals between 10 and 20 s, the white tracking circle

would change color to either red (the no-go signal) or green (the go-signal). Participants were instructed to press a button on the joystick with their non-tracking hand as soon as they saw a go signal, and to do nothing if they saw a no-go signal. In both cases, they were instructed not to let the dual task sacrifice their performance. SDRP and RT were dependent variables.

Analysis Strategy

Data preparation. Instantaneous frequency was computed for ECG data in the same manner as Experiment 1 (Barros & Ohnishi, 2001). Instantaneous frequency was computed for wavelet filtered EOG data in a manner similar to movement data in Experiment 1 (i.e., Hilbert Transform) because EOG data were very oscillatory, no doubt from tracking an oscillating stimulus. EEG data were pre-processed by passing data through a bandpass filter (1-120 Hz) before applying independent component analysis (ICA; Hyvärinen, 2000). EEG data are often contaminated by numerous bodily signals such as those that arise from the movement of the eyes as well as EMG signal from clinching the jaws and other muscles. ICA is considered the gold standard for removing artifacts, and the current work used the implementation found in the EEGLAB toolbox for Matlab (Delorme & Makeig, 2004; Mathworks, Inc., Natick, MA). ICA was applied to EEG data to remove eye-blink artifacts, EOG, and EMG contaminants. Data from two subjects had too many artifacts to be corrected by ICA and were removed from further analysis. Three EEG (F3, Oz, & Cz) channels were selected for analysis by MLR, corresponding to frontal, motor, and visual cortices. These channels reflect three possible brain areas that have been implicated in oculomotor behavior, namely, the dorsolateral

pre-frontal cortex, and the primary visual and motor cortices (Cohen, 2016; Nagel et al., 2006). Other brain regions were not examined further.

Multiscale coordination and performance. As in Experiment 1, MLR was applied pairwise for many of the signals described in the Data Preparation section. For neural signals, MLR was calculated on scales ranging from 0.04 s to 6.4 s increments of 0.04 s and lag ranges from 0.0 s to 6.4 s in increments of 0.004 s. The same number of scales and lags were analyzed as in Experiment 1. However, those numbers corresponded to different amounts of clock time across the two experiments: 0 – 32 s in Experiment 1 and 0 – 6.4 s in Experiment 2. That decision was made for two reasons – one practical and one physiological. The practical reason is that, in its current form, the MLR algorithm is computationally very expensive with long time series like EEG, and using the same clock time range exceeded the capability of available computing power. The physiological reason is that brain dynamics are thought to take place at time scales much faster than respiratory rate or heart rate, which often occur at frequencies much lower than 1 Hz. For that reason, a smaller clock time window, relative to Experiment 1, was chosen to closer match the characteristic time scale of neural dynamics.

The average $\beta_1(s,l)$ was then taken at each lag, in each B, and for each process pair. Total power was calculated from the FFT of the average lag-wise $\beta_1(s,l)$ (Figure 9). A series of linear regression analyses were then conducted to assess the dependence of SDRP on total power. Separate analyses were conducted for the movement perturbation and go/no-go conditions because of the marked dissimilarity in the two tasks. The go/no go task did not have a discrete time structure (e.g., pre, during, post) like the movement perturbation condition.

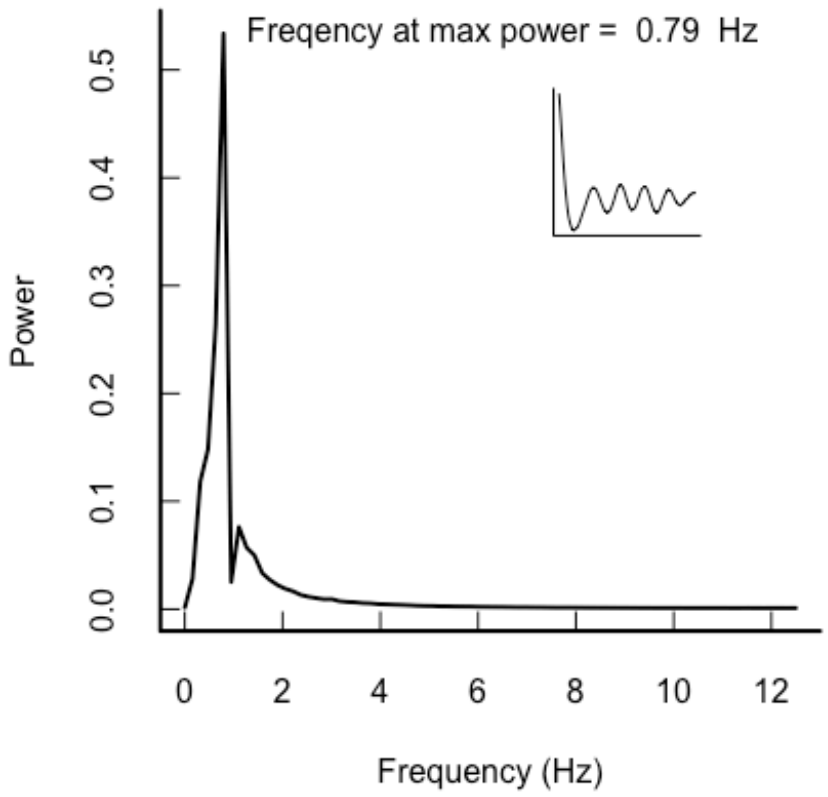

Figure 9. Power spectrum average lag-wise *B* when Cz is regressed on Oz with MLR. Note that peak power occurs at a frequency very near the tracking stimulus frequency of 0.80 Hz. The insert is the series of average regression coefficients on which the power spectrum was based.

Results

The results for Experiment 2 will follow a template similar to that used in Experiment 1. MLR plots for brain dynamics are presented first. For the data involving brain regions, I also introduce another MLR visualization method that depicts the same data but emphasizes the observed regularity (e.g., Figure 10). The x-axis is the same time lag depicted in the matrix plots from Experiment 1; the y-axis is the magnitude of $\beta_1(s,l)$,

with each plotted line (and color) depicting a single time scale. The color legend ranges from red to blue, with the smallest scales (0.04 s) in red, moderate scales in green, and the largest scales (6.4 s) in blue. Following description of those figures, performance (i.e., SDRP, and when appropriate, RT) is regressed on total power in the average lag-wise MLR coefficients. In the case of the movement perturbation, time (pre, during, and post perturbation) was also included as a predictor in the model.

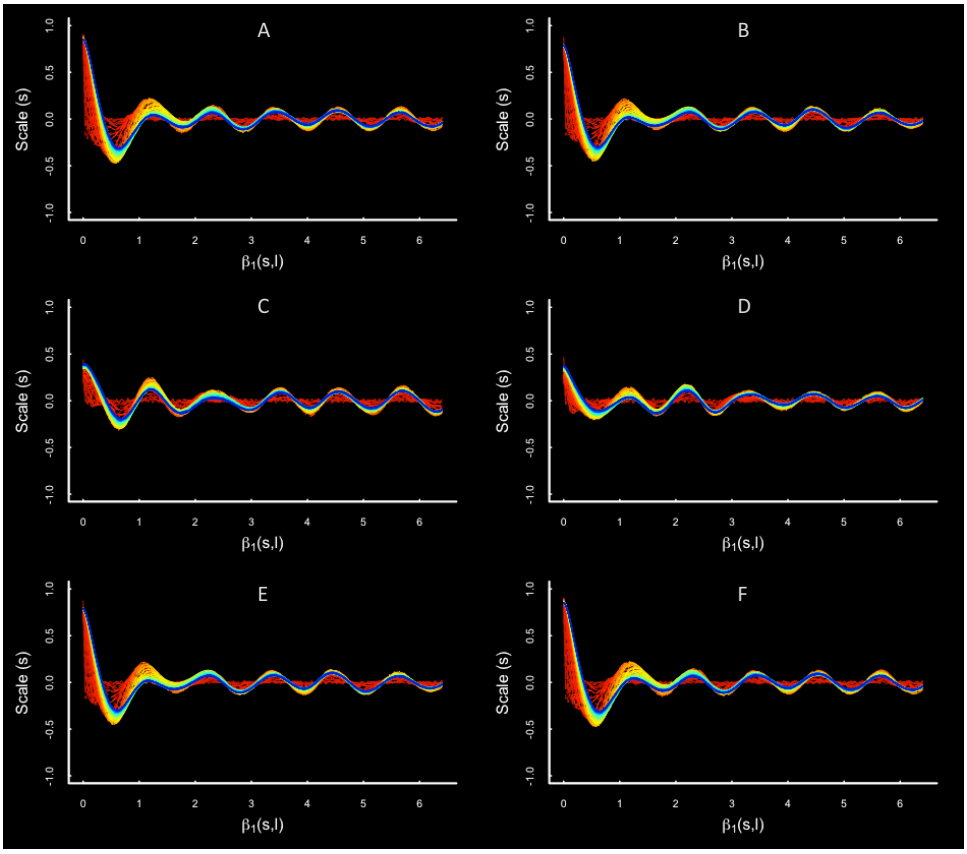

Figure 10. MLR plots depicting bidirectional relationships between neural measurement sites in the go/no-go condition. (a) Oz regressed on Cz; (b) Cz regressed on Oz; (c) Oz regressed on F3; (d) F3 regressed on Oz; (e) F3 regressed on Cz; and (f) Cz regressed on F3.

Figure 10 depicts pairwise MLR plots for one representative participant and the three neural measurement sites. The graphs highlight both the regularity across lags and the symmetry across MLR directions. For example, the relationship between activity at Oz [Figure 10 (a)] and Cz [Figure 10 (b)] starts strong, but quickly dampens into a regular, sinusoidal pattern. That is, the structure in the plot shows that the relationship between activity at Oz and activity at Cz is strongly oscillatory in nature, at least at moderate and large scales. In addition to being sinusoidal, Figure 10 suggests that oscillations over many scale sizes may also exhibit phase alignment. The structure at the smallest scales quickly decays near zero and has a noisy appearance. That description applies equally well whether Oz is regressed on Cz or Cz is regressed on Oz and when involving other measurement sites as shown in Figure 10 (c) – (f). Furthermore, the description carries over to the movement perturbation condition as shown in Figure 11. Next, statistical results predicting performance from total power are presented within each task for each process pair.

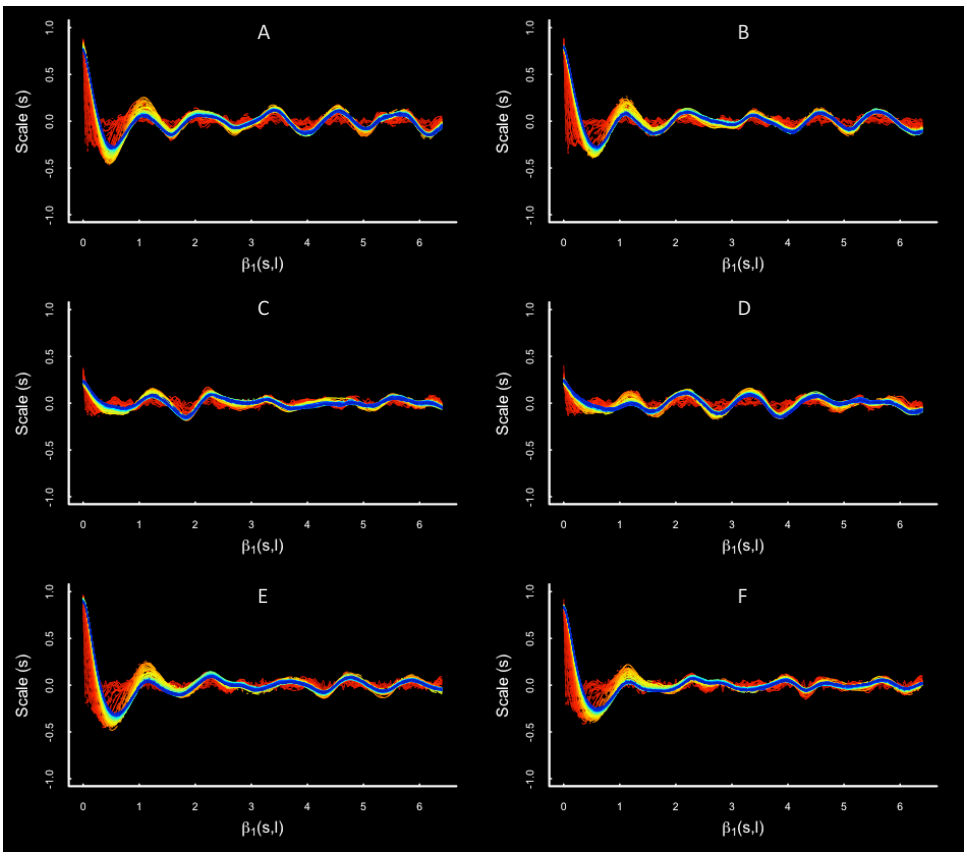

Figure 11. MLR plots depicting bidirectional relationships between neural measurement sites in the movement perturbation condition. (a) Oz regressed on Cz. (b) Cz regressed on Oz. (c) Oz regressed on F3. (d) F3 regressed on Oz. (e) F3 regressed on Cz. (f) Cz regressed on F3.

Oz and Cz

Performance Results. The relationship between reaction time and total power was explored using ordinary least squares regression; that is, average reaction time for each participant was regressed on total power. In this, and proceeding analyses, data from one participant was omitted because their average RT was more than 2.5 times the standard deviation of the sample. The results concerning MLR of Cz on Oz showed that total power did not predict reaction time. In contrast, the results for MLR of Oz on Cz found that a one unit increase in total power predicted a 0.14 s decrease in average RT, $F(1, 6) = 8.07$, $p < 0.05$. The relationship between total power and SDRP was also assessed by linear regression. The results showed only a marginal effect for MLR of Oz on Cz where a one unit increase in total power predicted a 0.55 decrease in SDRP.

Concerning the movement perturbation task, linear mixed-effects models revealed that the only significant results were related to the perturbation, such that SDRP increased during perturbation, $F(2, 18.21) = 6.62$, $p < 0.05$, stemming from the fact that SDRP was higher during-perturbation than pre-perturbation period. In contrast, SDRP was lower post-perturbation than pre-perturbation. The same result was obtained for MLR of Oz on Cz and MLR of Cz on Oz.

Oz and F3

Performance Results. The relationship between reaction time and total power was explored using ordinary least squares regression, that is, average reaction time for each participant was regressed on total power. The results concerning MLR of Oz on F3 showed that total power did not predict reaction time. However, there was a marginal relationship revealed for MLR of F3 on Oz, such that one unit increase in total power

predicted a 0.09 s decrease in average RT, $F(1, 6) = 5.08$, $p = 0.07$. The relationship between total power and SDRP was also assessed by linear regression. The results showed no effect of total power on SDRP.

Concerning the movement perturbation task, the only significant results were related to the perturbation, such that SDRP increased during perturbation, $F(2, 17.75) = 7.30$, $p < 0.05$, stemming from the fact that SDRP was higher during-perturbation than pre-perturbation. SDRP was lower post-perturbation than pre-perturbation. The same result was obtained for both directions of MLR.

F3 and Cz

Performance results. The relationship between reaction time and total power was explored using ordinary least squares regression, that is, average reaction time for each participant was regressed on total power. The results concerning MLR of F3 on Cz gave evidence of a marginal trend, where a one unit increase in total power predicted a 2.0 s decrease in RT, $F(1,6) = 4.56$, $p = 0.07$. While the regression coefficient seems extreme, total power in this case only ranged from about 0.02 to 0.08, implying that small changes in power might predict dramatic changes in reaction time. More convincing, though, are the results concerning Cz on F3 which showed a significant linear trend where a one unit change in power predicted a 1.69 s decrease in RT, $F(1,6) = 15.36$, $p < 0.05$, and carry the same implication as the preceding case involving MLR of Cz on F3. The relationship between total power and SDRP was also assessed by linear regression. The results showed no effect of total power on SDRP.

Concerning the movement perturbation task, the only significant results were related to the perturbation, such that SDRP increased during perturbation, $F(2, 18.79) =$

6.31, $p < 0.05$, stemming from the fact that SDRP was higher during-perturbation than pre-perturbation period. In contrast, SDRP was lower post-perturbation than pre-perturbation. The same result was obtained for both directions of MLR.

The above results illustrate two points. First, it seems that total power, as measured from FFT of the lag-wise average of MLR coefficients, does not predict SDRP. However, the above results suggest RTs do depend on total power, at least when comparing some measurement sites. Given the regularity in MLR plots and the strong peak in Figure 9, one conclusion is that total power reflects the degree of coordination across neural time scales. If so, then the implication is that increases in synchronization across neural time scales is related to performance of speeded reactions.

Eye movement frequency and heart rate

The matrix plots used in Figures 4 -9 obscured the regularity in MLR revealed relationships between brain regions. Similarly, multiline graphs used to discuss brain behavior make it difficult to assess the structure between eye movement frequency and heart rate. The matrix plots used in Experiment 1 were used to depict the results of MLR of eye movement frequency on heart rate and vice versa (see Figure 12).

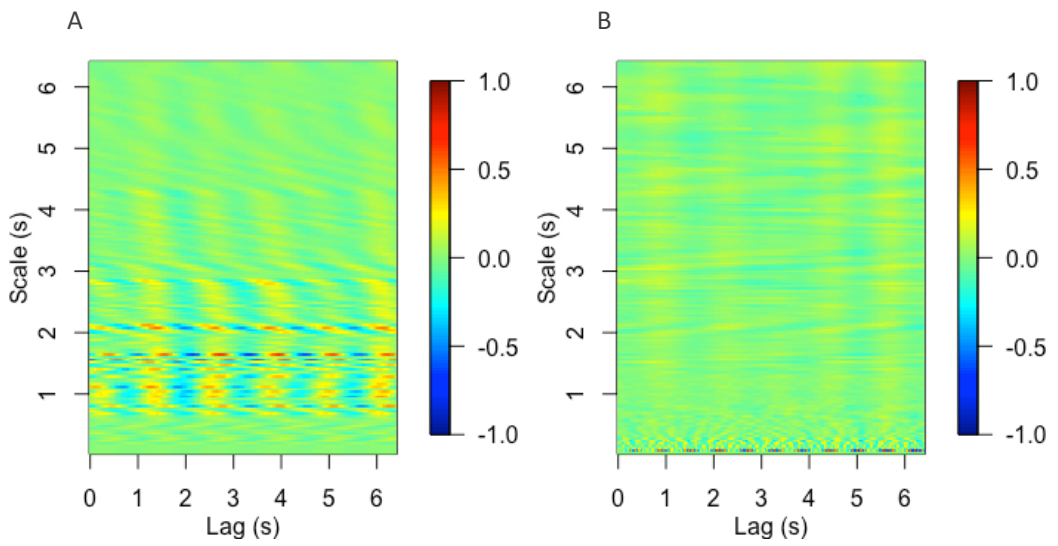

Figure 12 (a). MLR plot showing heart rate regressed on current and previous values of eye movement frequency.

(b) MLR plot showing eye movement frequency regressed on current and previous values of heart rate.

Figure 12 is visibly different than any plot examined in Experiment 1. Panel (a) of Figure 12 has a clearly delineated region of scales where heart rate predicts eye movement frequency, i.e., in the range of about 1 to 2 seconds. The pattern seems oscillatory across lags within that scale range, but has a wavy characteristic across scales (i.e., variability in phase). In contrast, eye movements only seem to predict heart rate at very small time scales and that relationship also seems regular and periodic. The pattern is also different than what was observed in brain data – MLR of brain areas suggested phase alignment across scales. That is, peaks and troughs are not aligned across scale (c.f. Figure 10). Total power was on a much different scale than RT because power was

relatively low. Both were converted to z-scores before entering into the linear regression model. Statistical analysis revealed that when MLR was used to regress eye movement frequency on heart rate [Figure 12(b)], a standard deviation change in total power predicted a 0.73 standard deviation increase in reaction time, $F(1,6) = 7.00$, $p < 0.05$. No other results involving RT or SDRP were significant for the go/no-go task.

The data in Figure 12 are representative of all participants when performing in the go/no-go condition. Hence, those patterns are reminiscent of findings from Experiment 1. However, the relationships revealed by MLR between eye movement frequency and heart rate in the movement perturbation condition are extremely variable from one participant to the next. Figure 13 shows the MLR results for three participants and highlights the variability that was observed. The small sample size prevents me from making general statements about clustering of patterns. For now, it is apparent that more research is needed to understand these results. For consistency with other process pairs, a linear mixed-effect model was estimated to regress SDRP on time and power. Not surprising was the lack of an effect of power but effects of time as in other processes already considered in Experiment 2: SDRP increased during perturbation before decreasing below baseline level post-perturbation, $F(2, 18.04) = 7.21$, $p < 0.05$.

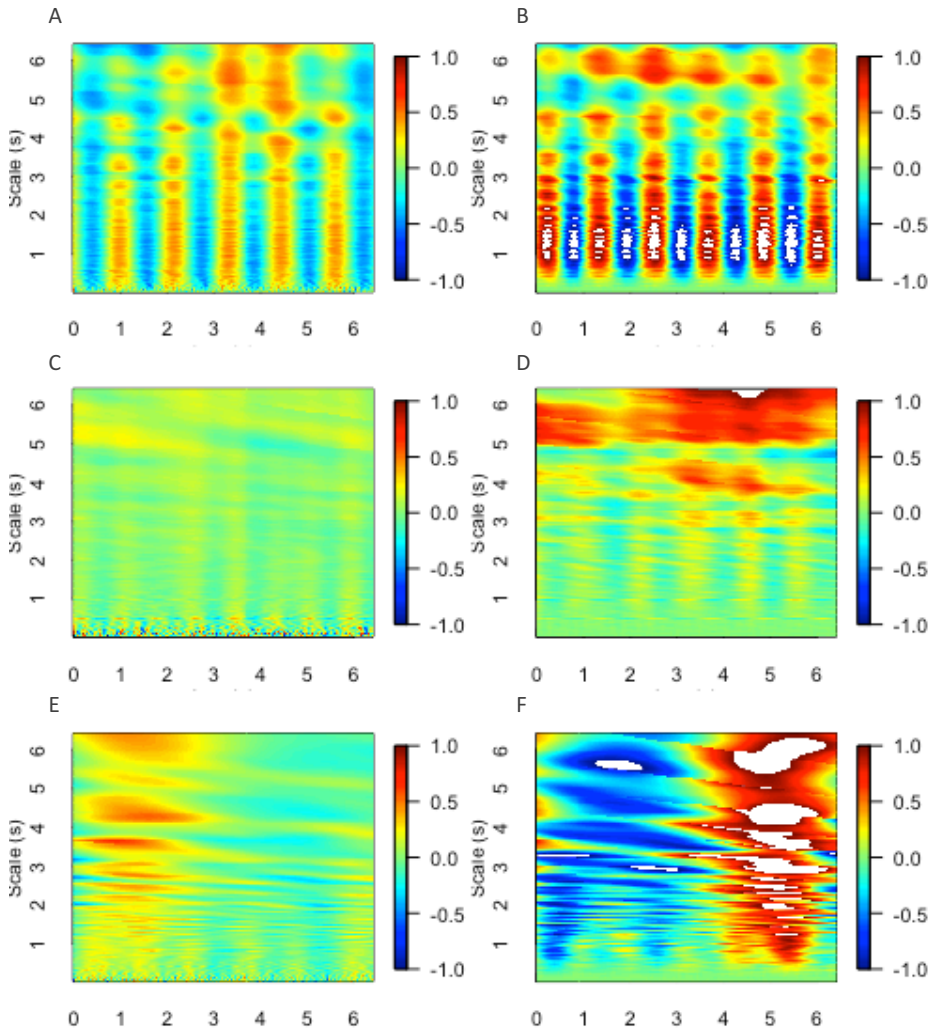

Figure 13 (a, c, e). MLR plot showing heart rate regressed on current and previous values of eye movement frequency. (b, d, f) MLR plot showing eye movement frequency regressed on previous values of heart rate. Each row is a different participant.

Eye movement frequency and neural measurements

This section reports the results for MLR involving eye movement frequency and the three EEG measures (Oz, Cz, & F3). Before going further, it should be noted that

total power did not predict performance in terms of either SDRP (in either tasks) or RT (in the go/no-go task). However, establishing a link between multiscale interactions and performance represents the secondary goal of this work. The primary goal was uncovering multiscale interactions. For that reason, representative MLR plots between eye movement frequency and each EEG measurement site are presented in Figures 14 (go/no-go) and 15 (movement perturbation. Those figures, for a single participants, capture interesting multiscale patterns.

Notable features in Figure 14 include an obvious similarity in the scaling patterns across pairwise MLRs. That pattern observed between eye movement frequency and Oz is similar to the pattern observed between eye movement frequency. There are also elements that are reminiscent of trends observed in Experiment 1. The plots seem exhibit strong directional dependences where large scales dominate in one direction and moderate and small scales dominate in the other directions. Figure 15 has that latter feature in common but the direction of dependence reverses. Also distinguishing Figure 15 from Figure 14 is the fact that there is less similarity across process pairs. In Figure 15, MLR of eye movement frequency on Oz shows that moderate scales show a prominent relationship over time; other pairs show that small time scales have the most in common. These results are interesting because the data in Figure 14 and Figure 15 are from two different tasks, the go/no-go task and the movement perturbation task, respectively. Hence, even though the relationships revealed by MLR do not predict performance variables, multiscale relationships eye movement frequency and neural activity do appear to depend on task constraints.

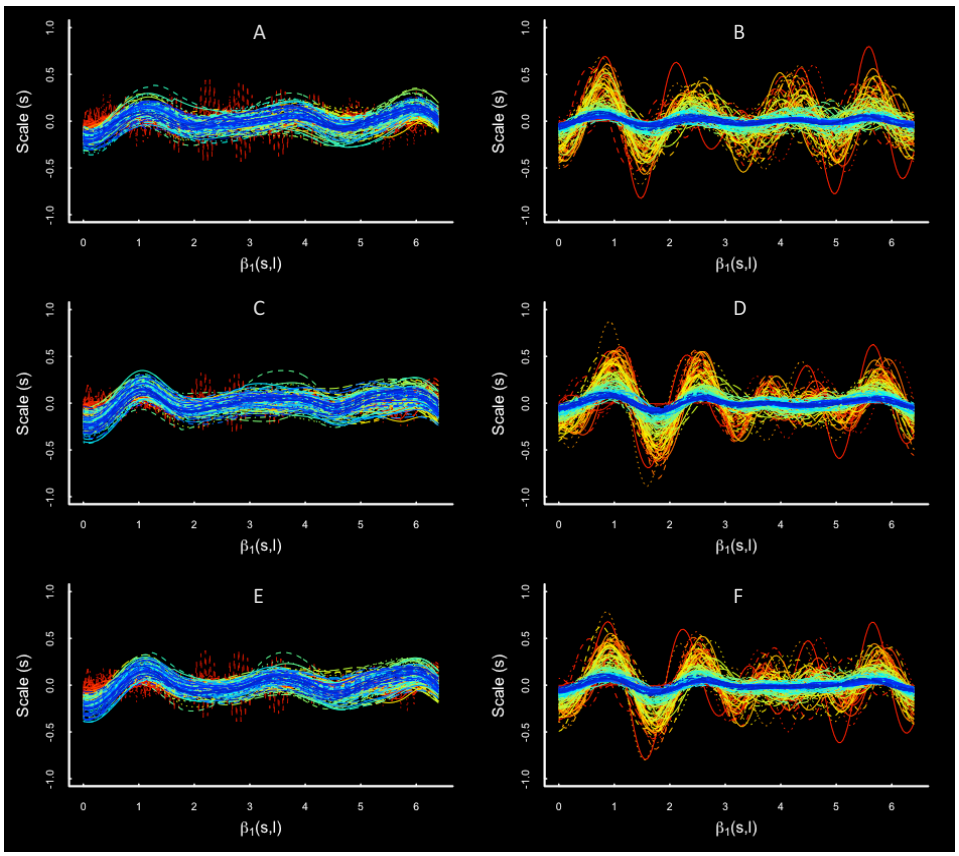

Figure 14. MLR plots depicting bidirectional relationships between eye movement frequency and neural measurement sites in the go/no-go condition. (a) Eye movement regressed on Oz. (b) Oz regressed on eye movement frequency (c) Eye movement frequency regressed on F3. (d) F3 regressed eye movement frequency. (e) Eye movement frequency regressed on CZ. (f) Cz regressed on eye movement frequency. All panels are from the go/no-go condition.

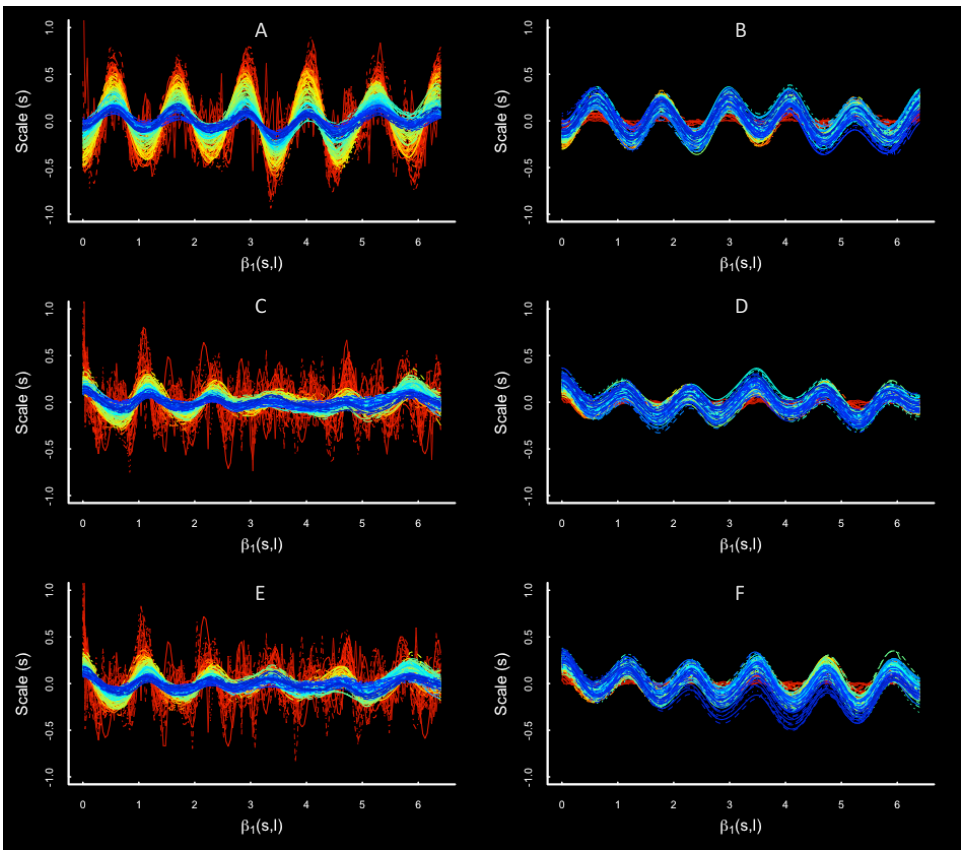

Figure 15. MLR plots depicting bidirectional relationships between eye movement frequency and neural measurement sites during the movement perturbation condition. (a) Eye movement regressed on Oz. (b) Oz regressed on eye movement frequency (c) Eye movement frequency regressed on F3. (d) F3 regressed eye movement frequency. (e) Eye movement frequency regressed on CZ. (f) Cz regressed on eye movement frequency. All panels are from movement perturbation condition before perturbation.

Discussion

Experiment 2 required that participants perform a pursuit-tracking task in two conditions, one involving a movement perturbation, the other involving a dual-task

component. The movement perturbation condition was identical to the one used in Experiment 1, except for a different apparatus and a slight decrease in tracking speed. Following expectations, the results showed that SDRP increased during the perturbation. A surprising result was that SDRP was lower at baseline post-perturbation. That result is surprising because participants in Experiment 1 seemed to exhibit a fatigue effect where SDRP was higher post-perturbation than pre-perturbation. The difference between Experiment 1 and Experiment 2 is likely do to the fact that controlling the manipulandum in Experiment 1 was more physically demanding than controlling the joystick in Experiment 2. Thus, the performance gain in Experiment 2 might simply reflect participants becoming more skilled at the task, as one might expect from previous literature (Pew, 1974). In the dual task condition, participants performed the same pursuit tracking task while simultaneously performing a go/no-go reaction time task. Reaction times were not expected to vary in a systematic way across the trial because no other manipulations were introduced; however, reaction times were in similar in magnitude to those observed in previous literature (e.g., Strayer & Johnston, 2001).

Across both conditions, hypotheses were explored concerning multiscale interactions and their involvement in performance of tracking and decision-making (i.e., to react or refrain). As in Experiment 1, expectations concerning multiscale coordination were more exploratory but follow the same basic question: Do measurements in Experiment 2 imply the presence of multiscale interactions so often implied by the fractal literature? The answer seems to be affirmative because several general patterns (e.g., oscillation, scale- and directional-dependence) emerged from MLR of neural data and other measurements. An important caveat is that the precise nature of those interactions

depends on the processes being compared. The coming paragraphs discuss those findings in additional detail while addressing eccentricities in the MLR-revealed relationships between psychophysiological processes.

For neural data, the defining feature was oscillation. In fact, the patterns captured in Figures 10 and 11 highlight the most striking case of oscillatory covariance captured by MLR in either Experiment 1 or Experiment 2. An interesting observation was that oscillations were near the frequency imposed by the tracking task. One might think the patterns stems from mechanical perturbations such as shaking of one's head while tracking. That explanation, however, can be ruled out because filtering prior to analysis was used to remove mechanical artifacts related to the frequency of the task. Thus, the results imply that the multiscale, temporal relationship between neural measurement sites is oscillatory in nature. A secondary feature was symmetry, that is, application of MLR in both directions yielded similar results. At first glance, that result is reminiscent of Simulations 1 and 7 in Appendix A, implying that MLR simply captured simple correlation between oscillatory variables. That intuition must be tempered by the knowledge that neural data generally exhibit fractal scaling (e.g., Voytek et al., 2015; Woyshville & Calebrese, 1994). Thus, oscillations in scaled and lagged neural covariance were found, even though neural data themselves were not oscillatory.

Oscillation was also found to be a defining feature of the temporal relationship between eye movement frequency and three neural measurement sites. Unlike neural data alone, those data, as shown in Figures 14 and 15, also appear to exhibit both scale- and directional-dependence, and so, those findings are reminiscent of the many patterns observed in Experiment 1. The addition of a dual-task component yielded an observation

not possible in Experiment 1: directional dependencies were not consistent across tasks. The implication is that different task constraints require specific organizations of the neuromuscular substrate (e.g., Bingham, 1988; Kelso, Buchanan, DeGuzman, & Ding, 1993). That idea could be explored in a manner similar to early applications of dynamical systems to motor coordination (e.g., Kelso, 1984). Driving the motor system to a point of instability and beyond could reveal lawful changes in the multiscale interactions that co-occur before, during, and after phase transitions.

The MLR results for eye movement frequency and heart rate were perhaps the most peculiar observed in either experiment because of a complete lack of consistency across participants (Figure 13). The idiosyncrasy in those results suggest two possible implications. One is that coordination between heart rate and eye movement frequency is irrelevant for a pursuit-tracking task. Discussion of that possibility is left for the general discussion. The alternative explanation is that idiosyncrasy reflects something meaningful about multiscale coordination of eye movements and heart rate in a pursuit-tracking problem. The *N* in Experiment 2 is too small make such conclusions but could easily be explored in a future study involving a larger sample. The goal would be to identify clusters of coordination patterns that could, in turn, reflect different solutions to the same problem. Where they exist, those clusters could help to explain performance on the pursuit-tracking task. In fact, that same approach could be applied to any of the process comparisons made in Experiment 2. The outcome of that approach could reveal which processes are most relevant to tracking a moving target.

Concerning performance, there was also an expectation that multiscale interactions would predict performance on a pursuit-tracking task. A positive conclusion

was cautious in Experiment 1; here caution is further justified. The results involving neural data showed that, regardless of which electrodes were being compared, there were a few marginal and significant relationships between power and reaction time such that increases in power predicted reduction in reaction time. The tenuous implication of those findings is that neural coordination across more than three orders of magnitude predicts one's ability to make simple decisions about whether to act or refrain. MLR of eye movement frequency on heart rate showed the opposite trend where increases in total power predicted dramatic increases in reaction time. The relationships between neural data and eye movement frequency were less revealing. Despite seemingly clear evidence of directed, oscillatory behavior in those plots, total power failed to predict either of the performance measures. Lastly, multiscale interaction results for Experiment 2 are distinct from those in Experiment 1 in that the magnitude of total power did not predict SDRP.

As an interim summary, the results from Experiment 2 provided additional evidence that the time varying relationships between the many processes that make up behavior do, in fact, interact over many different scales. Experiment 2 results further suggest that some multiscale interactions predict other meaningful aspects of behavior, albeit less convincingly than in Experiment 1. Null results here and in Experiment 1 raise interesting questions about the role of certain processes in the production of behavior. Treatment of those questions will be left for the General Discussion section.

General Discussion

The primary purpose of this dissertation was to uncover direct evidence of multiscale interactions in psychological processes. Participants performed a pursuit-tracking task while multiple behavioral and physiological measures were recorded. In Experiment 1, participants tracked an onscreen circle while experiencing perturbations of movement speed and respiration as well as a control condition that had no external perturbation. In Experiment 2, conditions involved a movement perturbation similar to the one from Experiment 1 and a second condition that involved a dual-task component, a go/go-go reaction time task. In both experiments, hypotheses were generated for both task performance and multiscale interactions. Each set of predictions and results are discussed in turn, beginning with performance data.

Treatment Effects on SDRP

Treatment effects on performance variables provide the context for further discussion of findings related to multiscale interactions. This paragraph restates the main findings concerning SDRP. In both experiments, we examined changes in SDRP that resulted from experimental perturbations; perturbations were expected to increase SDRP. Results from Experiment 1 were consistent with that prediction, at least during the movement perturbation. The respiratory perturbation had little effect likely because of variability in participant interpretations of instructions. The performance results in Experiment 2 were similar to Experiment 1 in that the movement perturbation led to an increase in SDRP relative to pre-perturbation. However, the movement perturbation condition in Experiment 2 produced an effect not observed in Experiment 1 where post-perturbation SDRP was lower than SDRP pre-perturbation. The results concerning

SDRP are reasonable given the constraints present in this task. Later in this discussion, those trends will inform more general statements concerning multiscale interactions and psychological performance.

Multiscale Interactions

Multiscale interactions have long been thought to be the causal agents behind observations of fractal scaling in any number of psychological time series (Van Orden et al., 2003; Ihlen & Vereijken, 2010; Likens et al., 2014). However, uncovering direct evidence of multiscale interactions has proven challenging. Historically, researchers have relied on fractal analysis to draw conclusions about distributed control of behavior, but fractal scaling alone is a shaky foundation for claims of multiscale coordination (Wagenmakers et al., 2012). It is true that complex systems entail multiscale interactions and that fractal scaling is a defining feature of those systems; however, there are many ways to generate fractal properties (Beran, 1994; Gardner, 1978; Gilden, 2001; Ihlen & Vereijken, 2010; Thornton & Gilden, 2005; Van Orden et al., 2003; Wagenmakers et al., 2004). Thus, fractal scaling can provide only indirect evidence of multiscale interactions in psychological performance. The current work sought to demonstrate the existence of multiscale coordination by more direct means.

In both experiments, multiple physiological and behavioral measures were recorded and compared with a new analytical method called multiscale lagged regression (MLR). The method assessed how dependence between psychological time series varies as function of both time and scale. This is a major advantage over fractal analysis of psychological time series that is commonly used to construct arguments of multiscale interactions (e.g., Kello et al., 2010; Kelty-Stephen et al., 2012; Van Orden et al., 2003).

As noted in the preceding paragraph, information gained from fractal analysis has limited value in identifying underlying dynamics. That is not say that observation of fractal scaling is unimportant. To the contrary, observation of fractal scaling provides a clue that observable behavior may be conceived as the product of a complex, dynamical system (e.g., Van Orden et al., 2003; Van Orden et al., 2005). Nonetheless, that is only a clue. Fractal analysis reveals that time series exhibit some form of multiscale relationship but tells very little about the nature of that relationship. The meaning of fractal scaling becomes even more opaque in multivariate forms of fractal analysis (Kristoufek, 2013; Podobnik & Stanley, 2008; Xiong & Shang, 2016). In contrast, MLR measures the magnitude and direction in the relationships between psychological time series. In the current work, MLR allowed the following question to be asked and answered: How do the multiple scales that make up behavior actually interact?

The results from both experiments showed evidence of multiscale interaction among the many processes that support psychological performance. Those patterns can be distilled into several general observations. The coming sections examine those observations by revisiting the multiscale patterns of interaction observed in each experiment before discussing those findings within the context of experimental manipulations and performance data.

Multiscale interactions in Experiment 1. The application of MLR to behavioral and physiological data was first explored in Experiment 1. In general, the results supported the hypothesis that psychological processes interact over multiple temporal scales. In all cases examined, the relationships among physiological and behavioral components of behavior are distinguishable from randomness. Simulation 3 in Appendix

A shows that when processes are unrelated over time and scale, $\beta_1(s,l)$ is practically zero for all scales and lags. None of the comparisons considered in Experiment 1 had that characteristic. At the most surface level, that means multiscale interactions are not random. At first, that result seems somewhat trivial; however, the deeper implication is that the multiscale randomness model of fractal scaling may not be a reasonable explanation of the complexity observed in human performance (Gardner, 1978; Wagenmakers et al., 2004). That result is also important because detecting deviations from randomness has figured prominently into theories concerning multiscale interactions (Ihlen & Vereijken, 2010; Kelty-Stephen et al., 2012). There are, however, an infinite number of ways to deviate from randomness. The purpose of this experiment was to investigate how multiscale interactions might be structured. The structure revealed in Experiment 1 took on several general forms.

The major observation was that the relationships between variables tended to be oscillatory in nature, suggesting that the relationship between psychological processes is not constant over time but ebbs and flows in a regular way. Simulations 1 and 7 (Appendix A) showed two ways in which time series might generate oscillations that persist across many temporal lags. The current results depart from those examples in important ways. The time series in those simulations were sinusoids and produced oscillating patterns of correlation across time, a pattern that persisted almost regardless of the scale of analysis. The time series in Experiment 1, on the other hand, were all empirical time series known to produce temporal variability typical of fractal scaling (Fine et al., 2015; Peng et al., 2001; Peng et., 2002; Collins & DeLuca, 1995). Thus, the

finding that the observed time series produced oscillatory relationships over time is surprising. Implications will be discussed in the concluding sections of this manuscript.

A further departure from Simulations 1 and 7 is fact that the frequency of oscillatory relationships did not persist across all time scales. Figure 6 showed that the MLR-revealed relationship between postural path length and respiratory rate was organized into distinct scale ranges that coincided with different frequencies of oscillation, a pattern observed in the comparisons of postural path length and heart rate (Figure 7) and heart rate and respiratory rate (Figure 8). Those findings are interesting because they may reflect the time course typical of coordination among bodily systems. Postural corrections are known to coincide with the time course of respiration (e.g., Bouisset et al, 1994; Hodges et al., 2002) as does variability in heart rate (Acharya et al., 2006). For example, frequency analysis of postural correction time series reliably produces significant power in frequency bands typical for human respiration (Bouisset et al, 1994). MLR appears to have also captured those relationships because oscillations found in the moderate scale sizes of Figures 6 and 7 are consistent with the typical rates of human breathing.

Other typical observations were that the magnitude of MLR coefficients tended to be graded across scales, and gradation was directionally dependent. For example, when MLR was used to predict changes in movement frequency from changes in heart rate, MLR coefficients tended to be small at small scales and large at large scales [Figure 5(a)]. That result implies that patterns in heart rate variability are seemingly inconsequential to movement frequency over small time windows but large scale heart rate variability may come to play a larger role in predicting movement frequency, at least

in the current task. In contrast, Figure 5 (b) showed that changes in movement frequency only tend to predict changes in heart rate at finer scales. Those patterns of results were not limited to movement frequency and heart rate. Figure 4 showed that changes in movement frequency predicted rapid, oscillatory changes in postural path length; however, changes in postural path length only predicted slowly undulating changes in movement frequency that registered at time scales greater than 15 seconds.

Results concerning gradation and directional dependence are exciting because they have great potential for application. One idea for applied research would be to investigate multiscale relationships in tasks involving expert manual dexterity. For instance, researchers could investigate the psychophysiological context of mistakes made during simulated surgeries. Are errors made in the context of brief, intermittent physiological flutters like sharp but fleeting increases in heart rate or respiratory rate? Alternatively, do errors emerge when changes in physiological processes extend over longer stretches of time? Trends revealed from those types of studies could be used to develop new monitoring techniques and introduce potentially life-saving interventions. Imagine a surgeon wearing unobtrusive monitoring gear that could alert her when her psychophysiological context predicts danger. Relatedly, MLR could characterize points of vulnerability in a system as well as provide a means to assess, and even predict, how perturbations are absorbed within a system (Likens et al., 2014). Simulation 6 in Appendix A readily captures that idea. In that simulation, regular perturbations introduced in one part of the system seem to cascade to larger and larger scales in another part of the system. Those results are likewise exciting because of the importance recent research has placed on understanding the effects of perturbations in team coordination

research (Gorman et al., 2010a, b; Likens et al., 2014). That is, researchers could introduce perturbations like a loss of communication at a specific point in time and observe how communication failure affects team performance at different temporal scales. Perhaps the effect is transient, only degrading performance, momentarily. Maybe the effect diffuses across both time and scale, causing widespread performance issues. The current result suggest that it may be possible to diagnose either case and understand the potency of perturbations in team coordination and many other applied research areas.

Multiscale Interactions in Experiment 2. Application of MLR revealed patterns both similar to and distinct from those in Experiment 1. Consistent across both experiments was the observation that relationships among the psychological processes tends to be oscillatory, scale-dependent in nature and, in many cases, appears to exhibit directional dependence. Experiment 2 data presented two deviations from those general tendencies. One departure emerged when MLR was used to compare eye movement frequency and heart rate during the movement perturbation task. In strict contrast to other process pairs considered in these experiments, those results were very inconsistent across participants (see Figure 13). There are at least two possible explanations for those results. One possibility is that the relationship between eye movement frequency and heart rate is idiosyncratic, meaning that there are large individual differences in the coordination of those behaviors. Another explanation is that multiscale coordination of eye movement frequency and heart rate may not be important in a pursuit-tracking task. If that is true, then those explanations could come from a common source.

Psychological systems are thought to self-organize into suitable configurations for accomplishing specific tasks (Bingham, 1988; Gibbs & Van Orden, 2003). There is no *a*

priori reason to suspect that coordination between eye movement frequency and heart rate is essential to the formation of a pursuit tracking device. If coordination of those systems is unimportant in the current task, then perhaps the peculiar patterns revealed in Figure 13 simply reflect idiosyncratic individual differences and task-irrelevant correlation between eye movement frequency and heart rate. The more general implication is that consistency in multiscale coordination observed across participants may reveal the subcomponents important for a particular task. That idea is speculative but could be explored empirically by changing tasks constraints abruptly within continuous performances.

MLR comparison across different neural measurement sites showed a more systematic deviation from the general tendencies observed in Experiment 1, excepting oscillatory behavior. In contrast to other process pairs, oscillations in the relationships between measured areas of brain activity seemed to maintain the same frequency of oscillation across many temporal scales, a frequency that seemed consistent with the required frequency of the task (Figure 9). That is, oscillatory relationships seemed to exhibit phase alignment across many temporal scales. Capturing oscillations among brain areas is probably not so surprising. EEG studies typically focus either on event related potentials or time-frequency analysis of EEG recordings. That latter of two is based on the premise that neural behavior is oscillatory in nature (Cohen & van Gaal, 2014). Functional connectivity in brain activity is a contemporary topic in neuroscience (e.g., Friston, 2011), and there is considerable evidence that regular stimuli produced regular neural oscillations often in time with frequency of the stimulus (Vialette, Maurice, Dauwels, & Cichocki, 2010). What is remarkable, though, is that oscillatory

patterns involving neural dynamics captured by MLR have so much in common with the dynamics observed among other bodily processes. That is, MLR results suggest that that oscillation is a general means with which systems of the body organize in service of behavior.

Multiscale Interactions in Pursuit-Tracking Systems. At the outset of this paper, the claim was made that finding evidence of multiscale coordination becomes interesting when grounded in other psychologically meaningful variables. Many patterns of multiscale interaction have been reported so far. The lingering issues to be explored in this paper are concerned with how those patterns might predict performance in the pursuit tracking task. To address those issues, total power in average lag-wise MLR coefficients was introduced as a singular measure of multiscale coordination. Hypotheses concerning the relationship between total power and performance variables (SDRP and RT) were necessarily two-tailed. The results show some promise in terms of prediction but must be interpreted with caution.

In Experiment 1, several process pairs gave evidence that multiscale interactions seem to play a role in performance of a pursuit tracking task. The results showed that total power from several process pairs predicted SDRP and was implicated in several interactions with perturbations. Unfortunately, the magnitude and direction of those effects is less than straight forward. For example, total power from MLR of movement frequency on respiratory rate shows a negative relationship with SDRP. MLR of respiratory rate on movement frequency shows the opposite trend. Based on the patterns present in Figure 4 (a) and (b), one might be tempted to think that differences in slope reflect directional dependence in gradation captured by MLR; however, there was simply

not enough consistency among results to draw that conclusion. Similar statements can be made concerning interaction effects. Interactions between total power and condition suggest that the relationship between multiscale interactions and SDRP depends on task constraints. Unfortunately, interaction effects were not consistent. Sometimes negative slopes became positive during a perturbation. Sometimes positive slopes became negative, making direct interpretation of those results difficult. However, the presence of any interaction warrants some discussion.

Interactions imply that relationship between multiscale coordination and performance during steady state behavior is somehow different when behavior is perturbed. One of the claims associated with a dynamical systems explanation of fractal scaling is that fractal variability reflects a system flexibly adapting to perturbations both internal and external to the system (Likens et al., 2014; Van Orden et al., 2003). The fly in the ointment is that fractal properties often degrade in the face of external constraints (e.g., Dingwell & Cusumano, 2010; Holden et al., 2011; Likens et al., 2015). That is, evidence of fractal scaling is most likely to be observed when a system is engaged but not overly restricted (e.g., Holden et al., 2011). The current results suggest a reason why, namely, coordinative structures vary according to the constraints of task.

Experiment 2 introduced a new task, a go/no reaction time task and found that, for neural process pairs, total power may predict RT in a consistent way. For each process pair, total power from at least one MLR direction was significant. Moreover, each of those slopes was negative, suggesting increases in total power predict faster responses. In contrast, there was no measurable relationship between total power and SDRP for any of the process pairs. The lack of an effect for total power concerning eye movement

frequency and heart rate is not surprising given the peculiar results already discussed at some length. However, given the results of Experiment 1 and the regularity present in Figures 10, 11, 14, & 15, null results concerning eye movement frequency and EEG are surprising. One possible explanation for that effect is statistical. The sample size is relatively small and it could be that the sample did not generate enough variability to reveal the same relationships observed in Experiment 1.

Limitations and Future Directions

The analyses and results presented in this dissertation hinge upon the new analytical technique introduced in Experiment 1 and Appendix A, namely, multiscale lagged regression. Therefore, it is important to discuss limitations of the MLR tool. Acknowledging those limitations in no way diminishes the current findings but provides a convenient segue to discuss ongoing and future developments of MLR. One important limitation is that MLR is only a bivariate tool. Future work will address extending the technique to include multiple predictor variables as a further compliment to existing regression techniques (Cohen et al., 2003; Hill et al., 2011). One of the most powerful aspects the regression framework is the ability to control for covariates when assessing the relationship between a predictor and a criterion. Extending that idea to the MLR tool will be challenging but, if possible, would allow researchers to control for the influence of covariates at many different time scales. Another limitation is that, in its current form, MLR does not asses model fit or provide other statistics common in regression procedures (e.g., R^2, F statistics, p values, and so on). Already, it is possible to assess scale-wise R^2 in the DFA-based regression introduced in Kristoufek (2015); however, future work will explore the generality of such measures in MLR.

Another limitation to the current findings is that total power may not be the best metric for summarizing MLR coefficients. The MLR tool is new and still under development, and future work will investigate other ways of characterizing MLR-revealed structure. If the oscillatory patterns shown in these experiments are general and replicable, then one possibility is the use of differential equation modeling of the activity observed at each scale (e.g., Butner, Amazeen, & Mulvey, 2005; Butner, Gagnon, Geuss, & Lassard, 2015). Oscillatory patterns across both experiments suggest damped oscillator models would be a good place to start. Estimation of those models via multilevel modeling techniques could reveal stability of oscillatory relationships at different time scales (i.e., Lyapunov exponents, Rosenstein, Collins, & DeLuca, 1993). This has implications for the earlier discussion regarding detecting points of vulnerability. Lyapunov exponents describe, among other things, the resistance of a system to external perturbations. Knowing the Lyapunov exponents for a given scale of analysis is then tantamount to knowing how vulnerable that scale level is to perturbation. Ongoing work is exploring the utility of those modeling approaches in settings similar to those explored in this dissertation.

The current results make clear the fact that MLR uncovers multiscale interactions among the systems that make up a pursuit-tracking system. However, it is also clear that establishing the importance of those relationships in psychological contexts means characterizing multiscale interactions in the most appropriate way. There are many possible means of distilling those relationships that future work concerning MLR will address.

Multiscale Interactions in Psychological Systems

The results from these experiments suggest that an oscillatory form of coordination is a default behavior among the many systems involved in pursuit-tracking, even when the systems themselves are not oscillatory. That was stated explicitly with respect to measures from Experiment 1 (Fine et al., 2015; Peng et al., 2001; Peng et., 2002; Collins & DeLuca, 1995) but holds true for measures used in Experiment 2. These findings stand to impact a field that has long relied on indirect evidence to make conclusions about the underlying dynamics in psychological systems. Measurements of fractal scaling have come to dominate much of the contemporary literature on dynamical systems approaches to cognition, perception, and action. Indeed, the large literature reviewed in the introduction gives the impression that once the Hurst exponent is known, the system under study is understood. The results of these experiments propose an alternative point of view.

Fractal analysis of rough-looking time series is just the starting point for dynamical systems approaches to understanding psychological systems. Without a doubt, it is an exciting idea that such a simple measure like the Hurst exponent could somehow provide a general metric of health (e.g., Peng et al., 2001), learning (e.g., Nourritt-Lucas et al., 2015), social coordination (e.g., Fine et al., 2015; Marmelat & Delignieres, 2012) and so on. However, persistent pursuit of fractal scaling leads down a blind alley, without fully appreciating why fractal properties are so pervasive. It has already been established that understanding the meaning and significance of fractal scaling requires understanding the experimental contexts in which it is reasonable to observe fractal scaling (e.g., Likens et al., 2015). The current results take that notion one step further

because direct demonstration of multiscale interactions means it should be possible to explain why fractal properties vary across experimental contexts, in the first place.

References

Aks, D. J., Zelinsky, G. J., & Sprott, J. C. (2002). Memory across eye-movements: 1/f dynamic in visual search. *Nonlinear dynamics, psychology, and life sciences*, *6*(1), 1-25.

Almurad, Z. M., & Delignières, D. (2016). Evenly spacing in detrended fluctuation analysis. *Physica A: Statistical Mechanics and its Applications*, *451*, 63-69.

Amazeen, P. G., Amazeen, E. L., & Turvey, M. T. (1998). Dynamics of human intersegmental coordination: Theory and research. *Timing of behavior: Neural, psychological, and computational perspectives*, 237-259.

Anastas, J. R., Stephen, D. G., & Dixon, J. A. (2011). The scaling behavior of hand motions reveals self-organization during an executive function task. *Physica A: Statistical Mechanics and its Applications*, *390*(9), 1539-1545.

Andersson, B. J., Ortengren, R. O. L. A. N. D., Nachemson, A. L., Elfström, G., & Broman, H. (1975). The sitting posture: an electromyographic and discometric study.

Acharya, U. R., Joseph, K. P., Kannathal, N., Lim, C. M., & Suri, J. S. (2006). Heart rate variability: a review. *Medical and biological engineering and computing*, *44*(12), 1031-1051.

Barros, A. K., & Ohnishi, N. (2001). Heart instantaneous frequency (HIF): an alternative approach to extract heart rate variability. *IEEE transactions on biomedical engineering*, *48*(8), 850-855.

Bashan, A., Bartsch, R., Kantelhardt, J. W., & Havlin, S. (2008). Comparison of detrending methods for fluctuation analysis. *Physica A: Statistical Mechanics and its Applications*, *387*(21), 5080-5090.

Beran, J. (1994). *Statistics for Long Memory Processes.* Boca Raton, Florida: Chapman Hall/CRC.

Bernstein, N. A. (1967). The co-ordination and regulation of movements.

Bingham, G. P. (1988). Task-specific devices and the perceptual bottleneck. *Human Movement Science*, *7*(2), 225-264.

Buchheit, M., Al Haddad, H., Laursen, P. B., & Ahmaidi, S. (2009). Effect of body posture on postexercise parasympathetic reactivation in men. *Experimental Physiology*, *94*(7), 795-804.

Butner, J. E., Gagnon, K. T., Geuss, M. N., Lessard, D. A., & Story, T. N. (2015). Utilizing topology to generate and test theories of change. *Psychological methods*, *20*(1), 1.

Chen, Y., Ding, M., & Kelso, J. S. (1997). Long memory processes ($1/f^{\alpha}$ type) in human coordination. *Physical Review Letters*, *79*(22), 4501.

Coey, C. A., Washburn, A., Hassebrock, J., & Richardson, M. J. (2016). Complexity matching effects in bimanual and interpersonal syncopated finger tapping. *Neuroscience letters*, *616*, 204-210.

Cohen, J., Cohen, P., West, S. G., & Aiken, L. S. (2003). *Applied multiple regression/correlation analysis for the behavioral sciences*. Mahwah, New Jersey: Lawrence Erlbaum Associates.

Collins, J. J., & De Luca, C. J. (1993). Open-loop and closed-loop control of posture: A random-walk analysis of center-of-pressure trajectories. *Experimental Brain Research, 95*, 308-318.

Cohen, M. X., & van Gaal, S. (2014). Subthreshold muscle twitches dissociate oscillatory neural signatures of conflicts from errors. *Neuroimage*, *86*, 503-513.

Davis, T. J., Brooks, T. R., & Dixon, J. A. (2016). Multi-scale interactions in interpersonal coordination. *Journal of Sport and Health Science*, *5*(1), 25-34.

Delorme, A., & Makeig, S. (2004). EEGLAB: an open source toolbox for analysis of single-trial EEG dynamics including independent component analysis. *Journal of neuroscience methods*, *134*(1), 9-21.

Demos, A. P., Chaffin, R., & Kant, V. (2014). Toward a dynamical theory of body movement in musical performance. *Frontiers in psychology*, *5*, 477.

Diniz, A., Wijnants, M. L., Torre, K., Barreiros, J., Crato, N., Bosman, A. M., ... & Delignières, D. (2011). Contemporary theories of 1/f noise in motor control. *Human Movement Science*, *30*(5), 889-905.

Dixon, J. A., Holden, J. G., Mirman, D., & Stephen, D. G. (2012). Multifractal dynamics in the emergence of cognitive structure. *Topics in Cognitive Science*, *4*(1), 51-62.

Eke, A., Herman, P., Sanganahalli, B. G., Hyder, F., Mukli, P., & Nagy, Z. (2012). Pitfalls in fractal time series analysis: fMRI BOLD as an exemplary case. *Frontiers in physiology*, *3*, 417.

Eke, A., Herman, P., Kocsis, L., & Kozak, L. R. (2002). Fractal characterization of complexity in temporal physiological signals. *Physiological measurement*, *23*(1), R1-R38.

Fine, J. M., Likens, A. D., Amazeen, E. L., & Amazeen, P. G. (2015). Emergent complexity matching in interpersonal coordination: Local dynamics and global variability. *41*(3), 723-737.

Gardner, M. (1978). White and brown music, fractal curves and one-over-f fluctuations. *Scientific American*, *238*(4), 16-27.

Gibbs Jr, R. W., & Van Orden, G. C. (2003). Are emotional expressions intentional?: A self-organizational approach. *Consciousness & emotion*, *4*(1), 1-16.

Gilden, D. L. (2001). Cognitive emissions of 1/f noise. *Psychological review*, *108*(1), 33.

Gilden, D. L., Thornton, T., & Mallon, M. W. (1995). 1/f noise in human cognition. *Science*, *267*(5205), 1837-1839.

Granger, C. W., & Newbold, P. (1974). Spurious regressions in econometrics. *Journal of econometrics*, *2*(2), 111-120.

Hausdorff, J. M., Ashkenazy, Y., Peng, C. K., Ivanov, P. C., Stanley, H. E., & Goldberger, A. L. (2001). When human walking becomes random walking: fractal analysis and modeling of gait rhythm fluctuations. *Physica A: Statistical mechanics and its applications*, *302*(1), 138-147.

Hausdorff, J. M., Mitchell, S. L., Firtion, R., Peng, C. K., Cudkowicz, M. E., Wei, J. Y., & Goldberger, A. L. (1997). Altered fractal dynamics of gait: reduced stride-interval correlations with aging and Huntington's disease. *Journal of applied physiology*, *82*(1), 262-269.

Hausdorff, J. M., & Peng, C. K. (1996). Multiscaled randomness: A possible source of 1/f noise in biology. *Physical review E*, *54*(2), 2154.

Hausdorff, J. M., Purdon, P. L., Peng, C. K., Ladin, Z. V. I., Wei, J. Y., & Goldberger, A. L. (1996). Fractal dynamics of human gait: stability of long-range correlations in stride interval fluctuations. *Journal of applied physiology*, *80*(5), 1448-1457.

Hill, R. C., Griffiths, W. E., Lim, G. C. (2011). *Principles of Econometrics, 4th Edition*. Hoboken, New Jersey: John Wiley & Sons.

Holden, J. G., Choi, I., Amazeen, P. G., & Van Orden, G. (2011). Fractal 1/*f* dynamics suggest entanglement of measurement and human performance. *Journal of Experimental Psychology: Human Perception and Performance*, *37*(3), 935.

Hyvärinen, A., & Oja, E. (2000). Independent component analysis: algorithms and applications. *Neural networks*, *13*(4), 411-430.

Ihlen, E. A., & Vereijken, B. (2010). Interaction-dominant dynamics in human cognition: Beyond $1/f$ α fluctuation. *Journal of Experimental Psychology: General*, *139*(3), 436.

Ihlen, E. A., & Vereijken, B. (2013a). Multifractal formalisms of human behavior. *Human movement science*, *32*(4), 633-651.

Ihlen, E. A., & Vereijken, B. (2013b). Identifying multiplicative interactions between temporal scales of human movement variability. *Annals of biomedical engineering*, *41*(8), 1635-1645.

Ivanov, P. C., Amaral, L. A. N., Goldberger, A. L., Havlin, S., Rosenblum, M. G., Stanley, H. E., & Struzik, Z. R. (2001). From 1/f noise to multifractal cascades in heartbeat dynamics. *Chaos: An Interdisciplinary Journal of Nonlinear Science, 11*(3), 641-652.

Ivanov, P. C., Amaral, L. A. N., Goldberger, A. L., Havlin, S., Rosenblum, M. G., Struzik, Z. R., & Stanley, H. E. (1999). Multifractality in human heartbeat dynamics. *Nature, 399*(6735), 461-465.

Kello, C. T., Anderson, G. G., Holden, J. G., & Van Orden, G. C. (2008). The pervasiveness of 1/f scaling in speech reflects the metastable basis of cognition. *Cognitive Science*, *32*(7), 1217-1231.

Kello, C. T., Brown, G. D., Ferrer-i-Cancho, R., Holden, J. G., Linkenkaer-Hansen, K., Rhodes, T., & Van Orden, G. C. (2010). Scaling laws in cognitive sciences. *Trends in cognitive sciences*, *14*(5), 223-232.

Kelso, J. A. (1984). Phase transitions and critical behavior in human bimanual coordination. *American Journal of Physiology-Regulatory, Integrative and Comparative Physiology*, *246*(6), R1000-R1004.

Kelso, J. A. S., Buchanan, J. J., DeGuzman, G. C., & Ding, M. (1993). Spontaneous recruitment and annihilation of degrees of freedom in biological coordination. *Physics Letters A*, *179*(4), 364-371.

Kelty-Stephen, D. G., & Dixon, J. A. (2014). Interwoven fluctuations during intermodal perception: Fractality in head sway supports the use of visual feedback in haptic perceptual judgments by manual wielding. *Journal of Experimental Psychology: Human Perception and Performance*, *40*(6), 2289.

Kelty-Stephen, D. G., Palatinus, K., Saltzman, E., & Dixon, J. A. (2013). A tutorial on multifractality, cascades, and interactivity for empirical time series in ecological science. *Ecological Psychology*, *25*(1), 1-62.

Kristoufek, L. (2013). Mixed-correlated ARFIMA processes for power-law cross-correlations. *Physica A: Statistical Mechanics and its Applications*, *392*(24), 6484-6493.

Kristoufek, L. (2015). Detrended fluctuation analysis as a regression framework: Estimating dependence at different scales. *Physical Review E*, *91*(2), 022802.

Kugler, P. N., & Turvey, M. T. (1987). *Information, Natural Law, and the Self-Assembly of Rhythmic Movement*. New York, New York: Routledge.

Lemoine, L., Torre, K., & Delignières, D. (2006). Testing for the presence of 1/f noise in continuation tapping data. *Canadian Journal of Experimental Psychology/Revue canadienne de psychologie expérimentale*, *60*(4), 247.

Likens, A. D., Amazeen, P. G., Stevens, R., Galloway, T., & Gorman, J. C. (2014). Neural signatures of team coordination are revealed by multifractal analysis. *Social neuroscience*, *9*(3), 219-234.

Likens, A. D., Fine, J. M., Amazeen, E. L., & Amazeen, P. G. (2015). Experimental control of scaling behavior: What is not fractal? *Experimental Brain Research, 233*(10)*,* 2813-2821.

Mandelbrot, B. B. (1967). How long is the coast of Britain. *Science*, *156*(3775), 636-638.

Mandelbrot, B. (1974). Intermittent turbulence in self-similar cascades: Divergence of high moments and dimension of the carrier. *Journal of Fluid Mechanics, 62,* 331-358.

Mandelbrot, B. B. (1975). Stochastic models for the Earth's relief, the shape and the fractal dimension of the coastlines, and the number-area rule for islands. *Proceedings of the National Academy of Sciences*, *72*(10), 3825-3828.

Mandelbrot, B. (1982). *The Fractal Geometry of Nature.* New York, New York: W.H. Freeman and Company.

Marmelat, V., & Delignières, D. (2012). Strong anticipation: complexity matching in interpersonal coordination. *Experimental Brain Research*, *222*(1), 137-148.

Nagel, M., Sprenger, A., Zapf, S., Erdmann, C., Kömpf, D., Heide, W., ... & Lencer, R. (2006). Parametric modulation of cortical activation during smooth pursuit with and without target blanking. An fMRI study. *Neuroimage*, *29*(4), 1319-1325.

Nonaka, T., & Bril, B. (2014). Fractal dynamics in dexterous tool use: The case of hammering behavior of bead craftsmen. *Journal of Experimental Psychology: Human Perception and Performance*, *40*(1), 218-231.

Nourrit-Lucas, D., Tossa, A. O., Zelic, G., & Delignieres, D. (2015). Learning, motor skill, and long-range correlations. *Journal of motor behavior*, *47*(3), 182-189.

Palatinus, Z., Kelty-Stephen, D. G., Kinsella-Shaw, J., Carello, C., & Turvey, M. T. (2014). Haptic perceptual intent in quiet standing affects multifractal scaling of postural fluctuations. *Journal of Experimental Psychology: Human Perception and Performance*, *40*(5), 1808-1818.

Peng, C. K., Havlin, S., Stanley, H. E., & Goldberger, A. L. (1995). Quantification of scaling exponents and crossover phenomena in nonstationary heartbeat time series. *Chaos: An Interdisciplinary Journal of Nonlinear Science*, *5*(1), 82-87.

Peng, C. K., Henry, I. C., Mietus, J. E., Hausdorff, J. M., Khalsa, G., Benson, H., & Goldberger, A. L. (2004). Heart rate dynamics during three forms of meditation. *International journal of cardiology*, *95*(1), 19-27.

Peng, C. K., Mietus, J. E., Liu, Y., Lee, C., Hausdorff, J. M., Stanley, H. E., ... & Lipsitz, L. A. (2002). Quantifying fractal dynamics of human respiration: age and gender effects. *Annals of biomedical engineering*, *30*(5), 683-692.

Pew, R. W. (1974). Levels of analysis in motor control. *Brain Research, 71,* 393-400.

Podobnik, B., & Stanley, H. E. (2008). Detrended cross-correlation analysis: a new method for analyzing two nonstationary time series. *Physical review letters*, *100*(8), 084102.

Pomeranz, B., Macaulay, R. J., Caudill, M. A., Kutz, I., Adam, D., Gordon, D. A. V. I. D., ... & Cohen, R. J. (1985). Assessment of autonomic function in humans by heart rate spectral analysis. *American Journal of Physiology-Heart and Circulatory Physiology*, *248*(1), H151-H153.

Rhodes, T., & Turvey, M. T. (2007). Human memory retrieval as Lévy foraging. *Physica A: Statistical Mechanics and its Applications*, *385*(1), 255-260.

Riley, M. A., & Van Orden, G. C. (2005). Tutorials in Contemporary Nonlinear Methods for the behavioral sciences. Retrieved from http: //www.nsf.gov/sbe/bcs/pac/nmbs /nmbs.jsp

Rosenstein, M. T., Collins, J. J., & De Luca, C. J. (1993). A practical method for calculating largest Lyapunov exponents from small data sets. *Physica D: Nonlinear Phenomena*, *65*(1-2), 117-134.

Stephen, D. G., & Anastas, J. (2011). Fractal fluctuations in gaze speed visual search. *Attention, Perception, & Psychophysics*, *73*(3), 666-677.

Stephen, D. G., Anastas, J. R., & Dixon, J. A. (2012). Scaling in cognitive performance reflects multiplicative multifractal cascade dynamics. *Frontiers in physiology*, *3*.

Stephen, D. G., Arzamarski, R., & Michaels, C. F. (2010). The role of fractality in perceptual learning: exploration in dynamic touch. *Journal of Experimental Psychology: Human Perception and Performance*, *36*(5), 1161.

Stephen, D. G., Broncoddo, R. A., Magnuson, J. S., & Dixon, J. A. (2009). The dynamics of insight: Mathematical discovery as a phase transition. *Memory & Cognition*, *37*(8), 1132-1149.

Stephen, D. G., & Hajnal, A. (2011). Transfer of calibration between hand and foot: Functional equivalence and fractal fluctuations. *Attention, Perception, & Psychophysics*, *73*(5), 1302-1328.

Stephen, D. G., Hsu, W. H., Young, D., Saltzman, E. L., Holt, K. G., Newman, D. J., ... & Goldfield, E. C. (2012). Multifractal fluctuations in joint angles during infant spontaneous kicking reveal multiplicativity-driven coordination. *Chaos, Solitons & Fractals*, *45*(9), 1201-1219.

Stephen, D. G., & Mirman, D. (2010). Interactions dominate the dynamics of visual cognition. *Cognition*, *115*(1), 154-165.

Strayer, D. L., & Johnston, W. A. (2001). Driven to distraction: Dual-task studies of simulated driving and conversing on a cellular telephone. *Psychological science*, *12*(6), 462-466.

Szary, J., Dale, R., Kello, C. T., & Rhodes, T. (2015). Patterns of interaction-dominant dynamics in individual versus collaborative memory foraging. *Cognitive processing*, *16*(4), 389-399.

Takahashi, T., Okada, A., Saitoh, T., Hayano, J., & Miyamoto, Y. (2000). Difference in human cardiovascular response between upright and supine recovery from upright cycle exercise. *European journal of applied physiology*, *81*(3), 233-239.

Thornton, T. L., & Gilden, D. L. (2005). Provenance of correlations in psychological data. *Psychonomic Bulletin & Review*, *12*(3), 409-441.

Torre, K., & Wagenmakers, E. J. (2009). Theories and models for $1/f^{\beta}$ noise in human movement science. *Human movement science*, *28*(3), 297-318.

Turvey, M. T., & Carello, C. (2011). Obtaining information by dynamic (effortful) touching. *Philosophical Transactions of the Royal Society B*, *366*(1581), 3123-3132.

Van Orden, G. C., Holden, J. G., & Turvey, M. T. (2003). Self-organization of cognitive performance. *Journal of Experimental Psychology: General*, *132*(3), 331.

Van Orden, G. C., Holden, J. G., & Turvey, M. T. (2005). Human cognition and 1/f scaling. *Journal of Experimental Psychology: General*, *134*(1), 117.

Vialatte, F. B., Maurice, M., Dauwels, J., & Cichocki, A. (2010). Steady-state visually evoked potentials: focus on essential paradigms and future perspectives. *Progress in neurobiology*, *90*(4), 418-438.

Voss, R. F., & Clarke, J. (1975). 1/f ‘noise' in music and speech. *Nature*, *258*, 317-318.

Voytek, B., Kramer, M. A., Case, J., Lepage, K. Q., Tempesta, Z. R., Knight, R. T., & Gazzaley, A. (2015). Age-related changes in 1/f neural electrophysiological noise. *The Journal of Neuroscience*, *35*(38), 13257-13265.

Wagenmakers, E. J., Farrell, S., & Ratcliff, R. (2004). Estimation and interpretation of 1/fα noise in human cognition. *Psychonomic bulletin & review*, *11*(4), 579-615.

Wagenmakers, E. J., van der Maas, H. L., & Farrell, S. (2012). Abstract Concepts Require Concrete Models: Why Cognitive Scientists Have Not Yet Embraced Nonlinearly Coupled, Dynamical, Self-Organized Critical, Synergistic, Scale-Free, Exquisitely Context-Sensitive, Interaction-Dominant, Multifractal, Interdependent Brain-Body-Niche Systems. *Topics in cognitive science*, *4*(1), 87-93.

Watkins, N. W., Pruessner, G., Chapman, S. C., Crosby, N. B., & Jensen, H. J. (2015). 25 Years of Self-organized Criticality: Concepts and Controversies. *Space Science Reviews*, 1-42.

Webber, C. L., Marwan, N. (2015). *Recurrence Quantification Analysis -- Theory and Best Practices.* New York, New York: Springer International Publishing.

West, B. J., Griffin, L. A., Frederick, H. J., & Moon, R. E. (2005). The independently fractal nature of respiration and heart rate during exercise under normobaric and hyperbaric conditions. *Respiratory physiology & neurobiology*, *145*(2), 219-233.

Wijnants, M. L. (2014). A review of theoretical perspectives in cognitive science on the presence of scaling in coordinated physiological and cognitive processes. *Journal of Nonlinear Dynamics*, *2014*.

Wijnants, M., Cox, R., Hasselman, F., Bosman, A., & Van Orden, G. (2012). A trade-off study revealing nested timescales of constraint. *Frontiers in physiology*, *3*, 116.

Woyshville, M. J., & Calabrese, J. R. (1994). Quantification of occipital EEG changes in Alzheimer's disease utilizing a new metric: the fractal dimension. *Biological psychiatry*, *35*(6), 381-387.

Xiong, H., & Shang, P. (2017). Detrended fluctuation analysis of multivariate time series. *Communications in Nonlinear Science and Numerical Simulation*, *42*, 12-21.

APPENDIX A

MULTISCALE LAGGED REGRESSION

The literature on fractal scaling in psychological time series has principally relied on the idea that complexity emerges in psychological time series from coordination across multiple scales of analysis, and historically, documentation has relied heavily on a broad range of statistical methods known as fractal analysis (Eke et al., 2002; Eke et al., 2012; Beran, 1994). The purpose of this section is threefold: (1) it provides a brief and minimally technical overview of ordinary least squares regression and fractal analysis; (2) it discusses reasons why, on their own, those methods are insufficient for characterizing coordination across scales; and (3) it synthesizes those tools into a new method for analyzing temporal relationships across multiple temporal scales.

Ordinary least squares regression analysis. This section introduces a new method for the analysis of multiscale systems. The method draws from two methodological sources, ordinary least squares regression and fractal analysis (Cohen, Cohen, West, & Aiken, 2003; Eke et al., 2002; Kristoufek, 2015). Given its importance to the proposed analysis, a brief review of least squares regression is warranted before giving full attention to the new technique. Least squares regression is arguably the most general tool for studying the relationship between two or more variables. In the bivariate time series case, least squares regression is concerned with estimating the coefficients in the general equation,

$$Y_t = \beta_0 + \beta_1 X_t + \epsilon_t, \tag{1}$$

where X_t is a measured predictor at time t, Y_t is the measured criterion at time t, and the ϵ_t gives the difference between the predicted and observed criterion. Thus, β_0 gives the expected value of Y_t when X_t is equal to zero and β_1 gives the expected change in Y_t for a one unit change in X_t, assuming that β_0 is zero. When X is centered at zero, β_0 is

equivalent to the mean of Y_t. Estimation and statistical testing of β_1 is usually the focus and is captured in the following equation,

$$\widehat{\beta_1} = \frac{\sum_{t=1}^{T}(x_t - \bar{x})(y_t - \bar{y})}{\sum_{i=1}^{N}(x_i - \bar{x})^2} \sim \frac{\hat{\sigma}_{XY}}{\widehat{\sigma_X^2}} \quad (2)$$

where,

$$\bar{x} = \sum_{t=1}^{T} x_t \quad (3)$$

and,

$$\bar{y} = \sum_{t=1}^{T} y_t \quad (4)$$

For later development, special attention is given to the fact that the coefficient, $\widehat{\beta_1}$, is essentially ratio of covariance, $\hat{\sigma}_{XY}^2$, over variance, $\widehat{\sigma_X^2}$ because it provides a basic metric of the linear relationship between two variables.

The value of ordinary least squares regression cannot be overstated; however, the standard regression framework illustrated in equations (1) - (4) gives a potentially oversimplified picture of the relationships among psychological variables. In the introduction, numerous examples were given of psychological time series that have structure at multiple scales (e.g., Likens et al., 2014; Likens et al., 2015; Van Orden et al., 2003; Wagenmakers et al., 2004). To the extent that multiscale structure exists in psychological time series, it is reasonable to expect that the relationships among psychological time series might also depend on scale. If so, then the depiction of dependence given by the standard regression framework seems unreasonable, owing to its emphasis on a single temporal scale. In contrast, fractal analysis was developed to explicitly understand how variability changes as a function of scale (e.g., Mandelbrot, 1967), and recent developments in fractal analysis add multiscale resolution to the

regression framework (e.g., Kristoufek, 2013, 2015). The following sections given an overview of fractal analysis before integrating fractal analysis with the general regression framework and extending.

Fractal analysis. Fractal analysis comes in many forms with varying degrees of algorithmic complexity, but nearly all procedures provide a means to capture how some measure of variability changes as a function of scale size. Detrended fluctuation analysis (DFA) is generally considered to be the gold standard, despite newer and more complicated approaches (e.g., Bashan, Bartsch, Kantelhardt, & Havlin, 2008). It forms the basis for the new method introduced in this paper. The DFA algorithm involves five steps: (1) Create the profile by subtracting the mean and then taking the cumulative sum of the time series.

(2) Partition the time series of length, *N*, into *N*/*s* non-overlapping boxes such that each box contains *s* observations. (3) Fit local least squares line within each box and subtract the trend from each data point. (4) Square the residuals within each box. Repeat steps two and three for many *s*, computing the root mean squared residual for each *s*. The maximum *s* should be less than *N*/4, and the range of *s* can be divided either logarithmically (e.g., Peng et al., 1994; Likens et al., 2015) or linearly (e.g., Almurad & Deligniéres, 2016). The result of this step, the fluctuation function, $F_X^2(s)$, is the basic quantity used in fractal analysis (e.g., Mandelbrot, 1967).

(5) Regress the logarithm of $F_X^2(s)$on the logarithm of *s*. The slope resulting from step (5) gives a so-called scaling coefficient, α, and represents the relationship between the measure of variability and scale size. When the relationship between $logF_X^2(s)$ and $logs$ is linear, and α is in the interval, (0.5, 1), then the time series exhibits evidence of fractal

scaling. That is, variability is self-similar over many scales of analysis.

DFA has been extended to bivariate and multivariate settings (e.g., Podobnik & Stanley, 2008; Kristoufek, 2013; Kristoufek, 2015; Xiong & Shang, 2016), where scaling exponents represent the average of the scaling exponents that characterize component processes. The latter observation that bivariate and multivariate extensions to DFA capture the average scaling behavior is theoretically interesting. One implication is that the noise observed in a system's components comes from a common origin. A less obvious implication is that the relationships among a system's components might depend on temporal scale. So, while theoretically interesting, multivariate extensions of DFA are somewhat unsatisfying in that they identify that a multiscale relationship exists among component processes but do not specify what that relationship is, how it changes as a function of scale, or how it might change over time.

Multiscale lagged regression. Considered together, fractal analysis and standard regression make obvious a missing element in the analysis of psychological time series. Recall that variability in psychological performance is thought to emerge from the multiscale interactions among the many components that make up a psychological system (e.g. Van Orden et al., 2003). The litany of positive results from fractal analysis support that claim, but fractal techniques provide very little information concerning the nature of those interactions. Standard regression, while capturing the monoscale relationship between two series, ignores the multiscale structure inherent in psychological time series. What is needed is an analytical method that can elucidate the time-varying relationships among psychological processes, relationships that may be likewise depend upon the many temporal scales that make up behavior. The following paragraphs propose just

such a method.

Recently, Kristoufek (2013; 2015) observed that detrended cross correlation analysis (DCCA; Podobnik & Stanley, 2008) – the bivariate extension of DFA – could be leveraged to develop a multiscale form of regression. The main difference between DFA and DCCA is that DCCA is concerned with the combined fluctuation function, $F_{XY}^2(s)$, between two time series, X_t and Y_t (Podobnik & Stanley, 2008). That is, DCCA performs steps (1) - (3) of the DFA procedure independently for each time series; however, instead of computing the scale-wise variance, $F_X^2(l)$, for each variable in step (4), the scale-wise covariance, $F_{XY}^2(s)$, is computed by taking the cross-product of the scale-wise detrended series and averaging at each scale s. If the joint fractal properties are of interest to the researcher, then she can examine the linear relationship between the logarithm of $F_{XY}^2(s)$ and the logarithm of s.

The resulting slope reflects the average scaling exponent, $\bar{\alpha}_{XY}$, for X_t and Y_t, where $\bar{\alpha}_{XY} = (\alpha_X + \alpha_Y)/2$. However, the current interest is in characterizing how the relationship between X_t and Y_t changes as a function scale and time, not whether the processes have similar scaling properties. Referring back to Equation (2), one can appreciate that the regression coefficient, $\hat{\beta}_1$, is nothing more than the ratio between the covariance of X and Y and the variance of X (Kristoufek, 2015). Thus, the components of the standard regression coefficient are similar to estimates of variance, $F_X^2(s)$, and covariance, $F_{XY}^2(s)$, generated by the DFA and DCCA procedures. Kristoufek (2015) went on to show that scale-wise variance and covariance measures could be used to construct scale-wise regression coefficients,

$$\hat{\beta}_1(s) = F_{XY}^2(s)/F_X^2(s) \quad (5).$$

The current work extends the idea of scale-wise regression coefficient by exploring how the relationships estimated in Equation (5) change as a function of time-lag. Extending the DFA based regression in this way may help to answer questions concerning how changes in one variable at one time scale might be predicted by changes in another variable at a similar time scale, both contemporaneously and in the past. The outlined steps that follow this paragraph represent the new MLR algorithm. Steps 1 – 6 correspond to earlier work developing fractal analysis and DFA based regression. In step 7, the introduction of time lags, reflects my contribution to the DFA based regression framework:

8. Normalize each of two time series, X_t and Y_t, to have zero mean and unit variance.
9. Separate each time series into N/s bins of length s.
10. Within each bin, for each time series and several s, estimate the best fitting line and subtract that line from the binned time series. This step requires some justification. In the original DFA algorithm and in many other forms of fractal analysis (Eke et al., 2010), the interest is in analyzing the intrinsic fluctuations of a system, the ebb and the flow. The detrending procedure was introduced in fractal analysis by Peng and colleagues (1994) to address situations where nonstationarities such as a drift and singularities (e.g., sharp peaks or step-like jumps in time series) might bias estimates of scaling behavior by overestimation of long range correlations. However, detrending data before analysis by regressive techniques has long been a recommendation in time series analysis

where it has been shown that spurious trends lead to gross overestimation of temporal relationships between variables (Granger & Newbold, 1974).

11. Compute the residuals variances for *X* and *Y* as well as residual covariance between the binned series.
12. Compute the average covariance eat each scale, *s*.
13. For each scale, compute the scale-wise regression coefficient as $\hat{\beta}_1(s,l) = F_{XY}^2(s,l)/F_X^2(s,l)$, where *l* is lag of *X*. When *l* is zero, the procedure in Kristoufek (2015) is recovered.
14. Repeat Steps 1 through 6 for several scales and several lags to obtain an $s \times l$ matrix, *B*, that contains the regression coefficients for each scale and lag combination. The resulting rows of *B* give the temporal evolution of relationship between X_t and Y_t.

New analytical techniques require simulations to test and understand behavior of the algorithm. The following simulations help to illustrate the output of multiscale lagged regression (MLR) and demonstrate the generality of MLR in revealing the structure shared by time series data. The method also makes possible striking visualizations of scale by lag relationships, visualizations that prove very useful in making sense of empirical data, where properties are unknown or the series are extremely noisy.

Simulation 1 – Independent sine waves. Two 1 Hz sine waves were generated by at a sampling frequency of 100 Hz, both with zero phase offset and both with unit amplitude [Figure A1 (a) and (b)]. Figure A1 (c) and Figure A1 (d) show the outcome when we use the MLR algorithm on those sine wave series with scales ranging from 0.1 s to 50 s by intervals of 0.5 s and lags ranging from 0.0 s to 5 s in increments of 0.01 s – the graphs

are striking. Colors in Figure A1(c) represent the magnitude of scaled and lagged regression coefficient calculated in step (6). The range is from blue to red, such that blue represents the most negative coefficient (i.e., -1.0), red represents the most positive coefficient (i.e., 1.0) and green represents a coefficient of zero. White regions indicate regions outside the color scale. With that in mind, the results are exactly as one would expect. Moving your eyes from left to right over Figure A1 (c) reveals alternating bands of positive (red) and negative (blue) association, interspersed with zero association. Note that the relationship is the same, regardless of the scale at which one analyzes the data. Figure A1 (d) shows the average $\hat{\beta}_1(s, l)$ at each lag, a quantity used in later analysis. The smooth curve in Figure A1 (d) also captures the oscillatory nature of the sine waves.

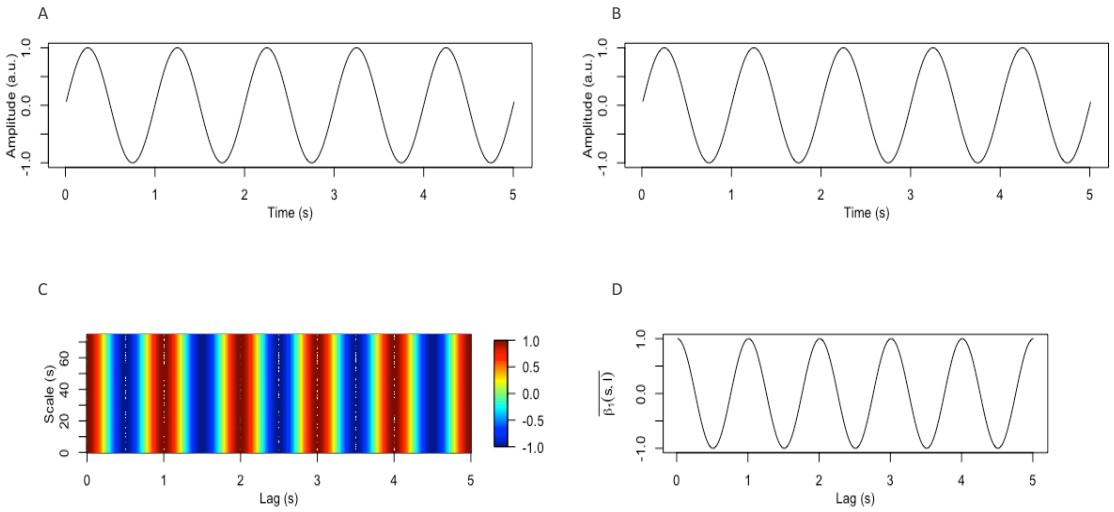

Figure A1. Multiscale lagged regression applied to simple oscillations. Panels (a) and (b) are time series plots of identical sine waves. Panel (c) is a graphical representation of the *B* matrix obtained in step (7) in MLR. As expected, the MLR reveals the oscillatory relationship between these variables. The oscillatory relationship that projects across time is further evident in panel (d), which shows $\hat{\beta}_1(s,l)$ averaged over columns of *B*.

Simulation 2 – Two identical white noise processes. This simulation compares two identical white noise processes [*N*s = 30,000; see Figure A2 (a) and (b)]. One would expect, in this case, that the regression coefficient for all scales should equal unity when the lag is zero but the coefficient should decay rapidly on successive lags. Figure A2 (c) shows that exact pattern as a strong, thin, red line that traverses all scales for a lag of zero but rapidly decays near zero for lags greater than zero and regardless of scale. Figure A2 (d) demonstrates that average $\hat{\beta}_1(s,l)$ is near 1.0 at lag zero but is close to zero for all other values.

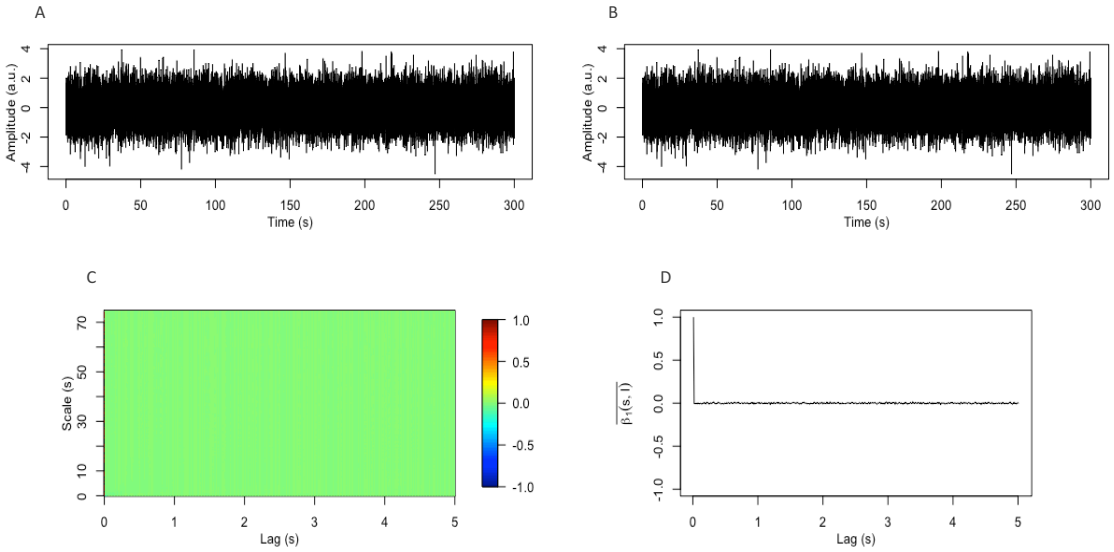

Figure A2. Multiscale lagged regression for identical white noise processes. Panels (a) and (b) are time series plots of identical white noise. Panel (c) is a graphical representation of the *B* matrix obtained in step (7) in MLR. The nature of the relationship is difficult to observe in (d) because, as expected, most lags and scales produce a $\hat{\beta}_1(s,l)$ very near zero. The singular exception is at lag zero when one time series perfectly predicts the other (i.e., itself).

Simulation 3 – Two independent white noise processes. Two distinct white noise processes were generated with zero mean and unit variance (*N*s = 30,000). Similar to the previous simulation, the expectation is that the majority of scaled and lagged regression coefficients should be zero. Where this example is expected to differ is that the lag zero coefficient is also expected to be near zero, regardless of scale. Figure A3 (a) and (b) show the simulated time series, and Figure A3 (c) and (d) show the expected result, namely, that the series are independent of one another, regardless of time or scale.

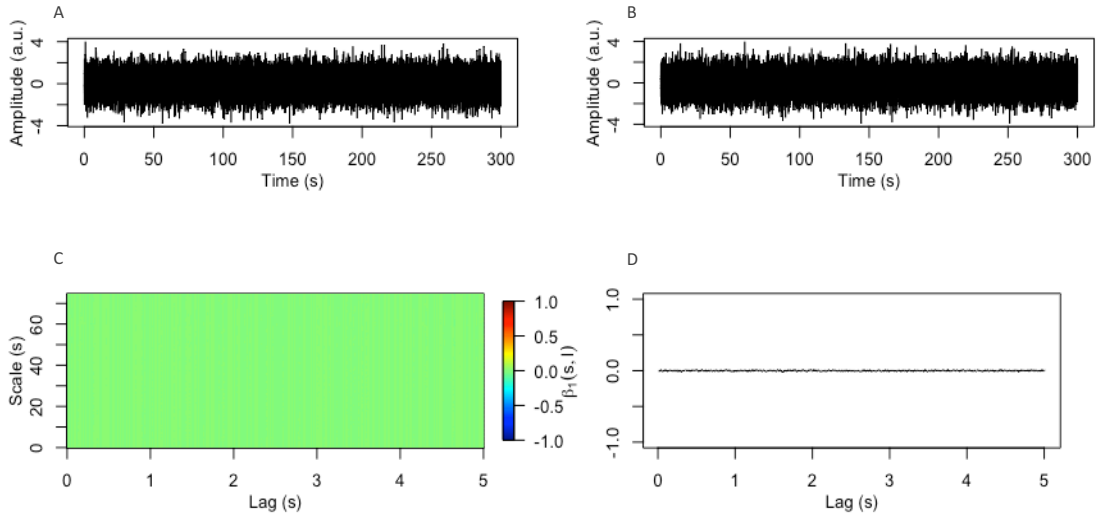

Figure A3. Multiscale lagged regression for independent white noise processes. Panels (a) and (b) are time series plots of identical white noise. Panel (c) is a graphical representation of the *B* matrix obtained in step (7) in MLR. The nature of the relationship between the independent series is obvious in that $\hat{\beta}_1(s,l)$ is always near zero in (d).

Simulation 4 – Two independent white noise processes with a common linear trend.

Here, two independent white processes were generated (N = 30,000), each with a superimposed linear trend that increases by one unit every second, assuming a 100 Hz sampling rate. This simulation is similar to the many examples given in introductory lectures on spurious correlations such as when a child's growth is correlated with growth in the stock market. The three prior simulations, while necessary, were somewhat unsurprising. Simulation 4, however, is arguably a little more interesting because there is a clear linear trend present in each of the series and the trend appears to be more or less the same (see Figure A4 (a) and (b)). An important result would be for MLR to reveal

the spuriousness of the common trend – Figure A4 shows the anticipated result. As expected, MLR shows the time series to be unrelated across all scales and lags. Figure A5 depicts the result without the detrending steps. In that case, not performing the detrending procedure gives the impression that strong positive relationship exists between the simulated series. That result is inaccurate because the two time series are random, independent noise that exert no influence on one another.

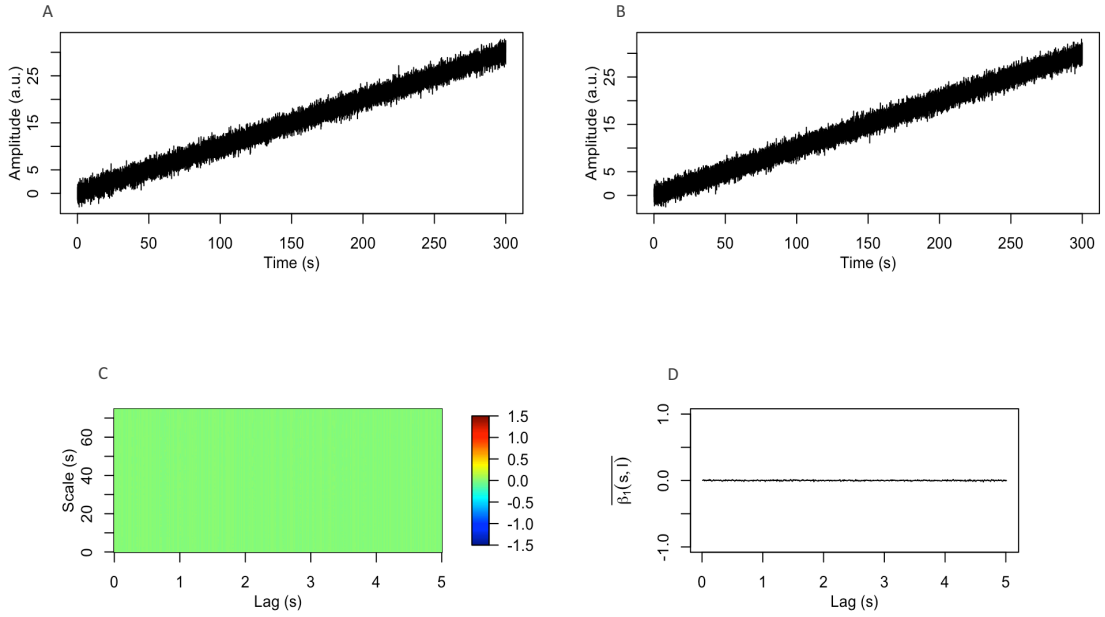

Figure A4. Multiscale lagged regression for independent white noise processes that share a common trend. Panels (a) and (b) are time series plots of identical white noise. Panel (c) is a graphical representation of the *B* matrix obtained in step (7) in MLR. The nature of the relationship between the independent series is obvious in that $\hat{\beta}_1(s,l)$ is always near zero in (d).

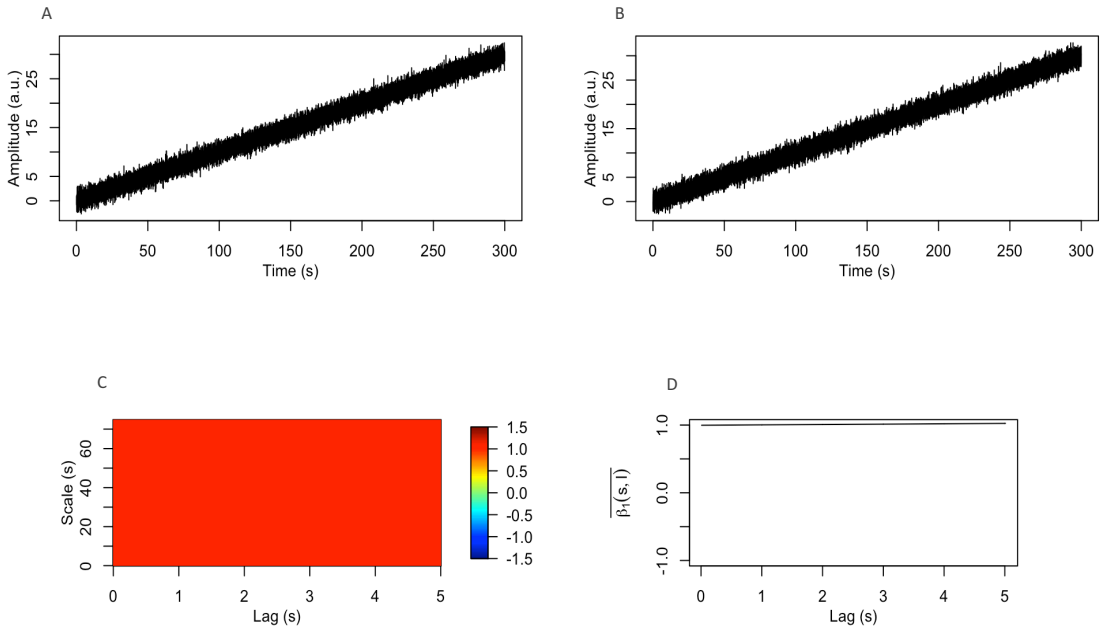

Figure A5. Multiscale lagged regression of spurious trends. Panels (a) and (b) are time series plots of identical white noise. Panel (c) is a graphical representation of the *B* matrix obtained in step (7) in MLR. Here, the spurious trend creates the illusion of a relationship in (d) when the detrending is omitted from MLR.

To contrast, consider an alternate situation in which two time series are correlated but share a common trend imposed by a source external to both series. The series in Figure A6 (a) and (b) were generated by simulating series with

$r \cong 0.75$ and, then giving them each the same trend as the previous simulation. Figure A6 (c) and (d) shows MLR's performance is also good in that scenario—MLR reveals a strong positive coefficient at lag zero that decays to zero at all other lags. Figure A7 depicts the (inaccurate) results that are obtained if the series are not detrended. Taken together, these two simulations show that detrending is beneficial in identifying spurious relationships while properly characterizing genuine dependence.

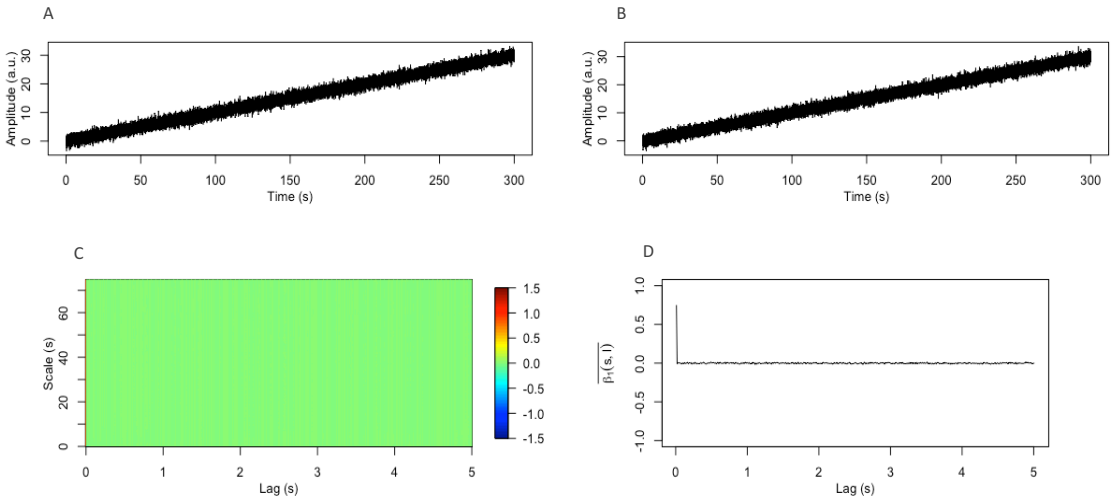

Figure A6. Multiscale lagged regression for independent white noise processes that share a common trend. Panels (a) and (b) are time series plots of correlated series that also share a common upward trend. Panel (c) is a graphical representation of the *B* matrix obtained in step (7) in MLR. Panel (d) shows that, as expected, the series have a strong contemporaneous relationship that decays rapidly over time.

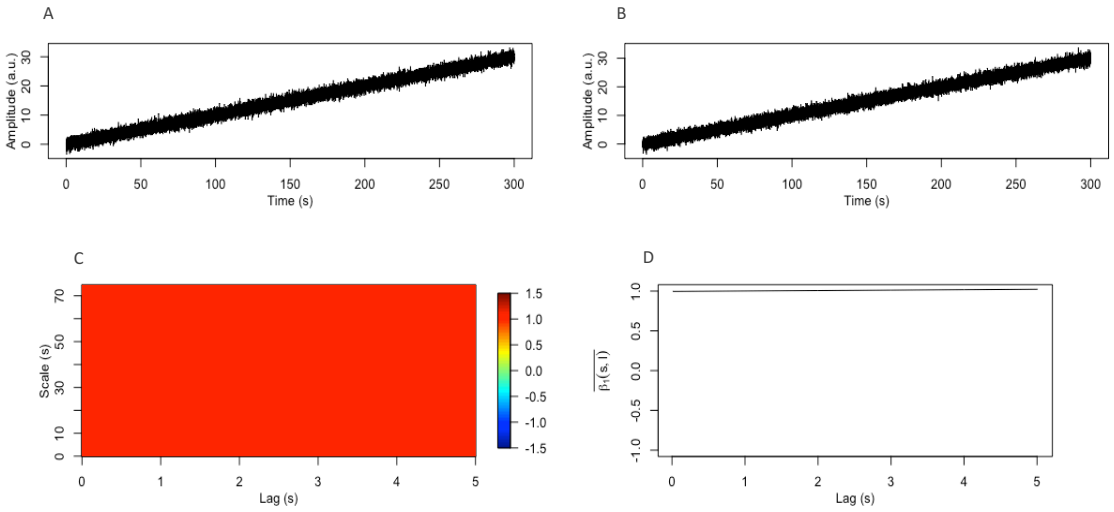

Figure A7. Multiscale lagged regression for independent white noise processes that share a common trend. Panels (a) and (b) are time series plots of correlated series that also share a common upward trend. Panel (c) is a graphical representation of the *B* matrix obtained in step (7) in MLR. Panel (d) shows that, without detrending, the algorithm overestimates the contemporaneous relationship but also projects that overestimation to all scale and lags.

Simulation 5 – Two long range correlated series with a contemporaneous relationship. Two time series were simulated in this example – a fractal time series, X_t, with scaling exponent, $\alpha \cong 0.8$, and a second time series, $Y_t = \beta_0 + \beta_1 X_t + \epsilon_t$, with $\beta_0 = \beta_1 = 1$, and where ϵ_t is a white noise process. In this case, the expectation for a well-performing algorithm is the ability to capture the contemporaneous relationship between X_t and Y_t as unity with slow decay indicative of long range correlation. Figure A8

confirms this finding. There is a strong positive relationship at lag zero that decays quite slowly over successive lags.

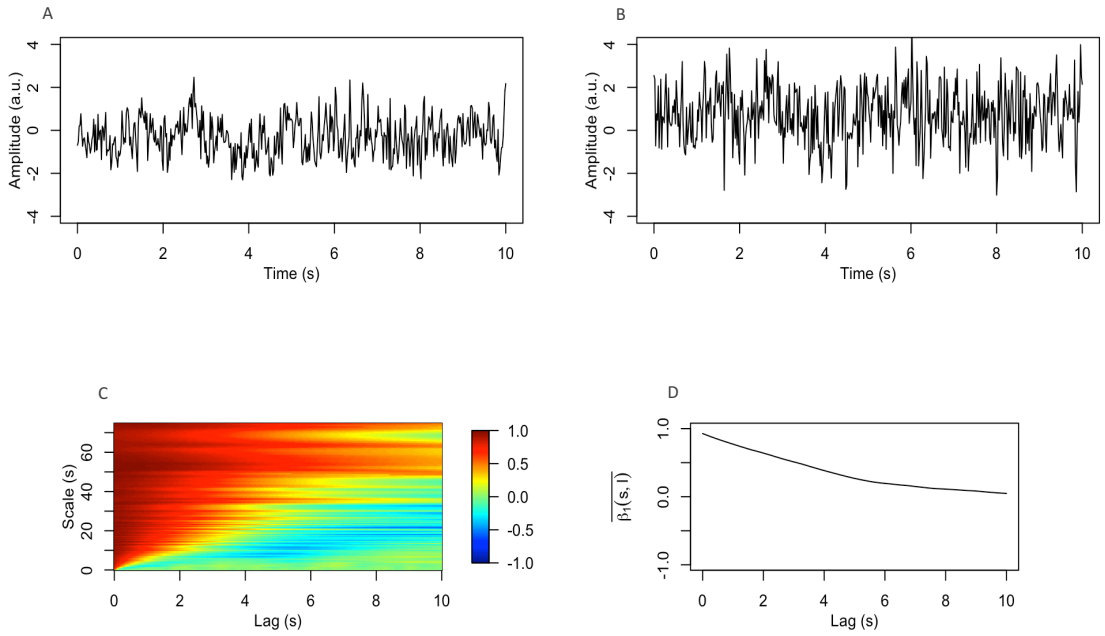

Figure A8. Multiscale lagged regression of long range correlated series that share a strong contemporaneous relationship. Panels (a) and (b) are time series plots of identical white noise. Panel (c) is a graphical representation of the *B* matrix obtained in step (7) in MLR. The spurious relationship between creates the illusion of relationship (d) when the detrending is omitted from MLR.

Simulation 6 – Time series related by multiple lags. This simulation shows that the method is sensitive to perturbations in one time series that originate in another time series. The time series in Figure A9 (a) and (b) were generated such that Figure A9 (b)

depends on previous values of Figure A9 (a). Specifically, the series in Figure A9 (a) perturbs the series in 8 (b) 1 s, 2 s, 3 s, 4 s, and 5 s in the past. The pattern of perturbations is clearly visible in Figure A9 (c) and (d). In Figure A9 (c), the perturbations are most visible at small scales and diffuse to longer and longer time scales. In Figure A9 (d), the pattern presents as a sequence of scallops resting at lags from 1 s to 5 s.

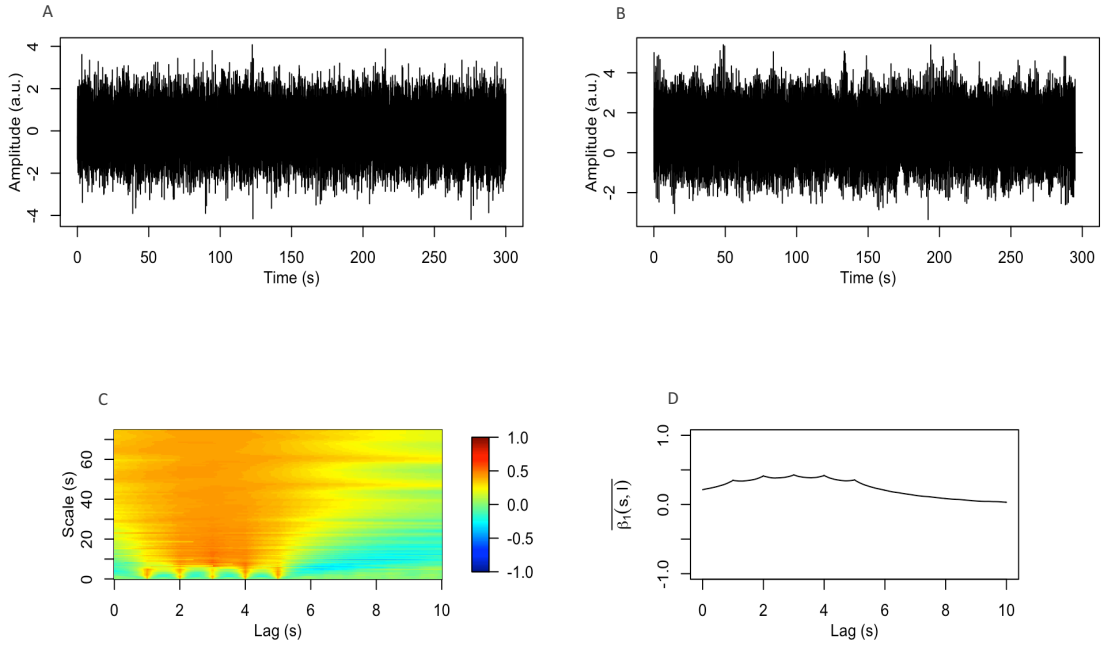

Figure A9. Multiscale lagged regression of spurious trends. Panels (a) and (b) are time series plots of identical white noise. Panel (c) is a graphical representation of the *B* matrix obtained in step (7) in MLR. The spurious relationship between creates the illusion of relationship (d) when the detrending is omitted from MLR.

***Simulation 7* – Two noisy sine waves.** The same sine waves generated in Simulation 1 were regenerated in current simulation (see Figure A10 (a) and (b)). The main difference was that the sine waves in the current simulation were contaminated by independent sources of white noise. Figure A10 (c) shows that the relatively small coefficients at small scales gives way to the expected oscillating pattern at large scales (c.f. Figure 1). That is interesting because it implies that if only small time scales were analyzed, then the relevant, oscillatory structure would be missed. MLR uncovered the oscillatory relationship between the time series, even though the relationship was buried in noise.

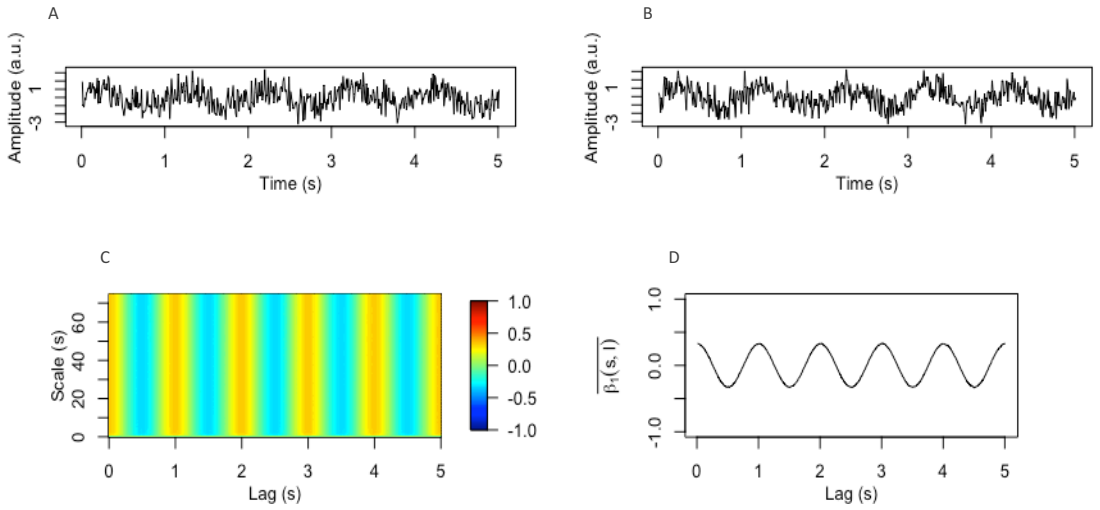

Figure A10. Multiscale lagged regression of noise corrupted sine waves. Panels (a) and (b) are time series plots of noisy sine waves. Panel (c) is a graphical representation of the *B* matrix obtained in step (7) in MLR. Despite considerable and independent noise in the time series, MLR still captures the tendency for oscillation across many scales as can be seen by average

It is clear from the simulations above that MLR reveals the multiscale temporal relationships between time series. The general utility of the MLR approach is its capability to capture structure not just contemporaneously, but also over successive lags. MLR functions well in the face of noise and misleading trends. Important for the analysis of psychological time series is the fact that MLR captures temporal dynamics at multiple time scales. Details of how those multiscale interactions are left to analysis sections involving experimental data as those summarization method are not a direct part of the algorithm.

APPENDIX B

LINEAR MIXED-EFFECTS MODELS FROM EXPERIMENT 1

Table B1. Linear mixed-effect model regressing total power on SDRP and other treatment effects. Model corresponds to MLR of respiratory rate on heart rate.

	B	*CI*	*p*	*B*	*CI*	*p*	*B*	*CI*	*p*	*B*	*CI*	*p*
Fixed Parts												
Intercept	0.53	0.45 – 0.62	**<.001**	0.44	0.35 – 0.53	**<.001**	0.40	0.30 – 0.50	**<.001**	0.44	0.33 – 0.55	**<.001**
Power	0.89	-0.24 – 2.03	.126	0.49	-0.55 – 1.52	.359	-0.12	-1.14 – 0.90	.814	1.47	-0.38 – 3.31	.124
Pre vs During				0.20	0.13 – 0.27	**<.001**	0.20	0.14 – 0.27	**<.001**	0.04	-0.06 – 0.15	.438
Pre vs Post				0.08	0.01 – 0.16	**.025**	0.08	0.02 – 0.15	**.017**	0.12	0.02 – 0.22	**.027**
Move vs Control							0.13	0.06 – 0.19	**<.001**	0.00	-0.10 – 0.10	.986
Breath Vs Control							-0.01	-0.08 – 0.06	.824	-0.02	-0.12 – 0.09	.732
Move Vs Control During										0.38	0.23 – 0.53	**<.001**
Move Vs Control Post										-0.01	-0.16 – 0.13	.857
Breath Vs Control During										0.07	-0.08 – 0.22	.361
Breath vs Control Post										-0.08	-0.23 – 0.06	.261
Power x Move										-1.47	-3.72 – 0.78	.203
Power × Breath										-3.19	-5.60 – -0.78	**.011**
Random Parts												
σ^2		0.038			0.030			0.027			0.020	
$\tau_{00,\,id}$		0.023			0.024			0.024			0.027	
ϱ_{01}								1.000			1.000	
N_{id}		15			15			15			15	
ICC_{id}		0.375			0.440			0.476			0.575	
Observations		135			135			135			135	
R^2 / Ω_0^2		.444 / .435			.556 / .551			.614 / .611			.724 / .722	

Table B2. Linear mixed-effect model regressing total power on SDRP and other treatment effects. Model corresponds to MLR of respiratory rate on movement frequency.

	B	*CI*	*p*	*B*	*CI*	*p*	*B*	*CI*	*p*	*B*	*CI*	*p*
Fixed Parts												
Intercept	0.53	0.43 – 0.62	**<.001**	0.43	0.32 – 0.53	**<.001**	0.39	0.29 – 0.50	**<.001**	0.48	0.36 – 0.60	**<.001**
Power	1.49	-5.90 – 8.88	.693	2.00	-4.68 – 8.67	.559	1.04	-5.35 – 7.43	.750	-10.53	-20.52 – -0.53	**.041**
Pre vs During				0.21	0.13 – 0.28	**<.001**	0.21	0.14 – 0.27	**<.001**	0.06	-0.04 – 0.16	.253
Pre vs Post				0.08	0.01 – 0.16	**.024**	0.08	0.02 – 0.15	**.017**	0.13	0.03 – 0.23	**.015**
Move vs Control							0.12	0.05 – 0.19	**<.001**	-0.09	-0.21 – 0.04	.172
Breath Vs Control							-0.00	-0.07 – 0.06	.909	0.02	-0.11 – 0.14	.794
Move Vs Control During										0.35	0.21 – 0.50	**<.001**
Move Vs Control Post										-0.02	-0.16 – 0.12	.793
Breath Vs Control During										0.04	-0.11 – 0.18	.632
Breath vs Control Post										-0.11	-0.26 – 0.03	.124
Power x Move										18.47	5.36 – 31.59	**.007**
Power × Breath										3.91	-7.83 – 15.64	.516
Random Parts												
σ^2	0.038			0.031			0.027			0.020		
$\tau_{00,\ id}$	0.023			0.023			0.024			0.030		
N_{id}	15			15			15			15		
ICC_{id}	0.373			0.431			0.473			0.604		
Observations	135			135			135			135		
R^2 / Ω_0^2	.435 / .425			.552 / .547			.612 / .608			.734 / .733		

Table B3. Linear mixed-effect model regressing total power on SDRP and other treatment effects. Model corresponds to MLR of respiratory rate on postural path length.

	B	*CI*	*p*	*B*	*CI*	*p*	*B*	*CI*	*p*	*B*	*CI*	*p*
Fixed Parts												
Intercept	0.53	0.45 – 0.62	**<.001**	0.44	0.34 – 0.53	**<.001**	0.40	0.29 – 0.50	**<.001**	0.41	0.30 – 0.52	**<.001**
Power	-0.95	-2.71 – 0.81	.294	-0.89	-2.49 – 0.71	.279	-1.04	-2.55 – 0.46	.176	-4.28	-7.09 – -1.47	**.003**
Pre vs During				0.21	0.13 – 0.28	**<.001**	0.21	0.14 – 0.27	**<.001**	0.10	0.00 – 0.21	.050
Pre vs Post				0.09	0.02 – 0.16	**.017**	0.09	0.02 – 0.16	**.010**	0.14	0.04 – 0.25	**.007**
Move vs Control							0.13	0.06 – 0.19	**<.001**	0.03	-0.08 – 0.13	.610
Breath Vs Control							-0.00	-0.07 – 0.06	.897	0.03	-0.07 – 0.14	.518
Move Vs Control During										0.32	0.18 – 0.47	**<.001**
Move Vs Control Post										-0.04	-0.18 – 0.11	.614
Breath Vs Control During										0.01	-0.14 – 0.15	.941
Breath vs Control Post										-0.12	-0.26 – 0.03	.111
Power x Move										4.53	1.06 – 8.00	**.012**
Power × Breath										4.40	0.53 – 8.27	**.028**
Random Parts												
σ^2	0.038			0.030			0.027			0.020		
$\tau_{00,\,id}$	0.024			0.024			0.025			0.025		
N_{id}	15			15			15			15		
ICC_{id}	0.383			0.445			0.481			0.556		
Observations	135			135			135			135		
R^2 / Ω_0^2	.441 / .432			.558 / .553			.618 / .615			.726 / .724		

Table B4. Linear mixed-effect model regressing total power on SDRP and other treatment effects. Model corresponds to MLR of heart on rate respiratory rate.

	B	*CI*	*p*	*B*	*CI*	*p*	*B*	*CI*	*p*	*B*	*CI*	*p*
Fixed Parts												
Intercept	0.53	0.43 – 0.62	**<.001**	0.42	0.32 – 0.53	**<.001**	0.39	0.28 – 0.50	**<.001**	0.37	0.24 – 0.50	**<.001**
Power	0.35	-1.83 – 2.54	.752	0.68	-1.29 – 2.66	.499	0.34	-1.60 – 2.28	.733	1.85	-0.39 – 4.09	.108
Pre vs During				0.21	0.13 – 0.28	**<.001**	0.21	0.14 – 0.27	**<.001**	0.09	-0.01 – 0.20	.091
Pre vs Post				0.09	0.01 – 0.16	**.020**	0.09	0.02 – 0.15	**.016**	0.15	0.04 – 0.26	**.009**
Move vs Control							0.12	0.06 – 0.19	**<.001**	0.03	-0.12 – 0.18	.699
Breath Vs Control							0.00	-0.07 – 0.07	.976	0.09	-0.04 – 0.22	.180
Move Vs Control During										0.35	0.20 – 0.50	**<.001**
Move Vs Control Post										-0.03	-0.19 – 0.12	.661
Breath Vs Control During										0.03	-0.12 – 0.19	.673
Breath vs Control Post										-0.11	-0.27 – 0.05	.167
Power x Move										-0.34	-4.61 – 3.94	.878
Power × Breath										-4.02	-10.34 – 2.30	.215
Random Parts												
σ^2		0.038			0.031			0.027			0.021	
$\tau_{00,\ id}$		0.024			0.024			0.025			0.026	
N_{id}		15			15			15			15	
ICC_{id}		0.383			0.445			0.480			0.554	
Observations		135			135			135			135	
R^2 / Ω_0^2		.437 / .428			.556 / .551			.613 / .610			.714 / .713	

Table B5. Linear mixed-effect model regressing total power on SDRP and other treatment effects. Model corresponds to MLR of heart on movement frequency.

	B	*CI*	*p*	*B*	*CI*	*p*	*B*	*CI*	*p*	*B*	*CI*	*p*
Fixed Parts												
Intercept	3	0.45 – 0.62	**<.001**	0.44	0.34 – 0.53	**<.001**	0.40	0.30 – 0.50	**<.001**	0.40	0.30 – 0.50	**<.001**
Power	4	-3.64 – 10.51	.343	2.69	-3.69 – 9.07	.410	2.69	-3.38 – 8.76	.387	-8.43	-19.80 – 2.94	.149
Pre vs During				0.20	0.13 – 0.28	**<.001**	0.20	0.14 – 0.27	**<.001**	0.18	0.11 – 0.25	**<.001**
Pre vs Post				0.09	0.01 – 0.16	**.023**	0.09	0.02 – 0.15	**.015**	0.08	0.01 – 0.15	**.018**
Move vs Control							0.12	0.05 – 0.19	**<.001**	0.12	0.05 – 0.19	**<.001**
Breath Vs Control							-0.01	-0.08 – 0.06	.850	0.00	-0.06 – 0.07	.961
Move Vs Control During										7.60	-7.19 – 22.39	.316
Move Vs Control Post										1.19	-11.68 – 14.06	.856
Breath Vs Control During										21.28	5.88 – 36.69	**.008**
Breath vs Control Post										5.95	-7.15 – 19.04	.375
Power x Move												
Power × Breath												
Random Parts												
σ^2	0.038			0.031			0.027			0.025		
$\tau_{00,\,id}$	0.022			0.023			0.024			0.026		
N_{id}	15			15			15			15		
ICC_{id}	0.367			0.432			0.467			0.506		
Observations	135			135			135			135		
R^2 / Ω_0^2	.436 / .427			.554 / .549			.612 / .609			.655 / .652		

Table B6. Linear mixed-effect model regressing total power on SDRP and other treatment effects. Model corresponds to MLR of heart on postural path length.

	B	*CI*	*p*	*B*	*CI*	*p*	*B*	*CI*	*p*	*B*	*CI*	*p*
Fixed Parts												
Intercept	0.57	0.49 – 0.66	**<.001**	0.47	0.37 – 0.57	**<.001**	0.43	0.32 – 0.54	**<.001**	0.48	0.36 – 0.61	**<.001**
Power	-2.36	-4.34 – -0.37	**.022**	-1.79	-3.60 – 0.02	.054	-1.38	-3.13 – 0.37	.125	-1.86	-4.14 – 0.41	.112
Pre vs During				0.20	0.13 – 0.27	**<.001**	0.20	0.13 – 0.27	**<.001**	0.06	-0.05 – 0.17	.283
Pre vs Post				0.08	0.01 – 0.15	**.034**	0.08	0.01 – 0.15	**.023**	0.09	-0.02 – 0.20	.099
Move vs Control							0.11	0.05 – 0.18	**.002**	-0.04	-0.17 – 0.09	.534
Breath Vs Control							-0.01	-0.08 – 0.06	.748	-0.03	-0.16 – 0.11	.692
Move Vs Control During										0.37	0.22 – 0.52	**<.001**
Move Vs Control Post										0.02	-0.13 – 0.17	.833
Breath Vs Control During										0.05	-0.10 – 0.20	.504
Breath vs Control Post										-0.06	-0.22 – 0.09	.408
Power x Move										1.66	-1.83 – 5.15	.353
Power × Breath										1.11	-3.19 – 5.40	.615
Random Parts												
σ^2	0.037			0.030			0.027			0.021		
$\tau_{00,\ id}$	0.023			0.024			0.024			0.025		
N_{id}	15			15			15			15		
ICC_{id}	0.381			0.442			0.476			0.539		
Observations	135			135			135			135		
R^2 / Ω_0^2	.457 / .449			.566 / .561			.619 / .616			.710 / .708		

Table B7. Linear mixed-effect model regressing total power on SDRP and other treatment effects. Model corresponds to MLR of movement frequency on respiratory rate.

	B	*CI*	*p*	*B*	*CI*	*p*	*B*	*CI*	*p*	*B*	*CI*	*p*
Fixed Parts												
Intercept	0.49	0.39 – 0.58	**<.001**	0.37	0.27 – 0.47	**<.001**	0.32	0.21 – 0.43	**<.001**	0.31	0.20 – 0.42	**<.001**
Power	0.88	0.06 – 1.71	**.038**	1.17	0.44 – 1.90	**.002**	1.13	0.43 – 1.83	**.002**	2.00	1.25 – 2.75	**<.001**
Pre vs During				0.22	0.15 – 0.29	**<.001**	0.22	0.15 – 0.28	**<.001**	0.09	-0.00 – 0.19	.061
Pre vs Post				0.08	0.01 – 0.15	**.021**	0.08	0.02 – 0.15	**.014**	0.08	-0.01 – 0.18	.085
Move vs Control							0.13	0.06 – 0.19	**<.001**	0.15	0.02 – 0.29	**.031**
Breath Vs Control							0.02	-0.05 – 0.08	.640	0.11	-0.02 – 0.24	.109
Move Vs Control During										0.33	0.19 – 0.46	**<.001**
Move Vs Control Post										0.02	-0.12 – 0.16	.772
Breath Vs Control During										0.02	-0.12 – 0.15	.805
Breath vs Control Post										-0.06	-0.19 – 0.08	.395
Power x Move										-2.35	-3.81 – -0.90	**.002**
Power × Breath										-1.41	-3.28 – 0.46	.142
Random Parts												
σ^2	0.037			0.028			0.025			0.018		
$\tau_{00,\,id}$	0.024			0.025			0.025			0.023		
N_{id}	15			15			15			15		
ICC_{id}	0.394			0.468			0.504			0.568		
Observations	135			135			135			135		
R^2 / Ω_0^2	.457 / .448			.589 / .585			.644 / .641			.761 / .760		

Table B8. Linear mixed-effect model regressing total power on SDRP and other treatment effects. Model corresponds to MLR of movement frequency on heart rate.

	B	*CI*	*p*	*B*	*CI*	*p*	*B*	*CI*	*p*	*B*	*CI*	*p*
Fixed Parts												
Intercept	0.53	0.45 – 0.62	**<.001**	0.44	0.35 – 0.53	**<.001**	0.39	0.29 – 0.49	**<.001**	0.43	0.33 – 0.53	**<.001**
Power	0.44	0.15 – 0.73	**.003**	0.53	0.28 – 0.78	**<.001**	0.51	0.27 – 0.75	**<.001**	0.73	0.49 – 0.98	**<.001**
Pre vs During				0.22	0.15 – 0.29	**<.001**	0.22	0.15 – 0.28	**<.001**	0.09	-0.00 – 0.19	.053
Pre vs Post				0.07	0.01 – 0.14	**.035**	0.07	0.01 – 0.14	**.024**	0.06	-0.03 – 0.16	.211
Move vs Control							0.13	0.06 – 0.19	**<.001**	0.01	-0.08 – 0.10	.823
Breath Vs Control							0.02	-0.05 – 0.08	.606	0.02	-0.07 – 0.11	.673
Move Vs Control During										0.33	0.20 – 0.46	**<.001**
Move Vs Control Post										0.05	-0.09 – 0.18	.495
Breath Vs Control During										0.02	-0.11 – 0.15	.788
Breath vs Control Post										-0.03	-0.17 – 0.10	.618
Power x Move										-0.86	-1.38 – -0.34	**.001**
Power × Breath										-0.45	-1.21 – 0.32	.256
Random Parts												
σ^2	0.036			0.027			0.024			0.017		
$\tau_{00,\,id}$	0.023			0.023			0.024			0.022		
N_{id}	15			15			15			15		
ICC_{id}	0.387			0.463			0.500			0.565		
Observations	135			135			135			135		
R^2 / Ω_0^2	.472 / .465			.608 / .604			.661 / .658			.771 / .770		

Table B9. Linear mixed-effect model regressing total power on SDRP and other treatment effects. Model corresponds to MLR of movement frequency on postural path length.

	B	*CI*	*p*	*B*	*CI*	*p*	*B*	*CI*	*p*	*B*	*CI*	*p*
Fixed Parts												
Intercept	0.56	0.47 – 0.65	**<.001**	0.46	0.37 – 0.56	**<.001**	0.42	0.31 – 0.52	**<.001**	0.45	0.34 – 0.57	**<.001**
Power	-0.50	-1.24 – 0.24	.190	-0.61	-1.27 – 0.05	.074	-0.44	-1.07 – 0.19	.175	-0.50	-1.35 – 0.35	.249
Pre vs During				0.21	0.14 – 0.28	**<.001**	0.21	0.14 – 0.28	**<.001**	0.08	-0.02 – 0.19	.118
Pre vs Post				0.08	0.01 – 0.15	**.024**	0.08	0.02 – 0.15	**.017**	0.11	0.01 – 0.22	**.036**
Move vs Control							0.12	0.05 – 0.19	**<.001**	-0.02	-0.16 – 0.11	.736
Breath Vs Control							-0.00	-0.07 – 0.06	.913	-0.01	-0.12 – 0.11	.928
Move Vs Control During										0.35	0.20 – 0.50	**<.001**
Move Vs Control Post										-0.00	-0.15 – 0.15	.982
Breath Vs Control During										0.02	-0.13 – 0.17	.752
Breath vs Control Post										-0.09	-0.24 – 0.06	.250
Power x Move										0.70	-1.03 – 2.43	.429
Power × Breath										0.49	-0.68 – 1.65	.415
Random Parts												
σ^2	0.038			0.030			0.027			0.022		
$\tau_{00,\ id}$	0.023			0.024			0.025			0.025		
N_{id}	15			15			15			15		
ICC_{id}	0.383			0.447			0.480			0.540		
Observations	135			135			135			135		
R^2 / Ω_0^2	.444 / .434			.565 / .561			.618 / .615			.707 / .705		

Table B10. Linear mixed-effect model regressing total power on SDRP and other treatment effects. Model corresponds to MLR of postural path length on respiratory rate.

	B	*CI*	*p*	*B*	*CI*	*p*	*B*	*CI*	*p*	*B*	*CI*	*p*
Fixed Parts												
Intercept	0.53	0.45 – 0.62	**<.001**	0.44	0.34 – 0.53	**<.001**	0.40	0.29 – 0.50	**<.001**	0.41	0.30 – 0.52	**<.001**
Power	-0.95	-2.71 – 0.81	.294	-0.89	-2.49 – 0.71	.279	-1.04	-2.55 – 0.46	.176	-4.28	-7.09 – -1.47	**.003**
Pre vs During				0.21	0.13 – 0.28	**<.001**	0.21	0.14 – 0.27	**<.001**	0.10	0.00 – 0.21	.050
Pre vs Post				0.09	0.02 – 0.16	**.017**	0.09	0.02 – 0.16	**.010**	0.14	0.04 – 0.25	**.007**
Move vs Control							0.13	0.06 – 0.19	**<.001**	0.03	-0.08 – 0.13	.610
Breath Vs Control							-0.00	-0.07 – 0.06	.897	0.03	-0.07 – 0.14	.518
Move Vs Control During										0.32	0.18 – 0.47	**<.001**
Move Vs Control Post										-0.04	-0.18 – 0.11	.614
Breath Vs Control During										0.01	-0.14 – 0.15	.941
Breath vs Control Post										-0.12	-0.26 – 0.03	.111
Power x Move										4.53	1.06 – 8.00	**.012**
Power × Breath										4.40	0.53 – 8.27	**.028**
Random Parts												
σ^2	0.038			0.030			0.027			0.020		
$\tau_{00,\,id}$	0.024			0.024			0.025			0.025		
N_{id}	15			15			15			15		
ICC_{id}	0.383			0.445			0.481			0.556		
Observations	135			135			135			135		
R^2 / Ω_0^2	.441 / .432			.558 / .553			.618 / .615			.726 / .724		

Table B11. Linear mixed-effect model regressing total power on SDRP and other treatment effects. Model corresponds to MLR of postural path length on heart rate.

	B	*CI*	*p*	*B*	*CI*	*p*	*B*	*CI*	*p*	*B*	*CI*	*p*
Fixed Parts												
Intercept	0.53	0.45 – 0.62	**<.001**	0.44	0.34 – 0.53	**<.001**	0.40	0.30 – 0.50	**<.001**	0.43	0.32 – 0.54	**<.001**
Power	-0.01	-0.27 – 0.24	.925	-0.02	-0.25 – 0.21	.872	-0.04	-0.26 – 0.17	.711	-0.19	-0.46 – 0.09	.182
Pre vs During				0.21	0.13 – 0.28	**<.001**	0.21	0.14 – 0.27	**<.001**	0.08	-0.02 – 0.18	.134
Pre vs Post				0.08	0.01 – 0.16	**.025**	0.08	0.02 – 0.15	**.017**	0.12	0.01 – 0.22	**.029**
Move vs Control							0.12	0.06 – 0.19	**<.001**	0.01	-0.10 – 0.11	.878
Breath Vs Control							-0.00	-0.07 – 0.06	.923	0.02	-0.09 – 0.12	.739
Move Vs Control During										0.35	0.20 – 0.49	**<.001**
Move Vs Control Post										-0.01	-0.15 – 0.14	.938
Breath Vs Control During										0.03	-0.12 – 0.18	.695
Breath vs Control Post										-0.09	-0.24 – 0.05	.220
Power x Move										0.26	-0.20 – 0.72	.263
Power × Breath										0.24	-0.33 – 0.81	.414
Random Parts												
σ^2	0.038			0.031			0.027			0.021		
$\tau_{00,\,id}$	0.024			0.025			0.025			0.027		
N_{id}	15			15			15			15		
ICC_{id}	0.385			0.447			0.484			0.560		
Observations	135			135			135			135		
R^2 / Ω_0^2	.438 / .428			.555 / .550			.614 / .610			.711 / .709		

Table B12. Linear mixed-effect model regressing total power on SDRP and other treatment effects. Model corresponds to MLR of postural path length on movement frequency.

	B	*CI*	*p*	*B*	*CI*	*p*	*B*	*CI*	*p*	*B*	*CI*	*p*
Fixed Parts												
Intercept	0.56	0.46 – 0.65	**<.001**	0.46	0.35 – 0.56	**<.001**	0.40	0.29 – 0.51	**<.001**	0.47	0.36 – 0.59	**<.001**
Power	-1.02	-2.07 – 0.02	.058	-0.59	-1.57 – 0.38	.233	0.81	-0.14 – 1.75	.101	-1.19	-2.18 – -0.21	**.019**
Pre vs During				0.20	0.12 – 0.27	**<.001**	0.20	0.13 – 0.26	**<.001**	0.05	-0.06 – 0.15	.396
Pre vs Post				0.08	0.00 – 0.15	**.042**	0.08	0.01 – 0.15	**.022**	0.09	-0.02 – 0.19	.112
Move vs Control							0.11	0.05 – 0.18	**.001**	-0.04	-0.16 – 0.08	.487
Breath Vs Control							-0.02	-0.08 – 0.05	.634	-0.02	-0.14 – 0.10	.727
Move Vs Control During										0.38	0.24 – 0.53	**<.001**
Move Vs Control Post										0.02	-0.12 – 0.17	.754
Breath Vs Control During										0.06	-0.09 – 0.21	.430
Breath vs Control Post										-0.06	-0.21 – 0.09	.405
Power x Move										1.51	-0.90 – 3.92	.222
Power × Breath										0.98	-0.99 – 2.96	.331
Random Parts												
σ^2		0.036			0.030			0.025			0.020	
$\tau_{00,\,id}$		0.028			0.027			0.032			0.029	
ϱ_{01}								-1.000				
N_{id}		15			15			15			15	
ICC_{id}		0.433			0.473			0.559			0.583	
Observations		135			135			135			135	
R^2 / Ω_0^2		.462 / .454			.564 / .559			.637 / .634			.722 / .721	